PHYSICAL REVIEW
LETTERS

VOLUME 4 MAY 15, 1960 NUMBER 10

POLARIZATION AND ANGULAR EXTENT OF THE 960-Mc/sec RADIATION FROM JUPITER*

V. Radhakrishnan and J. A. Roberts
Radio Observatory, California Institute of Technology, Owens Valley, California
(Received April 25, 1960)

Following the discovery by Sloanaker[1] of unexpectedly intense 10-cm radiation from Jupiter, Bolton initiated studies of the planet at a wavelength of 31 cm (960 Mc/sec) at the above observatory.[2] These and other investigations[3] have led to the suggestion that the radiation originates in a "Van Allen belt" surrounding Jupiter.[3] If the emission has its origin in such a belt of electrons spiralling in a trapping magnetic field, the angular extent of the source of the radiation is likely to be several times the diameter of the planet. In addition, some degree of polarization of the radiation would be expected.

Observations to test these predictions are being made with a variable-spacing interferometer, and some results are reported here. The source is found to be strongly linearly polarized, the radiation with the electric vector parallel to the equatorial plane of the planet being approximately 1.7 times as intense as in the orthogonal polarization. The radiation comes from a region several times the diameter of the disk and is more strongly polarized in the outer parts.

The observations were made possible by the advanced instrument available at this observatory, namely a phase-switched interferometer comprising two 90-foot antennas which can be moved on railroad tracks between stations with separations of 200, 400, 800, and 1600 feet. The corresponding fringe spacings at 960 Mc/sec are approximately 18, 9, 4.5, and 2 minutes of arc. (The diameter of Jupiter at the time of the observations was ~0.6 minute of arc.) The instrument can be used to completely determine the polarization of a radio source by observing with different orientations of the horn feeds on the two antennas.[4] Each horn can be rotated on its own axis; one is motorized and can be set alternately parallel and perpendicular to the other during an observation. Observations of non-polarized radio sources have shown that the signal received in the cross-polarized condition is approximately one percent of that received in the parallel condition.

The polarization of the planetary emission was demonstrated conclusively by the large interference pattern recorded when one horn was set to receive radiation with the electric vector in position angle -45° and the other to receive the orthogonal polarization. The phase of this interference pattern indicated that the polarization was linear, with the electric vector approximately in position angle 90° (E-W), i.e., in the planet's equatorial plane. No detectable pattern was observed when the antennas were cross polarized in position angles 0° and 90°. This implies the absence of any circularly polarized component ($\leq 6\%$), and that the direction of the electric vector of the linear component is within $\pm 12°$ of position angle 90°.

If the electric vector is assumed to lie directly E-W, the degree of polarization[5] is given by the ratio of the interference pattern recorded when the horns are cross polarized in position angles 45° and -45°, to that recorded when the horns are identically polarized at one of these position angles. Observations of this type, at an antenna separation of 400 ft made on April 2, 3, 11, and 12, 1960, gave values for the degree of polarization between 25 and 43%, with a mean value of 33%.

The polarization was also determined by comparing the intensity received with both horns parallel and oriented E-W and N-S on successive days (April 12, 13). These observations are in qualitative agreement, but given a lower degree of polarization (mean 22%). The significance of this difference is not yet clear.

From April 17 to April 21, observations were made with an antenna separation of 800 feet by one of the authors and David Morris. By observing the source at various hour angles, a range of effective baselines (and hence fringe separations) was obtained. The apparent intensity of all components of the radiation decreased with decreasing fringe size (Table I), indicating that the source was being resolved. However, the polarized component decreased more rapidly, and therefore the outer regions of the source are more strongly polarized. The present observations are insufficient to determine a detailed distribution of intensity, but are consistent with an equatorial ring of mean diameter about 2 minutes of arc, i.e., about three times the diameter of Jupiter.

Of the theories proposed to account for the Jovian decimeter radiation,[2,6] only the cyclotron and synchrotron theories predict strong linear polarization.

For the cyclotron theory the observed intensity of radiation can be accounted for on the basis of electron densities similar to those in the earth's outer Van Allen belt and a field ~300 gauss in the emitting region. This would imply a field $\sim 10^4$ gauss at the surface of the planet. It seems likely that such a field could be detected by optical means.

The synchrotron theory would not need such strong fields, but would demand a vastly greater density of relativistic electrons.

Observations of the polarization and source size as a function of frequency appear to be a powerful method of discriminating between the cyclotron and synchrotron theories. For the cyclotron case Field[7] has predicted a rapid change of the polarization with frequency. No detailed theory is yet available for the synchrotron case, but elementary considerations suggest that the observed sense of polarization would be predicted and that there would not be a rapid change with frequency. The latter result follows from the consideration that unless there is a relationship between the energy of the electrons and their pitch angles at the equator, electrons of all energies will have similar orbits and mirror points.

These observations were made possible by the unique instrument which is due to J. G. Bolton, and by the highly sensitive receiving equipment designed by G. J. Stanley. We wish to thank Dr. G. B. Field for informing us of his results prior to publication, and Professor Leverett Davis for helpful discussions.

*This work was supported by the Office of Naval Research.

[1]E. F. McClain and R. M. Sloanaker, Paris Symposium on Radio Astronomy, edited by R. N. Bracewell (Stanford University Press, Stanford, California, 1959), p. 61; C. H. Mayer, Astron. J. 64, 43 (1959).

[2]J. A. Roberts and G. J. Stanley, Publs. Astron. Soc. Pacific 71, 485 (1959).

[3]F. D. Drake and H. Hvatum, Astron. J. 64, 329 (1959).

[4]M. H. Cohen, Proc. Inst. Radio Engrs. 46, 172 (1958).

[5]Ratio of the intensity of the polarized component to the total intensity (2 planes of polarization).

[6]G. B. Field, J. Geophys. Research 64, 1169 (1959).

[7]G. B. Field, J. Geophys. Research (to be published).

Table I. Mean amplitude of interference fringes in arbitrary units.

Effective baseline (wavelengths)		390	780	Extinguished part at 780λ
Fringe spacing (minutes of arc)		8.8	4.4	
⇉	E-W component	40	23	17
⁄⁄	Position angle -45°	33	21	12
⇈	N-S component	26	17	9
⤡⤢	Cross polarized 45°, -45°	10	≤5	≥5
↑→	Cross polarized 0°, 90°	≤4	≤4	
Percentage polarization	Method 1	30	≤24	≥42
	Method 2	21	15	31

PVT ANOMALIES IN He^3 NEAR ITS MELTING CURVE*

S. G. Sydoriak, R. L. Mills, and E. R. Grilly
Los Alamos Scientific Laboratory, University of California, Los Alamos, New Mexico
(Received April 25, 1960)

Recent measurements[1] on the *PVT* melting properties of high-purity He^3 have been extended down to 0.3°K. A different apparatus and technique were required, however, because of the predicted[2] minimum, P_{min}, in the melting curve, at a temperature, T_{min}, recently reported[3,4] to be 0.32°K. A consequence of this phenomenon first pointed out[5] by one of us (SGS) is that all parts of a pressure sensing tube at temperatures below T_{min} will be plugged with solid. The present apparatus avoided this difficulty by use of a spring-loaded bellows, cell A, filled with high-pressure liquid He^3 and located inside a heavy-walled copper cell, B. The assembly was soldered to a He^3 bath equipped with a He^3 vapor pressure thermometer. The He^3 in cell A was raised above the melting pressure, P_m, by raising the B-cell pressure, P_B, from a low initial value. Subsequent variations in P_A were detected by observing P_B.

The difference in molar volume of liquid and solid He^3 at the melting point, $\Delta V_m \equiv V_l - V_s$, was determined as follows: Starting with A full of solid, small amounts of He^3 were removed from A into a low-pressure tank of known volume and measured pressure, p_t. The ratio, $\Delta P_B/\Delta p_t$, was used to indicate onset and completion of melting, being zero only during melting. Thermal disturbances verified these conditions. The material withdrawn from A during melting gave a measure of ΔV_m.

Calibrations of cell volumes $(v_A + v_B)$ and of v_A versus $(P_A - P_B)$ were made using liquid nitrogen and liquid He^3. For He^3 experiments at $T > T_{min}$, $(P_A - P_B)$ was a directly observable constant during the entire melting process. At $T < T_{min}$ the value of P_A at melting was determined from an extrapolation of pressure measurements made after P_A had dropped below P_{min}.

Values of V_l were determined in a separate series of experiments with A and B cells interconnected, using a stepwise bleed-out method which also yielded the compressibility coefficient $\beta_l = -V^{-1}(\partial V_l/\partial P)_T$, and the thermal expansion coefficient $\alpha_l = V^{-1}(\partial V_l/\partial T)_P$ near the melting point.

Figure 1 shows the V_l data and the values of V_s obtained by subtracting experimental values of ΔV_m from the V_l curve. Since ΔV_m does not become negative at T_{min}, the entropy change on melting must reverse sign at T_{min}. This was, in fact, observed in the present experiments: melting produced heating and cooling at $T_m = 0.308$°K and $T_m > 0.382$°K, respectively, which

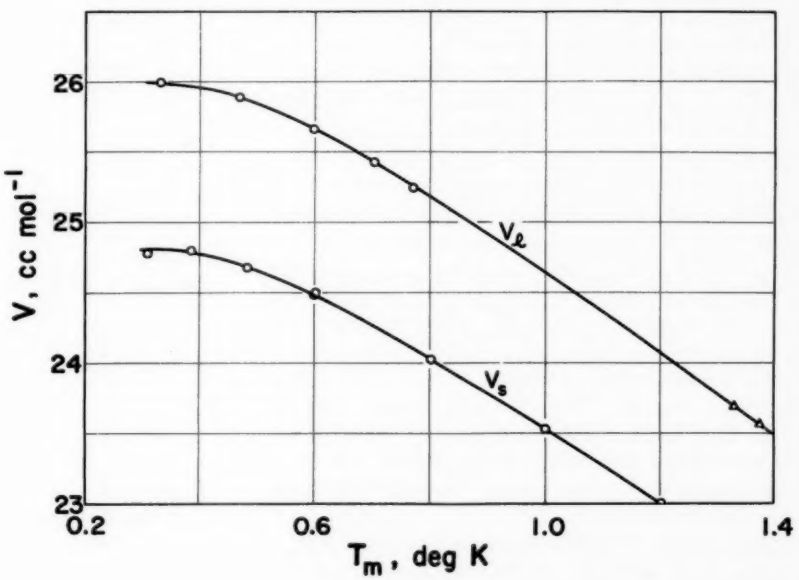

FIG. 1. Molar volume of liquid and solid He^3 along the melting curve. △ Grilly and Mills (reference 1), ○ present measurements.

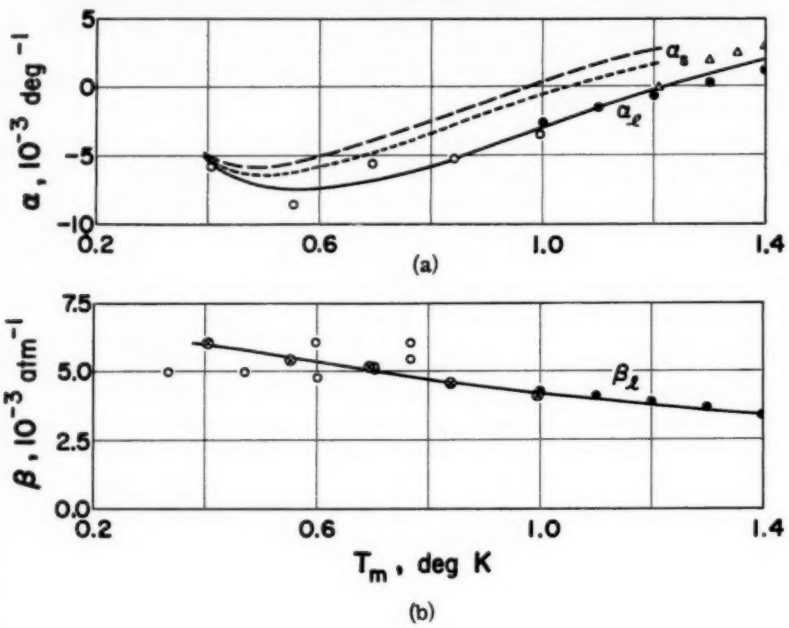

FIG. 2. (a) Thermal expansion coefficient (upper figure) and (b) compressibility coefficient (lower figure) of He^3 along the melting curve. △ Grilly and Mills (reference 1), ● Sherman and Edeskuty (reference 12), ○ present measurements, ⊗ computed from Eq. (1) using the present α_l points. Curves for α_S calculated from Eq. (2): ——— assuming $\beta_S = \beta_l$; ------ assuming $\beta_S = 0.99\beta_l$.

agrees qualitatively with the reversal temperature ~0.4°K of Walters and Fairbank.[6]

Values of α are shown in Fig. 2. The anomalous negative values of α_l found at lower pressures[7-9] are seen to persist up to the melting point. From the relation

$$\alpha_l = \left(\beta_l + \frac{1}{V_l}\frac{dV_l}{dP_m}\right)\frac{dP_m}{dT_m}, \qquad (1)$$

and the observation that dV_l/dP_m is nearly constant as $P - P_{\min}$, it appears likely that $\alpha_l \to 0$ as $T \to T_{\min}$. The data are inadequate, however, for a determination of the shape of the curve near $T_{\min}$. Measured and calculated values of β_l near the melting curve are shown in Fig. 2.

The thermal expansion coefficient of the solid was calculated from

$$\alpha_S = \alpha_l + \frac{1}{V_S}\frac{dV_S}{dT_m} - \frac{1}{V_l}\frac{dV_l}{dT_m} - (\beta_l - \beta_S)\frac{dP_m}{dT_m}. \qquad (2)$$

With the reasonable assumption that $\beta_l \geq \beta_S$, it is found (Fig. 2) that α_S becomes negative below $1.2 > T_m > 1.0$°K. This anomalous behavior is in accord with a suggestion of Goldstein[10] and in qualitative agreement with the theory of Bernardes and Primakoff.[11]

Each ΔV_m determination yielded a single P_m point. A modification of the above technique was used to increase substantially the number of points near $T_{\min}$. The P_m data indicate $P_{\min} = 28.91 \pm 0.02$ atm and $T_{\min} = 0.330 \pm 0.005$°K. The 39 points obtained between 0.3°K and 0.5°K fit the equation

$$P_m = 28.91 + 32.20(T_m - 0.330)^2 \text{ atm}$$

with an rms deviation of 0.02 atm, which is one-seventh of the least count of the A gauge, a 1000-psi Heise gauge calibrated in situ against a free piston gauge accurate to 0.001 atm. At higher temperatures the P_m data join smoothly to the melting points of Grilly and Mills[1] and Sherman and Edeskuty.[12]

The data of Baum et al.[4] gave $T_{\min} = 0.32$°K, in good agreement with the present determination. However, their $P_{\min} = 29.3 \pm 0.1$ atm exceeds the value reported here by 0.27 atm more than the combined estimated experimental error of the two determinations. Lee et al.[3] also gave $T_{\min} = 0.32$°K and reported a value of $P_{\min} = 29.1$ atm with no mention of their experimental error.

*Work performed under the auspices of the U. S. Atomic Energy Commission.

[1]E. R. Grilly and R. L. Mills, Ann. Phys. 8, 1 (1959).

[2]I. Pomeranchuk, J. Exptl. Theoret. Phys. (USSR) 20, 919 (1950).

[3]D. M. Lee, H. A. Fairbank, and E. J. Walker,

Bull. Am. Phys. Soc. 4, 239 (1959).
[4]J. L. Baum, D. F. Brewer, J. G. Daunt, and D. O. Edwards, Phys. Rev. Letters 3, 127 (1959).
[5]See E. F. Hammel in Progress in Low-Temperature Physics, edited by J. C. Gorter (North-Holland Publishing Company, Amsterdam, 1955), Vol. I., pp. 86-87.
[6]G. K. Walters and William M. Fairbank, Bull. Am. Phys. Soc. 2, 183 (1957); Symposium on Liquid and Solid He[3] (The Ohio State University Press, Columbus, Ohio, 1957), Suppl., p. 1.
[7]D. F. Brewer and J. G. Daunt, Phys. Rev. 115, 843 (1959).
[8]D. M. Lee and H. A. Fairbank (private communication).
[9]R. D. Taylor and E. C. Kerr (private communication).
[10]Louis Goldstein, Ann. Phys. 8, 390 (1959).
[11]N. Bernardes and H. Primakoff (private communication).
[12]R. H. Sherman and F. J. Edeskuty, Ann. Phys. (to be published).

HYDROMAGNETIC STABILITY OF FLOW BETWEEN ROTATING CYLINDERS*

R. J. Donnelly† and M. Ozima
Institute for the Study of Metals and Enrico Fermi Institute for Nuclear Studies,
The University of Chicago, Chicago, Illinois
(Received April 22, 1960)

The flow of an electrically conducting fluid between rotating cylinders in the presence of an axial magnetic field is one of the fundamental problems in magnetohydrodynamics. The stability of this flow was first discussed by Chandrasekhar[1] who gave theoretical estimates of the limit of stable flow for a number of magnetic field strengths. Chandrasekhar's calculations were for the case of perfectly conducting cylinder walls. Since then the corresponding problem for insulating cylinders has been considered by Niblett[2] and Chandrasekhar.[3] All these discussions are confined to the case where the gap between cylinders is small.

We have begun an experimental investigation of this problem using the rotating-cylinder viscometer technique developed by Donnelly.[4,5] In this experiment the cylinders are made of No. 302 stainless steel and the fluid is mercury. The inner cylinder is driven by means of a Graham variable-speed transmission. The outer cylinder is suspended freely on a tungsten wire 0.003 in. in diameter. A second wire holds the outer cylinder from below to balance the buoyant force of the mercury. The torque transmitted to the outer cylinder is measured by turning the upper torsion fiber until the torque just balances that due to the motion of the mercury. Thus the viscometer is a null-reading instrument. Fixed guard cylinders are provided at the top and bottom of the outer cylinder to shield the suspended part from end effects. The length of the suspended cylinder is 10 cm and the guard cylinders are each 0.95 cm long. These proportions are different from those of the earlier instrument because the wavelength of the motions at the critical speed in this experiment are quite large and it is desirable to make the suspended cylinder longer than a wavelength. The cylinders have radii $R_1 = 1.8$ cm and $R_2 = 0.2$ cm, leaving a gap $d = 0.2$ cm. The field was furnished by the magnet of the University of Chicago small cyclotron. The field was measured by a search coil calibrated against a nuclear resonance device.

The experimental procedure is to measure the effective viscosity of the fluid (which is proportional to the product of the torque and the period of rotation of the inner cylinder) as a function of speed of rotation. It was found that this curve shows a distinct change in slope at the critical rotation rate. Furthermore the time of response of the suspended cylinder to a small change in speed becomes longer and characteristic fluctuations in deflection appear as the critical speed is reached. All these features have been noticed with the earlier instrument.[4]

Since the properties of fluids are temperature dependent the results are best represented in dimensionless form. In Fig. 1 the critical Taylor number T_c is plotted as a function of Q, where

$$T = \frac{4R_1^2\Omega_0\Omega_1}{R_2^2 - R_1^2}\,\frac{d^4}{\nu^2}, \tag{1}$$

and

$$Q = \mu^2 H^2 \sigma d^2/\rho\nu. \tag{2}$$

In Eqs. (1) and (2), Ω_1 is the angular velocity of the inner cylinder, Ω_0 is a mean angular velocity

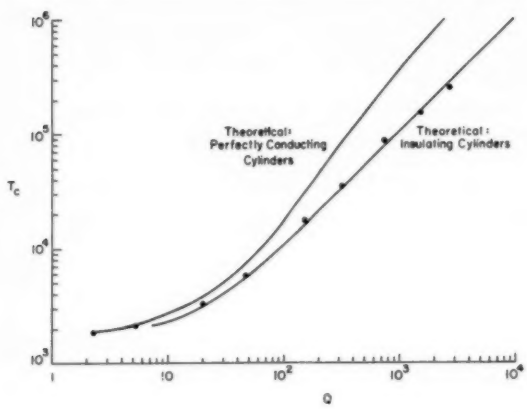

FIG. 1. Relation between the critical Taylor number T_C and Q. The solid curves are derived theoretically for the boundary conditions shown. The dots are experimental observations.

of the fluid given by $\Omega_0 = \frac{1}{2}\Omega_1[1 - 3d/2(R_2 + R_1)]$; $d = (R_2 - R_1)$; ν is the kinematic viscosity, σ the electrical conductivity, μ the permeability, and ρ the density of the fluid; and H is the magnetic field intensity.

From Fig. 1 one can see that the experimental data confirm the general feature of the calculations: an axial magnetic field tends to inhibit the onset of instability. The degree of inhibition can be appreciated from the fact that at $H = 0$ the critical rotation rate is $\Omega_1 = 0.42$ radian/sec, whereas at $H = 10\,000$ gauss, $\Omega_1 = 5.4$ radians/sec. The results are also seen to lie close to the theoretical curve for insulating cylinders. This is not surprising, as the case of perfectly conducting cylinders is to some extent artificial.

The experimental reliability of the preliminary data shown in Fig. 1 is estimated to be about $\pm 10\%$. At fields above 2000 gauss the effective viscosity in the laminar flow region is observed to increase as the rate of rotation increases. This is probably due to the effect of the finite length of the cylinders. The authors plan to try other cylinder sizes to study the effect of varying the ratio of length to gap width.

*Research supported in part by an Office of Naval Research contract with the Enrico Fermi Institute for Nuclear Studies, University of Chicago.

†Alfred P. Sloan Research Fellow.

[1]S. Chandrasekhar, Proc. Roy. Soc. (London) A216, 293 (1953).

[2]E. R. Niblett, Can. J. Phys. 36, 1509 (1958).

[3]S. Chandrasekhar, Hydrodynamic and Hydromagnetic Stability (Clarendon Press, Oxford, to be published).

[4]R. J. Donnelly, Proc. Roy. Soc. (London) A246, 312 (1958).

[5]R. J. Donnelly, Phys. Rev. Letters 3, 507 (1959).

RIGHT-ANGLED SUPEREXCHANGE*

T. N. Casselman
Department of Physics, University of Pittsburgh, Pittsburgh, Pennsylvania

and

F. Keffer†
Department of Physics, University of California, Berkeley, California

(Received April 18, 1960)

The standard model of superexchange[1] involves two paramagnetic cations at opposite ends of an anion dumbbell p_σ orbital, and this is generally believed to account for the next-nearest neighbor (nnn) antiferromagnetic ordering in MnO and similar compounds (ordering of the second kind). On the other hand, the molecular-field theory explanation of the large ratio of Curie-Weiss constant Θ to Néel temperature T_N invokes a relatively large nearest neighbor (nn) antiferromagnetic coupling.[2] We show below that this nn coupling arises because superexchange through the anion p_π orbitals is actually of the same magnitude as that through the p_σ orbital, in striking contradiction to the standard model. The origin of the π-like superexchange is a surprisingly large overlap between p_π anion orbitals and xy-like $3d$ cation orbitals.

According to molecular field theory, for ordering of the second kind,

$$\Theta/T_N = 1 + 2(J_{nn}/J_{nnn}). \quad (1)$$

In the case of MnO, with measured $\Theta/T_N = 5$, this requires the ratio of effective exchange integrals $J_{nn}/J_{nnn} = 2$. Recently Coles et al.[3] reported direct measurements of effective exchange coupling of isolated pairs of Mn^{++} impurity ions in MgO. Their result, $J_{nn}/J_{nnn} \approx 1$, while smaller than the molecular-field theory prediction for pure MnO, gives unambiguous evidence of very large J_{nn}.

We define the following overlap integrals between anion p orbitals centered at the origin and cation $3d$ orbitals centered at the lattice distance a along the x axis:

$$S_\sigma = \int \psi_{3x^2-r^2}(\vec{r} - a\hat{x})\psi_x(\vec{r})d\vec{r}, \quad (2)$$

$$S_\pi = \int \psi_{xy}(\vec{r} - a\hat{x})\psi_y(\vec{r})d\vec{r}. \quad (3)$$

In almost all treatments of superexchange and of related problems such as nuclear resonance shifts and optical spectra, it has been assumed (as seems plausible from crude plots of the orbitals) that S_π may be neglected compared to S_σ.

We have calculated S_π using Hartree-Fock orbitals appropriate to the free ions Mn^{++} and O^{--}. For O^{--} the analytic function of Yamashita and Kojima[4] was expanded about the Mn^{++} origin; for Mn^{++} the tabulated function was used. The result is, for MnO,

$$S_\pi \approx 0.050; \quad (4)$$

this is to be compared to

$$S_\sigma \approx 0.076, \quad (5)$$

which has been evaluated from the same Hartree-Fock radial functions by Kondo.[5]

Detailed analysis[6,7] of the various superexchange mechanisms shows that they all arise in the order S^4, and that this is composed of contributions of order S^2 from each cation-anion overlap in the cation-anion-cation chain. It is reasonable to suppose that these contributions are not only of order S^2 but proportional to S^2. This is because the principal contributions to all transfer and exchange integrals come from regions of large overlap.

For half-filled $3d$ shell the nnn cations along the x axis have the following couplings:

$$(3x^2 - r^2) - x - (3x^2 - r^2)$$

$$xy - y - xy$$

$$xz - z - xz,$$

giving rise to

$$J_{nnn} \sim S_\sigma^4 + 2S_\pi^4. \quad (6)$$

The nn cations in the xy plane have the following couplings through one anion:

$$\begin{array}{ccc} (3x^2 - r^2) & xy & yz \\ | & | & | \\ y - xy & x - (3x^2 - r^2) & z - xz, \end{array}$$

giving rise to

$$J_{nn} \sim 2(S_\pi^4 + 2S_\sigma^2 S_\pi^2). \quad (7)$$

The factor 2 in front takes account of the other anion.

The overlaps (4) and (5) then yield, for MnO,

$$J_{nn}/J_{nnn} \approx 1.5, \quad (8)$$

which is roughly what is required. The fact that the value of Coles et al.[3] is smaller than the result of Eq. (1) applied to pure MnO can possibly be accounted for by the smaller lattice constant of MgO. Two nnn impurity manganese ions will be pushed closer into their oxygen intermediary, increasing J_{nnn}, whereas two nn impurity manganese ions will tend to shove apart their two oxygen intermediaries, decreasing J_{nn}.

Kondo[5] has ascribed nn coupling to direct exchange, and he cites as evidence the values of Θ/T_N in the series MnO, MnS, MnSe, namely 5, 2, and 1.5. The increase of anion size across this series (1.40, 1.84, 1.98 A) causes increased separation of nn manganese and hence leads to decrease of direct exchange. However, the nn separation is already 3.14 A in MnO, and there is no evidence of large antiferromagnetic direct exchange at such distances. The ionic radius Mn^{++} is 0.8 A, and optical experiments on manganese salts indicate that the anions effectively shield the manganese from one another.

We suggest that the decrease of Θ/T_N across the series MnO, MnS, MnSe can be explained as follows. One of the reasons S_σ is not so very much larger than S_π in MnO is that the manganese wave function stretches well across the center of the oxygen, and therefore substantial portions of the integrand of (2) tend to cancel, whereas the integrand of (3) doesn't change sign on the far side of the oxygen nucleus. In the larger anions of MnS and MnSe there will be less cancellation within (2), and therefore we expect S_π/S_σ to decrease across the series.

The ratio Θ/T_N in the series MnO, FeO, CoO, NiO poses a much more complicated problem, involving d orbital occupancy, spin-orbit coupling, lattice distortion, and unreliable measurements of Θ. Kanamori has discussed this problem.[8]

Finally we make some remarks on the F^{19} nuclear resonance experiment of Shulman and Jaccarino[9] in MnF_2. An interpretation[10] of that experiment gave as the theoretical fraction of σ fluorine electrons participating in the hyperfine interaction,

$$f_{p\sigma} \approx (S_\sigma + \lambda_\sigma)^2 \approx (0.06 + 0.04)^2 \approx 0.01, \qquad (9)$$

where λ_σ is the fraction of Mn^+F configuration mixed into the ground state and in which the transfer is that of a p_σ electron. The measured value is

$$f_{p\sigma} - f_{p\pi'} \approx 0.003 \pm 0.003, \qquad (10)$$

where π' is one of the two π-like bonds. We must now not neglect $f_{p\pi'}$ in the calculation. Since $Mn^{++}F^-$ overlaps are very similar to $Mn^{++}O^{--}$ overlaps, we estimate

$$f_{p\pi'} \approx (S_\pi + \lambda_\pi)^2 \approx (0.05 + 0.03)^2 \approx 0.006, \qquad (11)$$

which, combined with (9), now brings theory and experiment into very good agreement. Nonneglect of π-like bonding introduces no purely π-like effects into the interpretation of the experiment since the measured hyperfine coupling constants all appear as $A_{p\pi} - A_{p\pi'}$.

We wish to thank Mr. James J. Pearson for checking the S_π calculation and Dr. Leland C. Allen for a number of stimulating discussions. After we had completed the manuscript we discovered that Dr. Walter Marshall has independently come to the conclusion that strong π-like bonding is responsible for right-angled superexchange.

---

*This work was supported in Pittsburgh by the Air Force Office of Scientific Research of the Air Research and Development Command and in Berkeley by the National Science Foundation.

†On leave from the University of Pittsburgh, Pittsburgh, Pennsylvania.

[1]P. W. Anderson, Phys. Rev. 79, 350 (1950).

[2]P. W. Anderson, Phys. Rev. 79, 705 (1950).

[3]B. A. Coles, J. W. Orton, and J. Owen, Phys. Rev. Letters 4, 116 (1960).

[4]J. Yamashita and M. Kojima, J. Phys. Soc. (Japan) 7, 261 (1952).

[5]J. Kondo, Progr. Theoret. Phys. (Kyoto) 22, 41 (1959).

[6]J. Yamashita and J. Kondo, Phys. Rev. 109, 730 (1958).

[7]F. Keffer and T. Oguchi, Phys. Rev. 115, 1428 (1959).

[8]J. Kanamori, J. Phys. Chem. Solids 10, 87 (1959).

[9]R. G. Shulman and V. Jaccarino, Phys. Rev. 108, 1219 (1957).

[10]F. Keffer, T. Oguchi, W. O'Sullivan, and J. Yamashita, Phys. Rev. 115, 1553 (1959).

INFRARED AND LOW-TEMPERATURE ACOUSTIC ABSORPTION IN SYNTHETIC QUARTZ

J. C. King, D. L. Wood, and D. M. Dodd
Bell Telephone Laboratories, Whippany, New Jersey
(Received April 20, 1960)

The infrared absorption bands in the region extending from 3000 to 4000 cm^{-1} in α quartz have been shown to arise from lattice defects.[1,2] In this part of the infrared, hydrothermally grown synthetic quartz exhibits a relatively strong band at 3620 cm^{-1} which is seen in Fig. 1, Curves A and B.[3] Mitchell and Rigden[2] designate this band by the letter χ and postulate that it is due to OH. The spectrum shown as Curve C of Fig. 1 describes the absorption for a specimen grown on an (0001) seed from D_2O solution. The absence of the absorption maximum at 3620 cm^{-1} in Curve C for the D_2O grown crystal corroborates the suggestion that the χ band relates to OH defects. The presence of the other bands in the D_2O grown crystal supports the contention that these are not due to OH.[4] The OD vibration corresponding to the 3620-cm^{-1} OH band was not observed because it lies among strong lattice overtone bands.

Stevels[5] has recently proposed that a dielectric relaxation loss in synthetic quartz at low temperatures derives from the same defect as the χ-band absorption. The mechanical analog[6] of this particular dielectric loss is identified at 50°K in Fig. 2, Curve A. Here the low-temperature acoustic absorption may be seen for 5-Mc/sec thickness shear resonators. Note that the

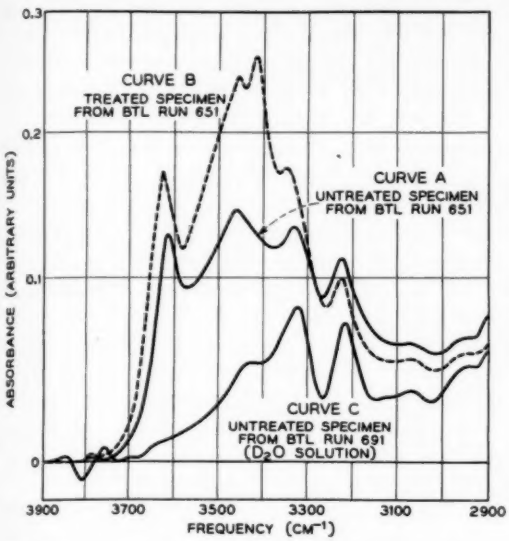

FIG. 1. Infrared absorption in Z-cut samples of synthetic quartz. Curve A is for untreated synthetic quartz. Curve B is for a sample heated in an electric field (1 kv/cm, 500°C, 24 hours). Curve C is for a sample grown from D_2O solution.

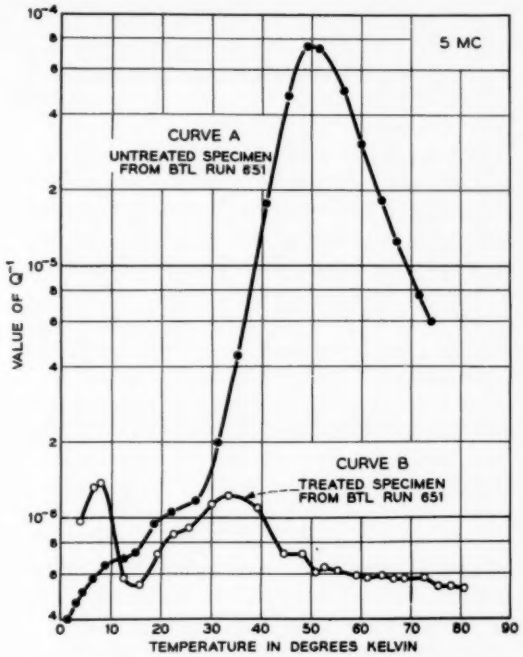

FIG. 2. Low-temperature acoustic absorption in 5-Mc/sec thickness shear synthetic resonators. Specimen used to obtain Curve B was derived from material treated in a field of the order of 1 kv/cm while at 500°C.

curves labeled A in both Fig. 1 and Fig. 2 obtain for specimens of the same synthetic crystal.

Profound changes in the acoustic behavior of synthetic quartz[7] occur when the material is "treated" at elevated temperatures with a static electric field, directed along the optic axis. For instance, the defect responsible for the 50°K absorption is virtually eliminated in a treated resonator, Curve B, Fig. 2. It follows that if the 50°K absorption and χ band are indeed related through a common defect, then the infrared absorption at 3620 cm^{-1} would also suffer changes in treated material. Such, however, is not the case as may be seen in Curve B, Fig. 1. The χ band is obviously impervious to the same treatment which removes the 50°K acoustic absorption.

These experiments permit two conclusions: First, the 3620-cm^{-1} infrared peak is due to OH, while the other peaks in this spectral region are not. Second, the 50°K acoustic absorption is not due to an OH defect.

[1]D. L. Wood, J. Chem. Phys. 27, 1438 (1957).

[2]E. W. J. Mitchell and J. D. Rigden, Phil. Mag. 2, 941 (1957).

[3]All synthetic crystals were kindly supplied by Mr. R. A. Laudise of the Bell Telephone Laboratories. Crystals from runs 651 and 691 were grown on basal-cut seed plates.

[4]D. L. Wood, J. Phys. Chem. Solids (to be published).

[5]J. M. Stevels, Conference on Noncrystalline Solids, Alfred, New York, 1958 (John Wiley & Sons, Inc., New York, to be published).

[6]J. C. King, Bell System Tech. J. 38, 573 (1959).

[7]J. C. King, Proceedings of the Thirteenth Annual Frequency Control Symposium, Asbury Park, 1959 (unpublished).

PARAMAGNETIC RESONANCE DETECTION OF TRAPPING IN A PHOTOCONDUCTOR

Reuben S. Title
International Business Machines Research Laboratory, Poughkeepsie, New York
(Received April 12, 1960)

The trapping of free carriers is necessary to explain many luminescent and photoconductive properties of ZnS-type phosphors. Information concerning the nature of the traps may be inferred from glow curve measurements, from the buildup and decay of photocurrents, from the voltage-current characteristic of the photoconductivity, and from the long-wavelength cutoff of absorptions in the material.

Where the trap is paramagnetic either before and/or after the trapping process, direct observation of the trapping may be made using paramagnetic resonance techniques.[1,2] Such a process has been observed at room temperature in a ZnS sample to which 0.02 molar percent Gd had been added during preparation. The apparatus used has been previously described[2] except that an improved cavity design suggested by Smith was used. The rectangular cavity operating in a TE_{102} mode had at one end a series of copper fins parallel to the narrow face of the waveguide. This enabled light to enter the cavity and irradiate the sample but constituted a set of waveguides beyond cutoff for the microwaves. Its Q was approximately twice that of a cavity using a screen at one end.

It was observed that in the dark there was a small Gd^{3+} electron paramagnetic resonance (EPR) signal. On irradiating the sample with light near 385 mμ, the Gd^{3+} signal increased twelve times in magnitude. Figure 1 gives the wavelength dependence of the Gd^{3+} resonance. If the irradiating light is removed, the Gd^{3+} resonance decreases slowly in magnitude to half value in approximately an hour and to tenth value in a few days. The decrease can be speeded up, that is, the Gd^{3+} resonance quenched by shining on the sample light of various wavelengths. The quenching of the Gd^{3+} resonance as a function of irradiating wavelength is plotted in Fig. 2. There is a broad peak centered around 650 mμ and with a long wavelength cutoff near 900 mμ. Quenching of the resonance was also observed for wavelengths between 280 mμ and 335 mμ.

The luminescent properties of the sample were found to have a correlation with the observed paramagnetic properties. Irradiation with 385 mμ caused it to fluoresce in the green. Removal of the 385 mμ resulted in a green phosphorescence. This phosphorescence could be quenched by irradiating with light between 475 and 900 mμ. This luminescent behavior is similar to that observed by Meijer[3] in ZnS:Cu and the model he proposed for that case can conveniently be applied to ZnS:Gd.

It is proposed that gadolinium is normally present in the lattice as Gd^{2+}. This is reasonable considering the divalent nature of the cation. Irradiation with 385-mμ light causes an electron to be released from the Gd^{2+} site to the conduction band. The electron is eventually trapped at some unknown sites near the conduction band.

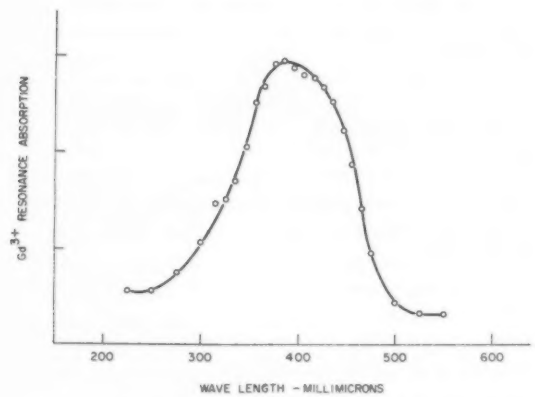

FIG. 1. Dependence of the magnitude of the Gd^{3+} resonance on irradiating wavelength.

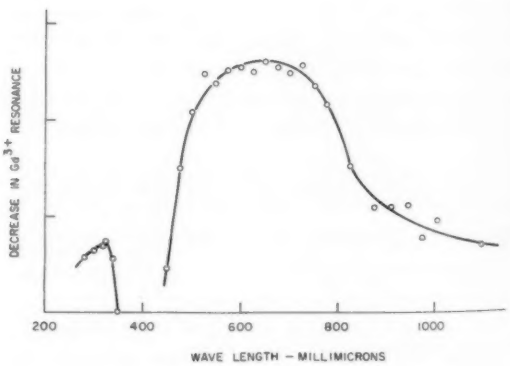

FIG. 2. The quenching of the Gd^{3+} resonance as a function of irradiating wavelength.

This process has the effect of converting Gd^{2+} to Gd^{3+}. The latter has an $^8S_{7/2}$ ground state and its EPR spectrum is easily observed at room temperature. The sites at which the electrons are trapped are sufficiently deep that thermal release of electrons is slow. It is these thermally released electrons recombining at Gd^{3+} sites which results in the green phosphorescence and accounts for the slow decrease in the magnitude of the Gd^{3+} EPR spectrum. The quenching of the Gd^{3+} resonance by radiation between 475 mμ and 900 mμ is caused by excitation of an electron from the valence band to the Gd^{3+} site, reconverting it to Gd^{2+}. This leaves a hole in the valence band which eventually recombines nonradiatively with the electrons in the traps. The quenching of the Gd^{3+} resonance by wavelengths between 280 mμ and 335 mμ is also easily understood. The band gap of ZnS at room temperature is 335 mμ.[4] Shining on light between 280 mμ and 335 mμ causes the formation of electron-hole pairs. Some of the electrons are captured at Gd^{3+} sites, accounting for the quenching of the Gd^{3+} resonance at these wavelengths. The holes recombine with the trapped electrons. Some of the quenching of the Gd^{3+} resonance, particularly at higher wavelengths, may be due to the excitation of electrons from the traps to the conduction band from where they recombine with Gd^{3+} ions. This is, however, believed to be small as no enhancement of the green emission is observed during quenching.

As indicated in the above explanation, associated with the ionization of Gd^{2+} by 385-mμ light, there should be a photocurrent due to the presence of electrons in the conduction band. Photoconductivity manifests itself as a loss in the electric susceptibility. The same apparatus used to measure the EPR spectrum was used to measure the photoconductivity. The sample was moved from maximum magnetic field at the center of the TE_{102} cavity to the position of maximum electric field (either the one-quarter or three-quarter position). The presence of photoconductivity disturbed the balance of the microwave bridge in which the cavity sat. The light producing the photoconductivity was chopped so that ac detection methods could be used. This measurement does not, of course, require the use of a magnetic field. The steady state photoconductivity as a function of wavelength of irradiating light is given in Fig. 3. It is noticed that there is a peak corresponding to the excitation peak of the Gd^{3+} resonance in Fig. 1. In addition, a conductivity due to the presence of holes in the valence band should manifest itself during the quenching of the Gd^{3+} resonance. To observe this, Gd^{3+} sites were created by irradiating the sample with 385-mμ light. Subsequent irradiation with the quenching radiation resulted in a photoconductivity which decreased as the number of Gd^{3+} sites decreased, in agreement with the proposed model.

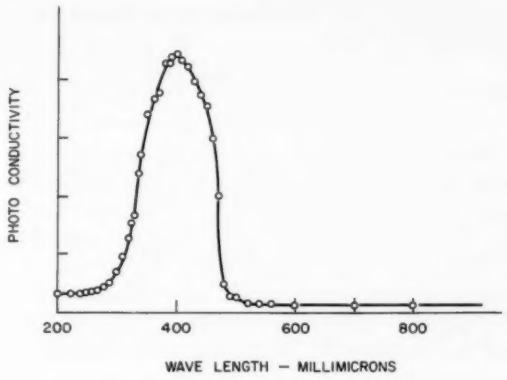

FIG. 3. Photoconductivity of ZnS:Gd as a function of irradiating wavelength.

These measurements represent the first direct observation of trapping in a photoconductor at room temperature. In addition, the technique of observing the trapping by paramagnetic resonance and using the same apparatus to measure the photoconductivity should prove generally useful. The technique has the added merit that the complications of electroding the sample are avoided.

I wish to thank J. A. Kucza for material preparation and S. P. Keller, W. V. Smith, and G. Cheroff for illuminating discussions.

[1]J. Lambe, J. Baker, and C. Kikuchi, Phys. Rev. Letters 3, 270 (1959).
[2]R. S. Title, Phys. Rev. Letters 3, 273 (1959).
[3]G. Meijer, J. Phys. Chem. Solids 7, 153 (1958).
[4]R. H. Bube, Proc. Inst. Radio Engrs. 43, 1836 (1955).

TRANSMITTED PHONON DRAG MEASUREMENTS IN SILICON*

Kurt Hubner† and William Shockley
Shockley Transistor, Unit of Clevite Transistors, Palo Alto, California
(Received April 18, 1960)

Figure 1 illustrates an experimental arrangement used for observing the transmitted phonon drag effect predicted earlier.[1,2] The current in the top n layer between outer current connections produces an input field E_1 measured between the voltage probes. The phonons in the associated phonon drag energy flow[3] move in all directions, and approximately 1/6 of them move towards the p layer. Some of these latter phonons reach the second n layer without scattering to produce a transmitted drag upon the electrons and set up an open-circuit output field E_2 of opposite polarity to E_1. (Since the phonon energy density has no gradient along the specimen, E_2 does not arise from ordinary thermoelectric effects.) The magnitude of the ratio of E_2 to E_1 is[4]

$$|E_2/E_1| = \exp(-W_p/L_p)[1+R_1\exp(-W_1/L_1)] \times [1+R_2\exp(-W_2/L_2)] \times \frac{[1-\exp(-W_1/L_1)][1-\exp(-W_2/L_2)][L_{\phi\phi}/6W_2]}{(1+n_1/n_c)(1+n_\phi/n_1)(1+n_2/n_\phi)}, \quad (1)$$

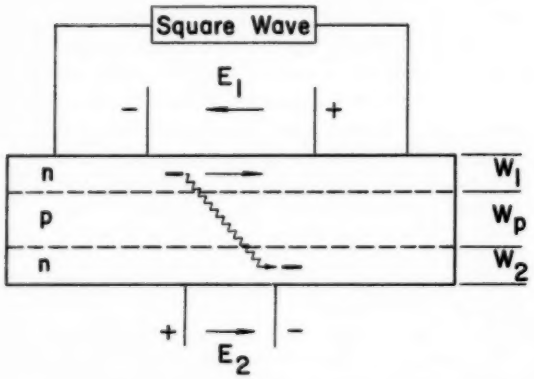

FIG. 1. Experimental arrangement used for measuring phonon drag transmitted from top input n layer of thickness W_1 through p layer of thickness W_p to output n layer of thickness W_2. The dimensions were: sample length 15 mm, width 1 mm, thickness 50 to 200 microns; probe spacings 13 mm for current source, 10 mm for E_1, and 3 mm for E_2.

where W_1, W_p, and W_2 are the thicknesses of the layers; n_1 and n_2 are the electron densities in the two n layers; $L_{\phi\phi}$ is the mean free path for relevant phonons (i.e., those which interact with current carriers) owing to phonon-phonon scattering only; $L_1 = L_{\phi\phi}n_\phi/(n_1+n_\phi)$, $L_p = L_{\phi\phi}p_\phi/(p+p_\phi)$, and $L_2 = L_{\phi\phi}n_\phi/(n_2+n_\phi)$ are for the three layers the mean free paths of relevant phonons including phonon-carrier contributions; p is the hole density; n_ϕ and p_ϕ are reference densities for which interaction with carriers halves the relevant-phonon mean free path; R_1 and R_2 are surface reflection coefficients for phonon momentum; and electron mobility is assumed to vary with n as $n_c/(n+n_c)$, where n_c is independent of n. Equation (1) has the necessary symmetry required by the Onsager relation for a four-pole.[5]

In the experiment, the input voltage was a 340-cps square wave. The distance from current contacts to output voltage contacts is about 20 thermal diffusion lengths in silicon; thus thermoelectric effects owing to heating from contact resistance are eliminated. The observed output wave form was square, with E_2 opposite to E_1, with rise time less than 10^{-4} second, and with output voltage linearly dependent on the input current. The specimen was submerged in liquid nitrogen.

The ratio of E_2/E_1 was measured for eight specimens, differing only in W_p, two each of four thicknesses, and decreased exponentially with W_p, as shown in Fig. 2, in keeping with the term $\exp(-W_p/L_p)$ of Eq. (1) and corresponding to an L_p value of 90 microns, which is consistent with estimates from thermoelectric data.[3] [Actually the simple exponential dependence of Eq. (1) is a result of simplifying assumptions.[1]]

All specimens were of 10-ohm cm boron-doped silicon with $p = 1.4\times10^{15}$ cm^{-3} at room temperature. From the saturation effect of thermoelectric power[3] one finds $p_\phi \approx n_\phi \approx 5\times10^{16}$ cm^{-3}. Since $p \ll p_\phi$, L_p and $L_{\phi\phi}$ are nearly equal. The n-type layers were diffused with junction depths of 15.6 microns and surface concentrations of about 1.3×10^{19} cm^{-3}. Thus L_1 and L_2 are much smaller than W_1 and W_2, so that the factors involving these quantities in Eq. (1) are nearly unity. Taking n_c as 2×10^{15} cm^{-3} from mobility

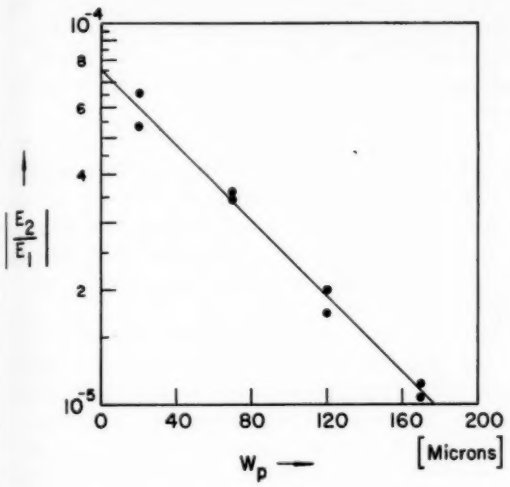

FIG. 2. Dependence of the transmitted phonon drag upon intermediate layer thickness.

data, Eq. (1) yields $n_1 = n_2 \approx 10^{18}$ cm^{-3} as an average effective electron concentration in order to fit the intercept at $W_p = 0$ in Fig. 2, a not unreasonable value since Eq. (1) is based on uniform nondegenerate n layers.

The experiment of Fig. 1 represents only one of a large family of experiments which may be carried out using the transmitted phonon drag effect. For example, by applying very large electric fields in the input layer, it will be possible to produce warm or hot electrons and study the differences in phonon mean free paths as a function of electron temperature. By varying electron concentration in degenerate samples, relevant phonon wave numbers may be varied. By applying stresses so as to alter occupancies of the valleys of the many-valley model, it should be possible to separate phonons produced by electrons having drift velocity in the small mass direction from phonons produced by drift velocity in the large mass direction. By varying the concentration of the carriers in the intermediate p layer, it should be possible to determine phonon-hole scattering cross sections quite directly for the relevant phonons. It may also be possible to study phonon transmission through insulators by applying conducting input and output coatings.

It is a pleasure to acknowledge helpful stimulation and encouragement from Paul Egli, George Busch, and Conyers Herring.

*This investigation has been supported by the Advanced Research Projects Agency, through the Office of Naval Research.

†The experimental part of this investigation was carried out in partial fulfillment of Ph.D. requirements of the Eidgenössische Technische Hochschule, Zurich, Switzerland.

[1]W. Shockley, Structure and Properties of Thin Films, edited by C. A. Neugebauer, J. B. Newkirk, and D. A. Vermilyea (John Wiley & Sons, Inc., New York, 1959), pp. 306-326.

[2]W. Shockley and K. Hubner, Bull. Am. Phys. Soc., 4, 455 (1959).

[3]C. Herring, Semiconductors and Phosphors (Interscience Publishers, Inc., New York, 1958), pp. 184-235.

[4]This equation is obtained by straightforward extensions of the methods of reference 1.

[5]H. B. G. Casimir, Revs. Modern Phys. 17, 343 (1945).

PIEZOELECTRICITY AND CONDUCTIVITY IN ZnO AND CdS

A. R. Hutson
Bell Telephone Laboratories, Murray Hill, New Jersey
(Received April 21, 1960)

Zinc oxide and cadmium sulfide (hexagonal form) have been found to be vigorous piezoelectrics with electromechanical coupling constants which considerably exceed that for quartz. Both ZnO and CdS are well known as extrinsic n-type semiconductors, and in the case of ZnO the single crystals available have almost always possessed room temperature conductivities in excess of 10^{-3} ohm^{-1} cm^{-1}. A conductivity of this magnitude effectively shorts out any macroscopic piezoelectric phenomena.

The present investigation of piezoelectricity in these compounds was undertaken to see if a piezoelectric interaction between conduction electrons and acoustical phonons could explain the large magnitude and the temperature dependence of the phonon-drag effect observed in thermoelectric-power measurements on ZnO.[1] (The

phonon-drag effect is necessarily proportional to the amount of acoustical-mode scattering.) Evidence has been presented in reference 1 and by Collins and Kleinman[2] which indicates that the inertial effective mass is only about $0.07m$ for electrons in ZnO. With this mass, deformation potential scattering could not give a coupling of the required magnitude unless the deformation potential constant were unreasonably large. Measurements of resistivity vs pressure by Hutson et al.[3] have shown that the deformation potential associated with lattice dilatation is not large.

Meijer and Polder[4] and Harrison[5] have developed a theory of piezoelectric scattering mobility for the zinc blende structure using a relaxation-time approximation. Despite differences in averaging procedures both papers derive for the mobility

$$\mu \cong 3000(m/m^*)^{3/2}(300/T)^{1/2},$$

based on a reported value of the piezoelectric constant for zinc blende of $d_{14} = -9.8\times10^{-8}$ statcoulomb/dyne.[6] The temperature dependence of this mobility would correctly predict the temperature dependence of phonon drag in ZnO, but a piezoelectric constant nearly an order of magnitude larger would be required. (Note that the constant obtained for zinc blende by applying pressure in the [111] direction to the ends of a bar is $d_{11}' = d_{14}/\sqrt{3} = 5.7\times10^{-8}$.)

In order to make piezoelectric measurements on ZnO it is necessary to quench the conductivity. This has been accomplished by compensating our n-type crystals with lithium acceptors.[7] This compensation raises the resistivity to the order of 10^{12} ohm cm at room temperature.

We have made the following sorts of piezoelectric measurements on ZnO doped with lithium: (A) Resonance-antiresonance measurements on vapor-phase grown needles, supported by nylon fibers and coupled capacitively at their ends to well-shielded micro-electrodes. (B) Direct squeeze measurements along the c axis (3 direction) of vapor-grown needles where the charge developed upon loading and unloading the crystal was captured on a large air capacitor whose voltage in turn was measured by a vibrating reed electrometer. (C) Resonance-antiresonance measurements on bars, cut from flux-grown platelets,[8] whose major faces had the c axis as their normal. (D) Resonance-antiresonance measurements on very small bars cut so that their length directions made angles of 45° and 20° with the c axis and so that the normals of the major faces were coplanar with the c axis and the length. (The lengths were only 2 to 4 mm and the transverse dimensions not ideally small since these bars had to be cut from a vapor-grown crystal.) The values of the piezoelectric d constants obtained for ZnO from these measurements are given in Table I.

Similar measurements performed on CdS crystals obtained from the Eagle-Picher Co. and annealed in sulfur vapor are reported in the Table.

It is interesting to compare the piezoelectricity in ZnO and CdS with that of quartz. The electromechanical coupling constant for an X-cut quartz plate is $k = 0.095$.[9] The comparable orientation for ZnO and CdS is a plate perpendicular to the c axis vibrating in a thickness longitudinal mode for which

$$k = (d_{33}c_{33}^{E} + 2d_{31}c_{31}^{E})\left(\frac{4\pi}{c_{33}^{D}\epsilon_3^{S}}\right)^{1/2}.$$

Making use of the elastic constants measured for CdS [10] without regard to whether they are at constant E or constant D and scaling them up for ZnO by the factor $s_{33}(\text{CdS})/s_{33}(\text{ZnO})$, and dielectric constants (ϵ) of 8.2 and 9 for ZnO and CdS, respectively, we obtain $k \cong 0.4$ for ZnO and $k \cong 0.2$ for CdS.

We have adapted Meijer and Polder's[4] calculation of piezoelectric scattering to our hexagonal symmetry and find that the electron mobility as limited by piezoelectric scattering alone is, in

Table I. Piezoelectric constants (d) and the elastic modulus s_{33} for ZnO and CdS.

	d_{33}[a]	d_{31}	d_{15}	s_{33}	
	(10^{-7} statcoulomb/dyne)			(10^{-12} cm²/dyne)	
ZnO	+3.6	-1.4	-3 to -4	0.83	
CdS	+3.2	-1.1	-4.3	1.35	1.60[b]

[a]The values of d have an estimated accuracy of about 10% except for d_{15} of ZnO where we would favor the larger of the two values.

[b]The second value of s_{33} for CdS was obtained from extremely weak resonances of c-axis bars and we believe it to be at constant E. Since this second value agrees with the measurement of reference 10, we believe that the conductivity of their CdS was high enough so that their measurements were at constant E.

cm^2/volt sec,

$$\mu \cong 50(m/m^*)^{3/2}(300/T)^{1/2} \text{ in ZnO}$$

and

$$\mu \cong 120(m/m^*)^{3/2}(300/T)^{1/2} \text{ in CdS.}$$

The piezoelectric scattering appears ample for the requirement of large phonon drag with a small effective mass. This calculation and these consequences will be discussed elsewhere.

Electrical conductivity in these piezoelectric materials results in a relaxation-type dispersion for the elastic constant c_{33} and also for c_{44} when propagation is perpendicular to the c axis. A theory of this dispersion has been developed and it successfully predicts the magnitude of the peak as well as the directional dependence of the photosensitive ultrasonic attenuation recently reported by Nine.[11] (K. Dransfeld of these Laboratories has observed that this attenuation does go through a maximum with light intensity.)

It also appears likely that the observations of luminescence occurring when excited (metastable) CdS is given an impact in the c-axis direction[12] have their origin in piezoelectric field ionization of shallow traps.

The author is grateful to W. P. Mason, H. J. McSkimin, and R. N. Thurston for helpful discussions, to R. B. Zetterstrom for sample preparation, and to C. Herring for a critical reading of the manuscript.

[1]A. R. Hutson, J. Phys. Chem. Solids 8, 467 (1959).
[2]R. J. Collins and D. A. Kleinman, J. Phys. Chem. Solids 11, 190 (1959).
[3]A. R. Hutson, W. Paul, W. Howard, and R. B. Zetterstrom, Z. Physik 156, 151 (1960).
[4]H. J. G. Meijer and D. Polder, Physica 19, 255 (1953).
[5]W. A. Harrison, Phys. Rev. 101, 903 (1956).
[6]K. S. Knol, Koninkl. Akad. Wetenschap. Amsterdam 35, 99 (1932).
[7]J. J. Lander (to be published).
[8]J. W. Nielsen and E. F. Dearborn, J. Phys. Chem. (to be published).
[9]W. P. Mason, Piezoelectric Crystals and Their Applications to Ultrasonics (D. Van Nostrand Company, Inc., Princeton, New Jersey, 1950).
[10]D. I. Bolef, N. T. Melamed, and M. Menes, Bull. Am. Phys. Soc. 5, 169 (1960).
[11]H. D. Nine, Phys. Rev. Letters 4, 359 (1960).
[12]C. H. Blakewood, D. M. Warschauer, and D. C. Reynolds, Bull. Am. Phys. Soc. 4, 45 (1959).

PRESSURE DEPENDENCE OF CUBIC CRYSTALLINE FIELD SPLITTINGS OF S-STATE IONS*

Walter M. Walsh, Jr.†
Gordon McKay Laboratory, Harvard University, Cambridge, Massachusetts
(Received April 25, 1960)

The detailed nature of the interaction between paramagnetic ions with half-filled shells (S ground states) and crystalline electric fields has been the subject of considerable discussion. The theoretical analysis of Watanabe[1] in particular has stimulated a good deal of experimental work. Recently Watanabe[2] has reviewed much of the pertinent experimental data and suggested that hydrostatic pressure might be used to clarify the problem. We had arrived at the same conclusion some time ago and had already performed such experiments prior to his suggestion. The majority of the results were presented at the Cambridge Meeting of the American Physical Society.[3] Complete reports on these and related investigations are to be submitted to the Physical Review in the near future. This note will summarize only those details which are pertinent to Watanabe's calculation.

Using apparatus similar to that previously described,[4,5] the paramagnetic resonance (PMR) spectra of Mn^{2+} and Fe^{3+} ($3d^5$, ^6S) present as trace ($\lesssim 0.01\%$) impurities in an MgO crystal have been observed as functions of hydrostatic pressure to 10 000 kg/cm^2 at room temperature. Details of these spectra and their analysis have been given by Low.[6,7] Of present interest is the cubic anisotropy energy represented by the spin-Hamiltonian term $(a/6)(S_x^4+S_y^4+S_z^4)$. The pressure-induced variations of the a parameters of both ions are shown in Fig. 1. Within experimental error the ratio $a_{Fe}/a_{Mn} = 10.70 \pm 0.02$ is independent of pressure. The fractional variation of a per kg/cm^2 is

$$(\partial \ln a/\partial P)_T = 4.03 \times 10^{-6} \text{ (kg/cm}^2)^{-1}. \quad (1)$$

In comparing this result with microscopic

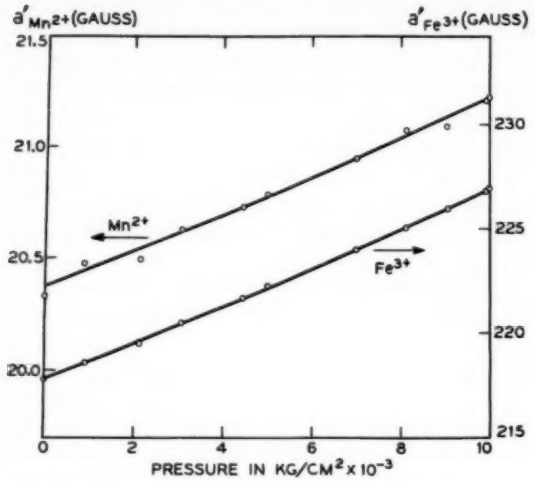

FIG. 1. Pressure dependence of the cubic field splitting parameters of Mn^{2+} and Fe^{3+} in MgO at room temperature. The units are "electron gauss": $a' \equiv a/g\beta$. (The g values are independent of pressure to at least 1 part in 10^5.)

crystalline field theory two principal assumptions are made: (I) The local compressibility in the immediate vicinity of the magnetic impurity is essentially unchanged from that of the undisturbed host lattice. (II) The effective electrostatic potential seen by the magnetic cation may be computed from a simple ionic model. The observed equality of $\partial \ln a/\partial P$ for both a doubly and a triply charged ion in the same lattice supports (I). Further confirmation of both (I) and (II) has been obtained from the pressure dependences of the g values of Cr^{3+} and Ni^{2+} in MgO.[8]

The volume dependence of a is computed using Bridgman's value[9] for the bulk compressibility of crystalline MgO:

$$(\partial \ln a/\partial \ln V)_T = -7.08 \quad (Mn^{2+} \text{ and } Fe^{3+} \text{ in MgO}). \quad (2)$$

According to Watanabe[1,2] the parameter a should be closely proportional to the square of the strength of the cubic potential. In the limit of zero overlap, such a potential varies as interionic distance to the inverse fifth power or $V^{-5/3}$, which means

$$(\partial \ln a/\partial \ln V)_T = -3.33 \quad \text{(theory)}. \quad (3)$$

While a number of cavils may be raised regarding the accuracy of Eq. (3) in the case of real complexes, our data on the better understood F-state ions indicate that for MgO Eq. (3) is valid to within ±20% at least. The disagreement between Eqs. (2) and (3) greatly exceeds such a margin and suggests that the cubic field splittings are more nearly proportional to the fourth power of the cubic potential in this lattice. Though consistent with Watanabe's conclusion that even powers of the cubic potential are dominant in determining a, this result conflicts with his numerical estimates for Mn^{2+} which indicate that any fourth power contribution is negative and much weaker than the positive second power term.

The pressure variation of a for Mn^{2+} in cubic ZnS has also been measured. Analysis similar to that described above leads to the volume dependence of the cubic field splitting,

$$(\partial \ln a/\partial \ln V)_T = -3.2 \quad (Mn^{2+} \text{ in ZnS}). \quad (4)$$

This apparently second-power-of-the-potential variation cannot safely be considered to support Watanabe's theory since the ionic model is not even approximately adequate in this case.[10] Failure of the simple model in tetrahedral coordination has been most clearly demonstrated by observations of a for Mn^{2+} in CdTe.[11] This splitting proves to be almost four times larger than for ZnS:Mn^{2+} whereas Watanabe's calculations lead to a value more than five times smaller.

A further indication that our understanding of crystalline field effects on the S-state ions is still quite incomplete has come to light in studying the temperature dependences of a for Mn^{2+} and Fe^{3+} in MgO. It is found that the effect can be accurately accounted for simply on the basis of Eq. (2) and the thermal expansion coefficient of the host lattice, i.e., there is no measurable explicit effect of lattice vibrations at constant crystal volume. This can be shown to imply an anomalous frequency dependence of the cubic field splitting[12] which is inconsistent with existing theory.

The constant support and encouragement of Professor N. Bloembergen is gratefully acknowledged as are numerous stimulating conversations with Dr. Jean Jeener and other associates. The MgO crystals used in these experiments were provided by the Norton Company. Professor C. Kikuchi of the University of Michigan kindly made available a natural zincblende crystal.

*This work was supported by the Joint Services.

†Now at Bell Telephone Laboratories, Murray Hill, New Jersey.

[1]H. Watanabe, Progr. Theoret. Phys. (Kyoto) 18, 405 (1957).
[2]H. Watanabe, Phys. Rev. Letters 4, 410 (1960).
[3]W. M. Walsh, Jr., Bull. Am. Phys. Soc. 4, 142 (1959).
[4]W. M. Walsh, Jr. and N. Bloembergen, Phys. Rev. 107, 904 (1957).
[5]W. M. Walsh, Jr., Phys. Rev. 114, 1473 (1959).
[6]W. Low, Proc. Phys. Soc. (London) B69, 1169 (1956).
[7]W. Low, Phys. Rev. 105, 793 (1957).
[8]W. M. Walsh, Jr. (unpublished).
[9]P. W. Bridgman, Proc. Am. Acad. Arts Sci. 67, 345 (1932).
[10]J. Baker, B. Bleaney, and W. Hayes, Proc. Roy. Soc. (London) A247, 141 (1958).
[11]J. Lambe and C. Kikuchi, Bull. Am. Phys. Soc. 5, 158 (1960).
[12]W. M. Walsh, Jr., J. Jeener, and N. Bloembergen (unpublished).

EVIDENCE FOR AN ANTIFERROMAGNETIC-FERRIMAGNETIC TRANSITION IN Cr-MODIFIED Mn_2Sb

T. J. Swoboda, W. H. Cloud, T. A. Bither, M. S. Sadler, and H. S. Jarrett
Central Research Department, E. I. du Pont de Nemours and Company, Wilmington, Delaware
(Received April 4, 1960)

We wish to report an unusual magnetization behavior found in the compound $Mn_{2-x}Cr_xSb_{1-y}In_y$, where $0.025 \leq x \leq 0.20$ and $0 \leq y \leq 0.05$. With decreasing temperature, the saturation magnetization undergoes a transition within about a 10° interval from a strongly ferrimagnetic state (σ = 20 to 30 gauss-cm³/g) to a weakly magnetic state ($\sigma \simeq 1$ gauss-cm³/g). This transition, which occurs in the temperature range 120 to 385°K depending on the amount of chromium present, is not accompanied by a change in crystal structure. At high temperatures, the magnetic properties of these compounds are similar to those of the parent compound Mn_2Sb,[1] but the saturation magnetization is too low to be accounted for entirely by the amount of chromium and indium present. As the temperature is lowered, transition to the weakly magnetic state takes place. This behavior is illustrated in Fig. 1, where the saturation magnetization is plotted as a function of temperature for two compounds, $Mn_{1.87}Cr_{0.13}Sb_{0.95}In_{0.05}$ and $Mn_{1.95}Cr_{0.05}Sb_{0.95}In_{0.05}$. The saturation magnetization for Mn_2Sb is included for comparison.

Below the transition temperature T_S, the materials exhibit an average saturation magnetization of 1 gauss-cm³/g. Metallurgical studies have shown, however, that there is a tendency toward nonstoichiometry on the manganese-deficient side resulting in precipitation of a small amount of MnSb. If the modified Mn_2Sb is formed with excess manganese, the residual magnetization is reduced but not eliminated completely. We attribute this residual magnetization to ferromagnetic MnSb precipitate. It appears then that the compound of interest may have no net magnetic moment below the transition temperature. The indium present in these compositions has but little effect on their magnetic properties and can in fact be eliminated without loss of the magnetic transition. However, in the absence of indium during the synthesis, it becomes even more difficult to avoid precipitation of MnSb.

The composition region in which ferrimagnetism occurs is designated by the cross-hatched area in Fig. 2. This area is bounded at high temperature by the normal Curie temperature and at low temperature by the transition at T_S. It is to be

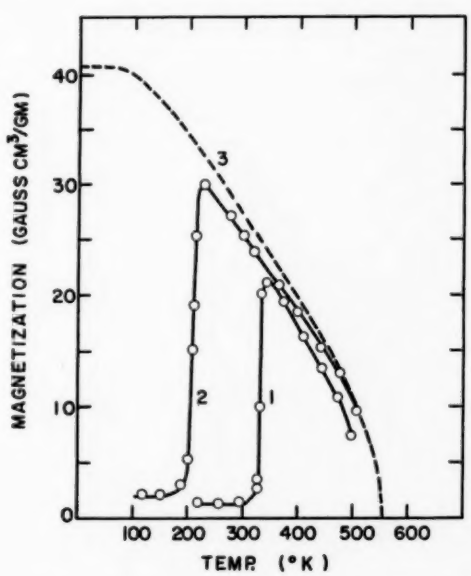

FIG. 1. Saturation magnetization of $Mn_{2-x}Cr_xSb_{1-y}In_y$. Curve 1, $x = 0.13$, $y = 0.05$; curve 2, $x = 0.05$, $y = 0.05$; curve 3, Mn_2Sb ($x = 0$, $y = 0$).

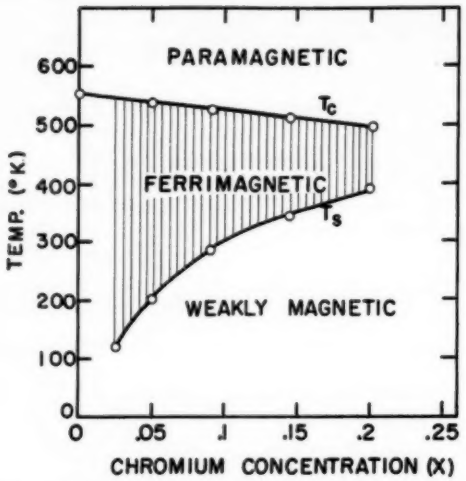

FIG. 2. Exchange inversion temperature T_S and Curie temperature T_C of $Mn_{2-x}Cr_xSb_{1-y}In_y$ as a function of x. Cross-hatched area defines temperature region in which compound is ferrimagnetic.

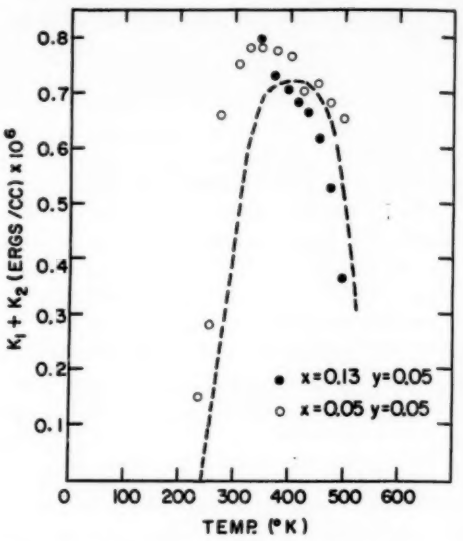

FIG. 3. The anisotropy constant, K_1+K_2, of $Mn_{2-x}Cr_xSb_{1-y}In_y$ for two different amounts of Cr. The dashed curve represents the anisotropy of Mn_2Sb.

noted that the Curie temperature decreases slightly with the addition of chromium, but this decrease is small compared to the strong dependence of T_S on x.

Measurement of the magnetization curves with fields applied parallel and perpendicular to the tetragonal axis of a crystal shows that the compounds have a uniaxial magnetocrystalline anisotropy similar to that observed in Mn_2Sb. The anisotropy constant K, representing the difference in energy required to magnetize parallel and perpendicular to the tetragonal axis, is shown in Fig. 3. This anisotropy can only be measured in the ferrimagnetic region, but in three examples with different chromium content, $x = 0.13$, $x = 0.05$, and $x = 0$, K is virtually the same.

The crystal structure of these compounds is identical to that of Mn_2Sb [2] (P^4/nmm) throughout the entire temperature range. X-ray studies of a single crystal with $x = 0.12$ and $y = 0.05$ show that the c axis of the unit cell contracts from 6.530 A to 6.516 A and that the a axes expand from 4.0875 A to 4.0882 A as the material is cooled through its magnetic transition at 50°C. This contraction leads to a net decrease in volume of approximately 0.18%. At the lowest temperature for which this compound remains ferrimagnetic, the c/a ratio is 1.598 compared to 1.608 for Mn_2Sb. The x-ray density, 7.04 g/cm^3, is slightly greater than that of Mn_2Sb, 7.02. Figure 4 shows the behavior of the c-axis lattice

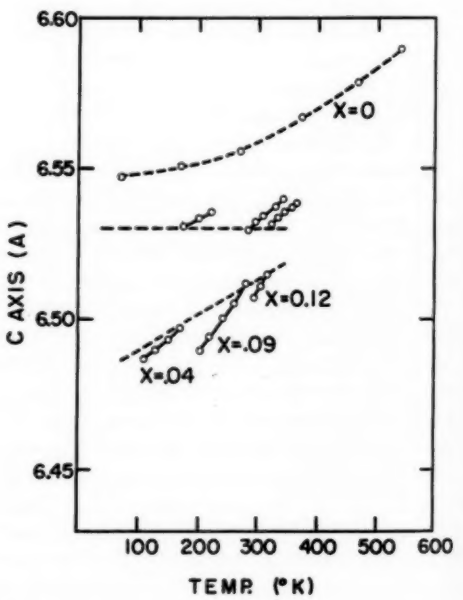

FIG. 4. c-axis dimension of $Mn_{2-x}Cr_xSb_{1-y}In_y$ as a function of temperature for various values of x and for Mn_2Sb ($x = 0$).

constant for several values of x. In all cases, the compounds transform to the weakly magnetic state for the same critical value of lattice constant.

Since it is unlikely that a transition from an ordered to a random state would occur with decreasing temperature, we propose that the low-temperature region possesses antiferromagnetic ordering rather than being paramagnetic. Preliminary results from neutron diffraction, obtained in cooperation with Battelle Memorial Institute, support this conclusion, and detailed results will be reported soon.

To account for the transition, we suggest that at least one of the exchange interactions changes sign near the critical dimension 6.53 A. Such a change in sign might occur because of possible opposing effects of certain superexchange and indirect exchange[3] interactions. It is not necessary to assume that a large change in either interaction must accompany the magnetic transition but only that their relative contribution is altered by the contraction of the crystal near the critical c-axis dimension. We propose to designate this temperature as the "exchange inversion temperature."

The authors wish to thank Dr. J. J. Cox of the Engineering Research Laboratory for the results from his metallurgical studies and Dr. F. J. Darnell for the data on the anisotropy of Mn_2Sb reported here. Mr. Keith Babcock performed the x-ray measurements on the unit-cell dimensions.

[1]Charles Guillaud, thesis, University of Strasbourg, 1943 (unpublished).

[2]L. Heaton and N. S. Gingrich, Acta. Cryst. 8, 205 (1955).

[3]M. A. Ruderman and C. Kittel, Phys. Rev. 96, 99 (1954).

[111] DIRECT TRANSITION EXCITON AND MAGNETOREFLECTION IN GERMANIUM

Benjamin Lax

Lincoln Laboratory,* Massachusetts Institute of Technology, Lexington, Massachusetts

(Received April 14, 1960)

From theoretical considerations of the g factor of electrons in germanium[1,2] and infrared[3] and microwave[4] experiments, it was deduced that a direct transition at an energy of ~2 ev[5] exists between the L_3' and L_1 bands at the edge of the Brillouin zone along the [111] direction. (See Fig. 1.) This suggests the possibility of carrying out reflection experiments at liquid helium temperatures with magnetic fields and high-resolution grating spectrometers that could provide information about the L_3' valence band. Under these experimental conditions it would be possible to observe a third exciton in germanium consisting of the [111] electron and a [111] hole. In addition the magneto-reflection would permit the observation of the fine structure of the Zeeman effect of this [111] exciton and also the direct transition between Landau levels of the L_3' valence and L_1 conduction bands along two sets of principal crystal directions. The information to be obtained by these experiments consists of the effective-mass parameters of the L_3' holes, the g factor of both electrons and holes and their anisotropies, an accurate determination of the energy gap between the two bands, and a measurement of the binding energy of the exciton. The purpose of this Letter is to predict theoretically some of these quantities and to specify those pertinent aspects of the experiments required for obtaining the desired information.

If second order perturbation theory using the $\vec{k}\cdot\vec{p}$ technique is applied to the L_1 conduction band, it can be shown that the matrix elements between this and the L_3' band are essentially those that

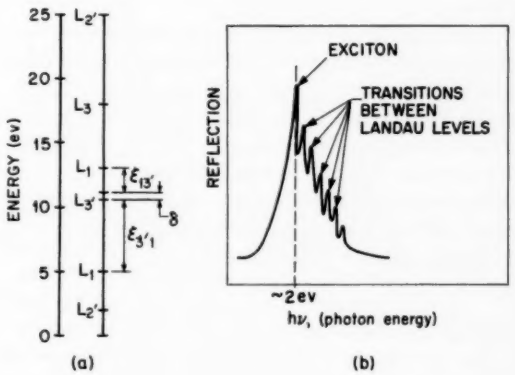

FIG. 1. (a) Approximate energy positions of band edges at the [111] zone edge in germanium. $\delta \approx 0.2$ ev is the spin-orbit splitting of the L_3' band. (b) Sketch of expected [111] magnetoreflection spectrum. Fine structure is not indicated.

give rise to the transverse electron mass in germanium,[6] namely:

$$\alpha_t = \frac{m_0}{m_{t1}} \approx 1 + \frac{2M_{13'}^2}{m_0 \mathcal{E}_{13'}} = 12, \qquad (1)$$

where $M_{13'} = |(L_1|p_x|L_{3'})|$.

Since $L_{3'}$ is split by a spin-orbit coupling by ~0.2 ev, we need only consider just one half the interaction above, i.e., $M_{13'}^2/\mathcal{E}_{13'}$. However, in addition there are matrix elements of comparable magnitude between the $L_{3'}$ and L_3 bands and also between the $L_{3'}$ and lower L_1 valence bands. These make a smaller contribution since they are approximately 6 ev away. Using these results, one finds that the transverse effective mass of the $L_{3'}$ hole is given by

$$\beta_t = \frac{m_0}{m_{t3'}} \approx 1 - \frac{M_{13'}^2}{m_0 \mathcal{E}_{13'}} + \frac{M_{3'1}^2}{m_0 \mathcal{E}_{3'1}} - \frac{2M_{33'}^2}{m_0 \mathcal{E}_{33'}} \approx -6.3, \qquad (2)$$

where $M_{3'1}$ is the matrix to the lower L_1 band. It is assumed that the matrix elements $M_{13'}$, $M_{3'1}$, and $M_{33'}$ are of the same order of magnitude and that $\mathcal{E}_{13'} \approx 2$ ev, $\mathcal{E}_{3'1} \approx \mathcal{E}_{33'} \approx 6$ ev.

The longitudinal mass is obtained by taking the matrix elements for the coordinate along the [111] direction. From symmetry considerations, no matrix elements exist between the $L_{3'}$ and L_1 bands but the most important one is between the L_3 and $L_{3'}$ bands. The result is

$$\beta_l = \frac{m_0}{m_{l3'}} \approx 1 - \frac{2M_{33'}^2}{m_0 \mathcal{E}_{33'}} \approx -2.6, \qquad (3)$$

where $M_{33'} = |(L_3|p_z|L_{3'})|$.

From these estimates it appears that the holes of the $L_{3'}$ band move on ellipsoids of revolution with masses $m_t \approx 0.16 m_0$ and $m_l \approx 0.4 m_0$. With these values and those obtained from cyclotron resonance for electrons, the binding energy of the exciton can be readily estimated. From the effective-mass Schrödinger equation for the exciton moving on spheroidal energy surfaces, the reduced effective masses become

$$\frac{1}{\mu_t} = \frac{1}{m_{t1}} + \frac{1}{m_{t3'}} \approx 18,$$

$$\frac{1}{\mu_l} = \frac{1}{m_{l1}} + \frac{1}{m_{l3'}} \approx 3.2. \qquad (4)$$

From a variational calculation of the binding energy for an ellipsoidal hydrogenic structure from Lampert's curves[7] for the above values and a value of the dielectric constant $K = 16$, we obtain that this becomes $\mathcal{E}_{ex} \approx 0.0048$ ev. This value is larger than that of the direct exciton[8] ($\mathcal{E}_{ex} \approx 0.0015$ ev) or that of the indirect exciton[8] ($\mathcal{E}_{ex} \approx 0.0025$ ev).

The magnetoreflection spectrum can most distinctly be observed with the magnetic field parallel to a [111] direction or perpendicular to it, i.e., a [110] direction. For other directions no selection rules for Δn, the magnetic quantum number, exist since the magnetic field is not along a principal axis of an ellipsoid.[9] Hence along the [111] axis for a magnetic field of approximately 40 000 gauss, the interband transition between two sets of Landau levels of the same quantum number n for one of the four ellipsoids of each band will give an energy separation $\Delta\mathcal{E}_t = \hbar\omega_t$, where $\omega_t = eH/\mu_t c$. The value of $\Delta\mathcal{E}_t \approx 0.007$ ev. For the [110] direction $\Delta\mathcal{E} = \hbar\omega_c$, $\omega_c = eH/\mu_{lt}c$, where $\mu_{lt} = (\mu_\Delta \mu_t)^{1/2} = 0.13 m_0$ or $\Delta\mathcal{E} \approx 0.003$ ev. This time two sets of ellipsoids of each band will contribute to the magnetoreflection. There should be fine structure associated with the splitting of the lines due to spin for the magnetic field along the [111] direction with a separation $\Delta\mathcal{E}_m = g_\parallel \beta H$, where $g_\parallel$ is a combination of two g factors of the L_1 and $L_{3'}$ bands. Similarly for the [110] direction $\Delta\mathcal{E}_s = g_\perp \beta H$. These separations, which are of the order of 10^{-4} - 10^{-3} ev, should be resolvable with good accuracy spectroscopically. From the known g values of the L_1 band obtained from spin resonance,[1,4] those of the $L_{3'}$ band can be readily deduced.

The line shape of the magnetoreflection spectrum can be theoretically approximated by the following expressions for the change in reflection coefficient if we assume that the magnetic effects are a small perturbation on the zero-field background of the [111] direct transition:

$$\Delta R \approx 4 \frac{[(n_0^2 - 1) - k_0^2]\Delta n + 2n_0 k_0 \Delta k}{[(n_0+1)^2 + k_0^2]^2}. \qquad (5)$$

For germanium the index of refraction and the extinction coefficient are $n_0 \approx 5$ and $k_0 \approx 2$ so that to a reasonable approximation,

$$\Delta R \sim (\Delta n + \Delta k) = (n_0 - k_0)\sigma_i + (n_0 + k_0)\sigma_r, \qquad (6)$$

where[10]

$$\sigma_r \sim \left[\frac{(x_n^2+1)^{1/2} + x_n}{2(x_n^2+1)}\right]^{1/2}, \quad \sigma_i \sim \left[\frac{(x_n^2+1)^{1/2} - x_n}{2(x_n^2+1)}\right]^{1/2}, \qquad (7)$$

and $x_n = (\omega - \omega_n)$ and $\hbar\omega_n = \mathcal{E}_g + (n + \frac{1}{2})\hbar(\omega_{c1} + \omega_{c3'})$.

The line shape therefore should consist of maxima corresponding to the transitions between Landau levels. The exciton line shape is also similar and is hence favorable for accurate determination of the various parameters. The exciton Zeeman pattern should give discrete resolvable lines for all crystal directions and allow the measurement of the anisotropic g factors. This pattern in the [110] plane will have three branches due to the spin alone.

The above transition should be extremely attractive for use in an optically excited cyclotron resonance maser since the fundamental excitation is in a very desirable range of the optical spectrum where pulsed line sources of the order of several watts or more are possible. Furthermore, this transition fulfills the necessary requirements for such a maser.[11] The direct transition permits selective excitation to discrete magnetic levels deep into the bands allowing population inversion of holes or electrons relative to Landau levels of lower quantum number. Due to the interaction of the spin-orbit split L_3, valence bands, these should have large change of curvature. This will permit unequally spaced magnetic levels so that selective transitions downward in energy between only two unique levels can be chosen by the resonant radiation in an interferometer tuned to this frequency. Thus the induced electric dipole cyclotron resonance transition will be emissive. From the values estimated in this paper for H along a [111] direction, with fields of the order of 4×10^4 gauss or larger which are available and desired for the interband transitions, the maser should be operable in the submillimeter or far infrared region at approximately 600 microns.

The author is grateful to Dr. Laura Roth for several suggestions and for checking the estimates of the effective-mass values. He has also benefitted from discussions with Professor G. F. Koster, Dr. H. J. Zeiger, and Dr. S. Zwerdling.

*Operated with support from the U. S. Army, Navy, and Air Force.

[1]L. M. Roth and B. Lax, Phys. Rev. Letters 3, 217 (1959).

[2]J. C. Phillips, J. Phys. Chem. Solids 12, 208 (1960)

[3]K. J. Button, L. M. Roth, W. H. Kleiner, S. Zwerdling, and B. Lax, Phys. Rev. Letters 2, 161 (1959).

[4]G. Feher, D. K. Wilson, and E. A. Gere, Phys. Rev. Letters 3, 25 (1959).

[5]H. R. Philipp and E. A. Taft, Phys. Rev. 113, 1002 (1959).

[6]L. M. Roth (to be published).

[7]M. Lampert, Phys. Rev. 97, 352 (1955).

[8]S. Zwerdling, B. Lax, L. M. Roth, and K. J. Button, Phys. Rev. 114, 80 (1959).

[9]R. J. Elliott, J. P. McLean, and G. G. Macfarlane, Proc. Phys. Soc. (London) 72, 553 (1958).

[10]L. M. Roth, B. Lax, and S. Zwerdling, Phys. Rev. 114, 90 (1959); B. Lax and S. Zwerdling, Progress in Semiconductors (to be published).

[11]B. Lax, Conference on Quantum Electronics-Resonance Phenomena (Columbia University Press, New York, 1960).

DIRECTION OF THE EFFECTIVE MAGNETIC FIELD AT THE NUCLEUS IN FERROMAGNETIC IRON†

S. S. Hanna, J. Heberle, G. J. Perlow, R. S. Preston, and D. H. Vincent
Argonne National Laboratory, Argonne, Illinois
(Received April 28, 1960)

In a recent experiment[1] it was shown that in ferromagnetic iron the effective magnetic field at the iron nucleus is strongly correlated with the magnetization. The sense of the correlation, however, was not determined, i.e., it was not known whether the effective field was parallel or antiparallel to the magnetization. The sense of the correlation has now been established by observing the change in the hyperfine splitting of the nuclear energy levels of Fe^{57} on application of an external field of 17 to 20 koe.

In an earlier paper[2] we presented the hyperfine spectrum obtained in the resonant Mössbauer[3] absorption in Fe^{57}. The interpretation given to the spectrum has since been confirmed in detail. Several groups have shown the correctness of the hyperfine pattern by observing the spectrum when different alloys and compounds of iron are used.[4] Gossard, Portis, and Sandle[5] have observed the nuclear magnetic resonance in the ground state of Fe^{57} at a frequency corresponding to a value of the effective field in close agreement with the value of 333 koe deduced in reference 2. In addition, Ewan, Graham, and Geiger[6] have

found that the $E2$ admixture in the $M1$ radiation is less than 10^{-4}, which confirms that the effect of $E2$ radiation in the spectrum is indeed negligible.[3]

Experimentally it was feasible to apply a large magnetic field only to the source of the resonant radiation. The absorber was either in the fringing field of the electromagnet holding the source or in a small parallel magnetic field of its own, applied to produce a definite magnetization in the absorber. At the top of Fig. 1 is shown the velocity spectrum which is applicable if the hyperfine splittings in source and absorber are identical. The intensities are appropriate to the emission of polarized radiation from the source but to an unpolarized absorption process. If, on the other hand, the hyperfine splittings in the emitter are about 10% greater (for example) than those in the absorber, then the complex spectrum at the bottom of Fig. 1 is obtained. It is clear that a study of the singlet line 6 affords the best means of determining the change that an external field produces in the hyperfine splitting.

For the effective field at the nucleus we write

$$\vec{H}_n = H_{n0}\vec{M}_0 + \vec{H}_{ext}, \qquad (1)$$

where $\vec{M}_0$ is a unit vector along the direction of magnetization in a ferromagnetic domain, and H_{n0} is the magnitude of the effective field in the absence of the external field $\vec{H}_{ext}$. The latter quantity includes the demagnetizing field which is negligible for the planar samples used. Since $H_{ext}/H_{n0} \ll 1$ in the present experiment, it is assumed in Eq. (1) that H_{n0} is not appreciably influenced by $\vec{H}_{ext}$. The quantity of interest is the sign of H_{n0}. Since $\vec{M}_0$ and $\vec{H}_{ext}$ are parallel under saturation conditions, the sign can be determined by observing whether the hyperfine splitting increases or decreases on application of a field. With a field of 17.6 koe a shift of $\pm 2.65\%$ is expected in line 6.

The experimental technique was similar to that in our earlier work.[1,2,7] The carriage of a lathe was used to provide velocities by means of which the spectrum was scanned. The source was mounted in the narrow gap of an electromagnet capable of producing fields up to 20 koe. The magnet was attached rigidly to the end of the lathe and the absorber was mounted on the carriage. The result obtained for line 6 is shown in Fig. 2. On application of the field to the source, a shift to lower energy is unmistakable. The correlation

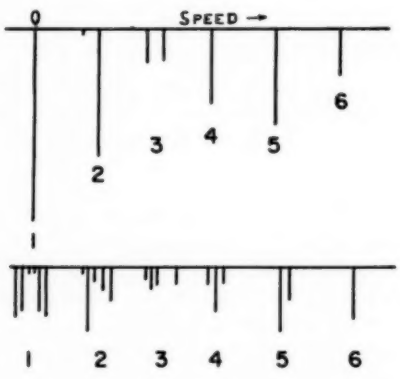

FIG. 1. Theoretical absorption spectra of 14.4-kev resonance radiation from Fe^{57}. Top: metallic source and absorber with identical hyperfine splittings. Bottom: same source and absorber but with the splitting in the source increased by 10%.

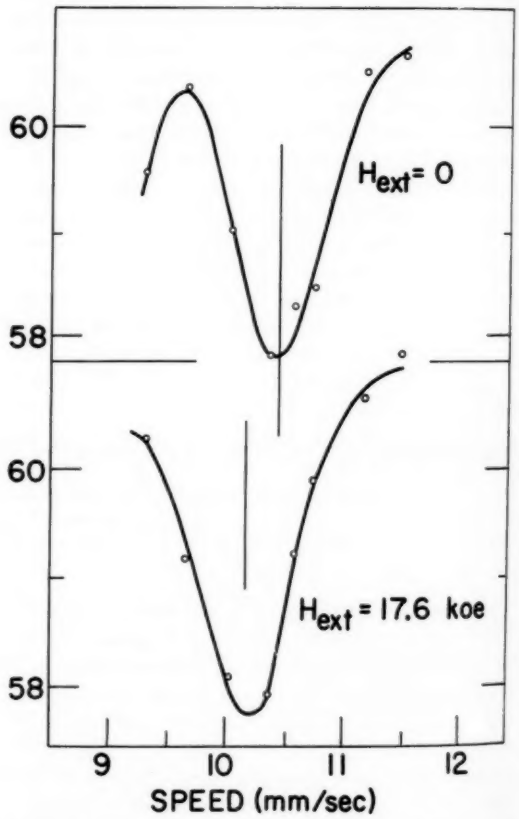

FIG. 2. Line 6 observed with $H_{ext} = 0$ and $H_{ext} = 17.6$ koe, where H_{ext} is the external field applied to the source of resonance radiation. The ordinate is in units of 10^3 counts.

is therefore negative. The magnitude of the observed shift is $(2.7 \pm 0.4)\%$ which is compatible with the linear relation $H_n = H_{n0} - H_{ext}$. A negative shift of about the correct magnitude was also observed in line 4. The multiplet structure in line 4 is symmetrical (Fig. 1) and so does not seriously interfere with the observation of a shift of its central member.

The effective field at the iron nucleus has now been determined both in sign and magnitude. The existence of such a large negative field (-333 koe) was unexpected. Marshall[8] has discussed a number of sources of the effective nuclear field. These consist mainly of direct effects of the $3d$ electrons and indirect effects of polarization of the various s electrons, which then contribute to the field via the Fermi contact interaction. The polarization of inner shells of electrons results in negative contributions to the field. In view of the experimental result these negative terms must completely dominate the other contributions.

We are grateful to S. Raboy for loan of the magnet. We wish also to thank M. R. Perlow for preparation of the source; F. J. Karasek for continuing to supply us with thin rolled iron foils; and E. Kowalski for assistance in taking the data. We have profited from a stimulating discussion with W. Marshall.

---

†This work was performed under the auspices of the U. S. Atomic Energy Commission.

[1]G. J. Perlow, S. S. Hanna, M. Hamermesh, C. Littlejohn, D. H. Vincent, R. S. Preston, and J. Heberle, Phys. Rev. Letters 4, 74 (1960).

[2]S. S. Hanna, J. Heberle, C. Littlejohn, G. J. Perlow, R. S. Preston, and D. H. Vincent, Phys. Rev. Letters 4, 177 (1960).

[3]R. L. Mössbauer, Z. Physik 151, 124 (1958).

[4](Ferrocyanide) S. L. Ruby, L. M. Epstein, and K. H. Sun (to be published); (ferrocyanide, stainless steel) G. K. Wertheim, Phys. Rev. Letters 4, 403 (1960); (Fe_2O_3) O. C. Kistner and A. W. Sunyar, Phys. Rev. Letters 4, 412 (1960).

[5]A. C. Gossard, A. M. Portis, and W. J. Sandle (to be published).

[6]G. T. Ewan, R. L. Graham, and J. S. Geiger (to be published).

[7]S. S. Hanna, J. Heberle, C. Littlejohn, G. J. Perlow, R. S. Preston, and D. H. Vincent, Phys. Rev. Letters 4, 28 (1960).

[8]W. Marshall, Phys. Rev. 110, 1280 (1958), and private communication.

RESONANCES IN C^{12} ON CARBON REACTIONS

E. Almqvist, D. A. Bromley, and J. A. Kuehner
Atomic Energy of Canada Limited, Chalk River Laboratories, Chalk River, Ontario, Canada
(Received March 28, 1960)

The reaction yield from C^{12} on carbon in the laboratory energy range 9-29 Mev has been investigated using C^{12} beams of precisely defined energy from the Chalk River tandem accelerator. The measured excitation curves for all reaction products studied reveal unexpected, sharp, isolated resonances at incident energies just below the Coulomb barrier corresponding to excitations in $Mg^{24} \approx 20$ Mev. At higher energies where strong interference structure was previously observed in the elastic scattering,[1] the reaction resonance structure is considerably less marked. In contrast to these results for the $C^{12} + C$ system, similar measurements for O^{16} ions on oxygen targets show no such resonant behavior; in this case the incident energy required to reach the top of the Coulomb barrier is somewhat higher and corresponds to 27-Mev excitation in S^{32}. It is noted that both reactions are restricted to only those states allowed to a system of two identical spin-zero Bosons.

The various excitation curves for C^{12} on carbon in Fig. 1 show marked similarity; particularly for incident energies below 6.5 Mev (center-of-mass system), sharp resonances appear in all curves at energies of 5.68 Mev, 6.00 Mev, and 6.32 Mev. The observed widths of these peaks are equal to the energy loss in the 40-$\mu g/cm^2$ carbon targets. This amounts to 100 kev in the c.m. system; consequently, in each case the true resonance width is almost certainly less than this. Additional measurements not shown in the figures on alpha particles detected[2] at 27° and 62° and protons detected[2] at 62° in the laboratory and on all gamma radiation of energy greater than 2.8 Mev also show these same sharp resonances below the Coulomb barrier. The fact that these resonance peaks appear at the identical incident energies for all reaction products independently of the angle of observation

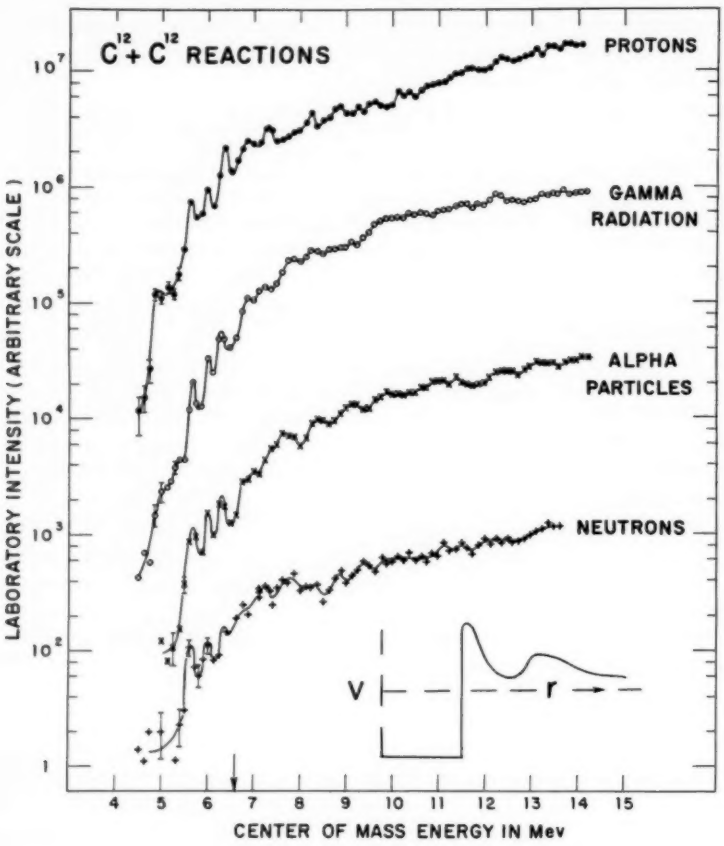

FIG. 1. Excitation curves for C^{12} on carbon reactions: protons at 27°, alpha particles at 42°, neutrons at 30°, and gamma radiation at 90°. The magnitudes of the corresponding differential cross sections (laboratory system) at 10 Mev (c.m. system) incident energy are: protons—15 mb/sr, alpha particles—34 mb/sr, and neutrons—3 mb/sr. These cross sections refer to protons >6 Mev laboratory energy, alpha particles >7.5 Mev, and all neutrons. Detectors were, respectively: Si p-n junctions (reference 2) covered by 0.007 inch of Al for protons, Au-Si surface barrier detectors (reference 2) covered by 0.001-inch Al for alpha particles, long counter of Hanson-McKibbon type for neutrons, and NaI crystal detectors biassed to detect gamma radiation >2.6 Mev energy. Target was a self-supporting ~40-μg/cm^2 C foil. Statistical errors are indicated where they are significantly larger than the points. The classical Coulomb barrier is indicated at 6.6 Mev. The inset shows the quasi-molecular potential envisaged.

precludes interference phenomena and suggests that isolated states of small total widths are involved. The measured separation of adjacent states for the three best defined resonances is nearly constant at 320 kev. There is some evidence that the regular structure persists but with increasing peak widths as the energy is raised above the Coulomb barrier. At still higher energies, the differential cross sections show similar but not identical excitation curves at different angles, suggestive of interference phenomena involving overlapping states in accord with the elastic scattering data.[1] The magnitudes of the differential cross sections (lab system) at 20 Mev are given in the figure captions for the reaction products studied and can be extrapolated to other energies using the excitation curves.

In marked contrast, the data in Fig. 2 for O^{16} on oxygen show yield curves that rise smoothly with energy. It does not appear tenable to attribute this smooth behavior solely to greater level density and widths of the compound system caused by the somewhat greater mass and excitation achieved in the O+O system relative to the C+C system. The top of the Coulomb barrier corresponds to an excitation of ~27 Mev in S^{32} for the former as compared with ~20 Mev in Mg^{24} for the latter. Rather it appears necessary to invoke a reaction mechanism which in the $C^{12}+C^{12}$ case, particularly below the Coulomb barrier, results in the formation of a few sharp, well-separated, states superimposed on the continuum arising from any broad overlapping levels of the compound nucleus. In addition, any such postulated mechanism must include an explanation of the absence of sharp structure in the $O^{16}+O^{16}$ data and in similar measurements on the O+C system.

The formation by two low-energy carbon nuclei of quasi-molecular states with a lifetime of ~10^{-20} second terminated either by the collapse of the

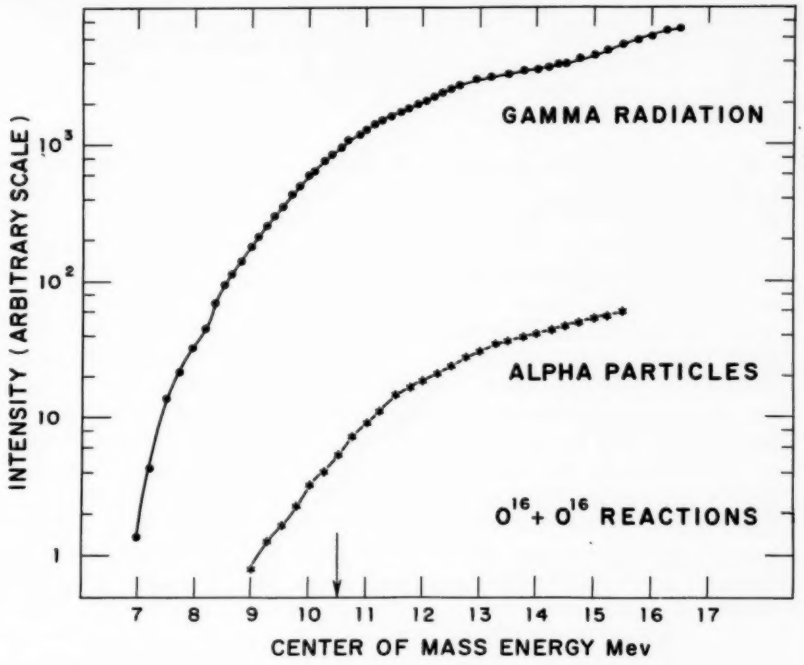

FIG. 2. Excitation curves for O^{16} on oxygen. The alpha particles were detected at 27° and the gamma radiation at 90° in the laboratory. The cross section for alpha-particle production at 10 Mev (c.m. system) incident energy is 4.5 mb/sr (laboratory system). The target was ~25 $\mu g/cm^2$ SiO. In the energy range covered, the reaction yield from Si is negligible. The classical Coulomb barrier is indicated at 10.5 Mev.

system into a compound state which de-excites by light-particle emission or by the re-emission of the carbon nuclei through the Coulomb barrier would, if it occurs, be in accord with the observation of resonances of $\lesssim$100-kev width both in the reaction and elastic scattering data. The possibility of forming such states at energies below the Coulomb barrier may arise from a minimum in the interaction potential caused by neutron interactions made possible by deformability of the reaction particles at a range where Coulomb and angular momentum forces are still effective in preventing immediate coalescence into a compound nucleus. The potential shape envisaged is shown in the inset in Fig. 1 with the resonances in question corresponding to states in the well of larger radius. At high energies, hence high angular momenta, as encountered in the elastic scattering, the centrifugal barrier is expected to modify the well shape to favor re-emission of the incident particles, i.e., compound elastic scattering, while at lower energies the lower orbital momenta are expected to favor coalescence leading to other reactions. The absence of such quasi-molecular states in O^{16} interactions may well arise from the closed shell structure of this nucleus. In this case nucleon transfer involves an exchange from p to d shells; furthermore, the greater rigidity of the closed shell structure will make less likely the distortion necessary to have neutron interactions at a range where Coulomb and angular momentum forces are still effective in causing repulsion. It is of interest to note that the Wigner limit to the reduced width and the level spacings in a square well appropriate to two carbon nuclei ($r \approx 10$ fermis) are in qualitative accord with the experimental data. The physical basis of the above potential is discussed more fully by Vogt and McManus.[3]

In view of the above results it is planned to examine interactions among other light nuclei to see if the lack of resonance structure is peculiar to interactions involving closed shell nuclei. In particular the C^{12} on Ne^{20} interaction which leads to the same excitation in S^{32} as O^{16} on O^{16} is being investigated.

We are indebted to Dr. E. Vogt and Dr. H. McManus for illuminating discussions regarding the nature of the reaction mechanisms involved.

[1]D. A. Bromley, J. A. Kuehner, and E. Almqvist, Phys. Rev. Letters 4, 365 (1960).

[2]J. M. McKenzie and D. A. Bromley, Bull. Am. Phys. Soc. 4, 422 (1959).

[3]E. Vogt and H. McManus, following Letter [Phys. Rev Letters 4, 518 (1960)].

"MOLECULAR" STATES FORMED BY TWO CARBON NUCLEI

Erich Vogt and Hugh McManus
Atomic Energy of Canada Limited, Chalk River, Ontario, Canada
(Received April 14, 1960)

Experiments with heavy ions by Bromley, Kuehner, and Almqvist[1,2] have led them to postulate the existence of "molecular" states of two C^{12} nuclei. We show that the partial widths of the observed resonance structure are in agreement with this suggestion. We discuss the physical origin of this new kind of state and its implications for nuclear structure. The experimental data[1,2] are the cross sections obtained by the bombardment of carbon and oxygen by C^{12} and O^{16} ions over an energy range from a few Mev to 15 Mev (in the center-of-mass system). In $C^{12}+C^{12}$ reactions, sharp resonances with a spacing of about 300 kev appear at the same energy in all reactions near the top of the Coulomb barrier. The elastic scattering above the barrier exhibits similar sharp structure. No such structure is observed in the $O^{16}+O^{16}$ data.

The width and spacing of the observed $C^{12}+C^{12}$ resonance levels cannot be attributed to the compound nucleus Mg^{24}. Even at the energy where the structure is first observed (~6 Mev in the center-of-mass system = 20-Mev excitation in Mg^{24}), the spacing[3] of the compound levels is at least an order of magnitude smaller than 300 kev. On the other hand, area analysis of the prominent reaction resonances at 6 Mev (as well as of the sharp structure at higher energies in the elastic scattering) yields partial widths, $\Gamma_{\lambda C^{12}}$, for formation of compound states by C^{12} of the same order of magnitude as the observed widths (~150 kev). Such a large width (corresponding to a reduced width approximately equal to the sum rule limit) is to be contrasted with the widths of a few kev which are estimated[4] for alpha-particle or proton emission in each channel from the levels of Mg^{24} at 20-Mev excitation. The observed resonances are thus attributed to almost pure single-particle states of two C^{12} nuclei. If these states occur within the normal compound nucleus, it is very hard to understand why they are not mixed into neighboring compound states more strongly. Moreover, the spacing of the C^{12} states is that of a well much larger than the usual Mg^{24} nucleus [see the spacing in the large well of Fig. 1(b), below]. States of the required spacing and width can be obtained if the resonance structure is attributed to "molecular" states in which both C^{12} nuclei retain their identities for appreciable periods, with relative motion over large distances. We suggest a model of such states which is intimately connected with the deformability of C^{12}—the lack of structure in the $O^{16}+O^{16}$ observations is attributed to the rigidity of O^{16}.

When two C^{12} nuclei come into contact, a nuclear attraction arises. Near the point of contact the attraction may occur fairly abruptly, due to a loss of surface energy, and it will be purely real because the C^{12} nuclei have a large Q value (~14 Mev) for nucleon transfer. Only at smaller separations are the two nuclei strongly absorbed into a compound system of Mg^{24}. If the surface vibrations of the two C^{12} nuclei are coupled with the center-of-mass motion resulting from the nuclear attraction of their touching surfaces, there are several normal modes. All but one of these have the high energy[5] ($\hbar\omega \sim 4$-10 Mev) of the surface vibrations of C^{12}. There is one mode, however, with a much lower energy ($\hbar\omega \sim 1$ Mev). In this mode every part of the system simultaneously stretches (or contracts), at constant density, along the axis joining the two C^{12} nuclei. Because of the high energy and small mass involved in the surface vibrations of C^{12}, we can approximate the motion in the low-energy "breathing" or stretching mode by assuming that for each value of separation, r, of the mass centers of the C^{12} nuclei, the nuclear surfaces will deform adiabatically to a minimum energy of the system. If $V_N(r)$ is the nuclear attractive potential of two spherical carbon nuclei, then $V_N[r/(1+\delta)]$ is the nuclear potential of the deformed nuclei, where δ is the fraction by which each C^{12} nucleus is stretched along the axis joining the nuclei. The adiabatic condition is then

$$\frac{d}{d\delta}V_N[r/(1+\delta)] = -\frac{d}{d\delta}V_D, \tag{1}$$

where

$$V_D \equiv C\delta^2 \tag{2}$$

is the distortion energy of the system and C is a constant.[5] In (1) we have neglected the change in Coulomb energy for the quadrupole distortions we are considering.

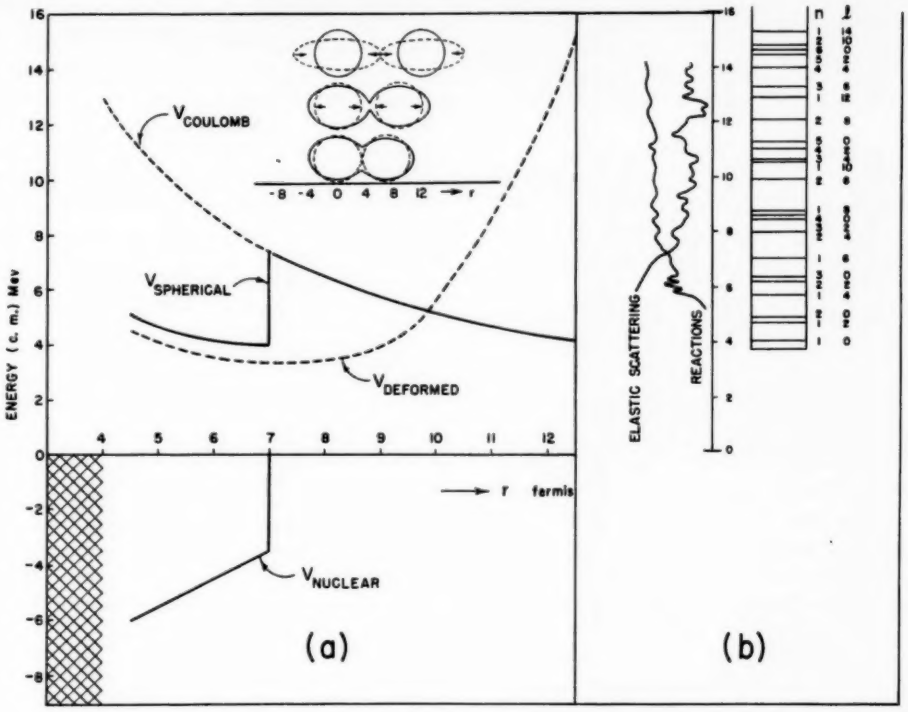

FIG. 1. (a) A qualitative illustration of the potentials connected with the motion of two C^{12} nuclei, as a function of their separation, r. The potential $V_{spherical} \equiv V_{nuclear} + V_{Coulomb}$ is the interaction between two spherical C^{12} nuclei. $V_{deformed}$ is the interaction between the nuclei in the breathing mode. The inset gives the shapes of the nuclei, both in $V_{spherical}$ and $V_{deformed}$, for various separations, r, of their centers of mass at a total energy of about 12 Mev. For $r = 7$ fermis the spheres are in contact and deform adiabatically by the amount shown. For $r = 9$ fermis the deformed mode is still energetically favored and the spherical incoming particles tend to snap together to form a mode in the well; for $r = 12$ fermis the spherical mode is energetically favored and the oscillating drops tend to snap apart, passing through a barrier to their favored spherical shape. (b) A qualitative comparison of the levels in $V_{deformed}$ with the structure of the $C^{12} + C^{12}$ data. The level scheme on the right is that for particles of six proton masses in an infinite square well of radius 10.8 fermis and the indicated depth—dimensions comparable to that of $V_{deformed}$ on Fig. 1(a). The surface energy step in V_N has been chosen so that the three prominent peaks seen in all reactions correspond to the $1g$, $2d$, and $3s$ levels in the well. No significance should be attached to this particular identification.

As two carbon nuclei approach each other their rapid surface vibrations, at any r, may bring their surfaces into contact, thus gaining contact or saddle point energy, although for $r > 7$ fermis (assumed to be the sum of the radii for two spherical C^{12} nuclei) the energy $V_N[r/(1+\delta)] + V_D$ constitutes a barrier that inhibits the contact if the gain in saddle point energy is sufficiently abrupt. However, once the nuclei touch, the same barrier prevents them from snapping apart. The center-of-mass motion is then given by the potential well:

$$V_{deformed}(r) = V_N[r/(1+\delta)] + V_D + V_{Coulomb}(r), \qquad (3)$$

where δ is determined for each r by (1). The attractive well V_N may extend to large distances before the repulsive term V_D takes over.

The motion of the two C^{12} nuclei as they stretch in $V_{deformed}$ is very reminiscent of fission.[6]

The present case has an essential simplicity in that the C^{12} nuclei cannot change their identities by nucleon transfer so that the effective potential, V_{deformed}, is intimately related to the structure of C^{12}.

The low frequency of the breathing mode ($\hbar\omega \sim 1$ Mev) implies that the nuclei make only a few vibrations before decay into the absorptive core (observed widths ~150 kev). The decay inward is inhibited by the centrifugal barrier (for states of high angular momentum), and by the rearrangement energy (Pauli principle) encountered when two C^{12} nuclei coalesce into a state of Mg^{24}.

To illustrate the properties of the states in the "molecular" potential V_{deformed}, Fig. 1(a) shows the V_{deformed} which is found for the particular V_N given on that figure and for a V_D ($C = 25$ Mev[5]) based on the structure of C^{12}. This deformability of C^{12} yields a well extending out to about 11 fermis. The saddle point energy which fixes the well depth has been chosen as 4 Mev on the figure. The slope of V_N between the saddle point and the absorptive core [shaded part of Fig. 1(a)] fixes the value of δ to be 0.15 for $r < 8$ fermis. For larger r the two C^{12} nuclei stretch retaining their saddle point energy, as in the breathing mode described above.

The "molecular" states are given in Fig. 1(b) for a square well of dimensions like that of V_{deformed} in Fig. 1(a). The spacing is similar to that observed. The form of spectroscopy implied by Fig. 1(b) should prove useful in studying the structure of any pair of nuclei which are easily deformed and which are stable against nucleon transfer reactions. The properties of the nuclear potential, V_N, and hence of the "molecular" states may be intimately connected with the fluid or superfluid properties of the nucleons in the surface of the coalescing drops.

The rigidity[7] of O^{16} not only narrows the "molecular" potential and increases the absorptive width of the "molecular" states, but it also strongly decreases the formation probability for such states; hence the lack of structure in the $O^{16}+O^{16}$ observations.

From detailed balance applied to the smoothly varying (compound nucleus) part of the $C^{12}+C^{12}$ data, the fission cross section, $Na^{23}(p, C^{12})C^{12}$ or $Ne^{20}(\alpha, C^{12})C^{12}$, for incident particles above 8 Mev should be of the order of 1% of the absorption cross section of the incident particles. The "molecular" resonances would not be expected to show prominently in the fission reactions.

The authors would like to acknowledge many useful discussions with E. Almqvist, D. A. Bromley, and J. Kuehner who initiated our interest in this problem and with L. G. Elliott and T. D. Newton who also contributed many helpful suggestions.

---

[1]D. A. Bromley, J. Kuehner, and E. Almqvist, Phys. Rev. Letters 4, 365 (1960).

[2]E. Almqvist, D. A. Bromley, and J. Kuehner, preceding Letter [Phys. Rev. Letters 4, 515 (1960)].

[3]If the spacing, $D_{J\pi}$, of levels of a given spin and parity is assumed to be $D_{J\pi} \equiv D/(2J+1)$, then at 13-Mev excitation in Mg^{24} the data give $D \sim 1$ Mev. Level density formulas give $D \sim 250$ kev at 20 Mev, yielding spacings for the 0+, 2+, 4+, 6+ levels of 250, 50, 27, 20 kev, respectively. For a nuclear radius of 7 fermis and a center-of-mass energy of 6 Mev the C^{12} penetrabilities for $l = 0$, 2, and 4 are all of the order of unity, so that approximately one compound level should be observed in every 20 kev.

[4]In the reactions involving Mg^{24} compound states at 13 Mev, as well as in nuclear reactions generally, reduced widths for nucleon or alpha emission have an average value of about $(0.05-0.10)D_{J\pi}$, where $D_{J\pi}$ is the level spacing discussed in reference 3. At 20-Mev excitation the reduced widths are therefore several kev on the average. For a typical compound state at that energy about 10 alpha-particle channels and 30 proton channels (and a few neutron channels) have penetrabilities of the order of unity, leading to the total widths (~150 kev) observed in the $C^{12}+C^{12}$ data as well as in $Na^{23}+p$ data at the same energy [H. E. Gove (private communication)]. Similarly, if the smoothly varying background lying underneath the resonance structure of the $C^{12}+C^{12}$ data is taken to be due to "normal" compound nucleus formation one finds $\gamma_{C^{12}}{}^2/D_{J\pi} \approx 0.025$, yielding "normal" widths for formation of compound states by C^{12} of a few kev.

[5]The low-lying levels of C^{12} have appreciable collective character [D. Kurath, Nuclear Phys. 14, 398 (1960)]. If the energy required to produce a prolate distortion of C^{12} is assumed to be $\frac{1}{2}C\delta^2$, where δ is the fractional elongation of the major axis, then the constant C has been calculated by T. D. Newton (private communication), see also Can. J. Phys. (to be published), to be ~25 Mev, in agreement with the quoted value of $\hbar\omega$.

[6]N. Bohr and J. A. Wheeler, Phys. Rev. 56, 426 (1939); D. L. Hill and J. A. Wheeler, Phys. Rev. 89, 1102 (1953); A. Bohr, Proceedings of the International Conference on the Peaceful Uses of Atomic Energy, Geneva, 1955 (United Nations, New York, 1956), P/199.

[7]J. J. Griffin, Phys. Rev. 108, 328 (1957).

GRAZING COLLISIONS OF COMPLEX NUCLEI*

R. H. Davis
Department of Physics, Florida State University, Tallahassee, Florida
(Received April 25, 1960)

The recent production of heavy-ion beams of variable and well-defined energies makes it possible to study the details of nuclear interaction between complex nuclei.[1] Interpretations of earlier work by either the sharp-cutoff model introduced by Blair,[2] or the optical model as applied by Igo[3] and Porter,[4] suggest that elastic scattering of complex nuclei is restricted to grazing collisions because of the highly absorbent nuclear interior.

When a complex nuclear projectile is incident on a target nucleus at a grazing collision impact parameter, a simple liquid-drop model calculation shows that the attractive and repulsive forces acting on the particle cancel for small interpenetrations provided the orbital angular momentum is sufficiently large. Because of the uncertainties in the "neck" radius and deformation inherent in a liquid-drop model analysis, it is attractive to assume the experimentally determined real optical model potential[3,4] for the specifically nuclear part of the interaction.[5] The potential for the incoming particle is given by

$$V = V_n + V_c + V_m. \tag{1}$$

The quantities V_n, V_c, and V_m are the real optical model potential, the Coulomb potential, and the centrifugal potential, respectively. As-

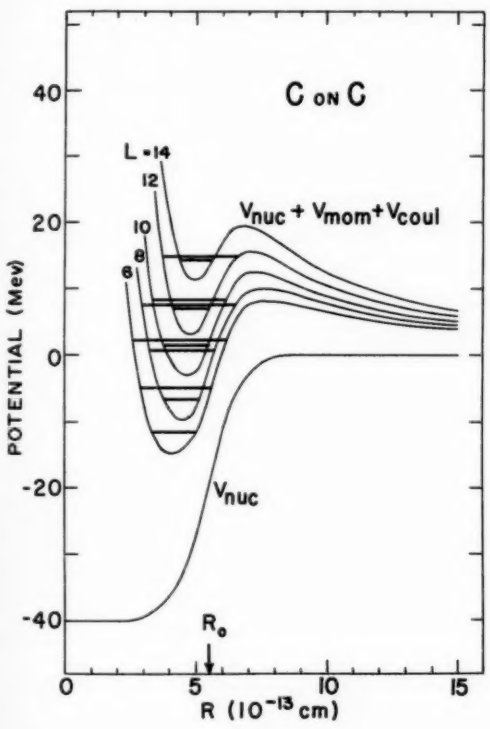

(a)

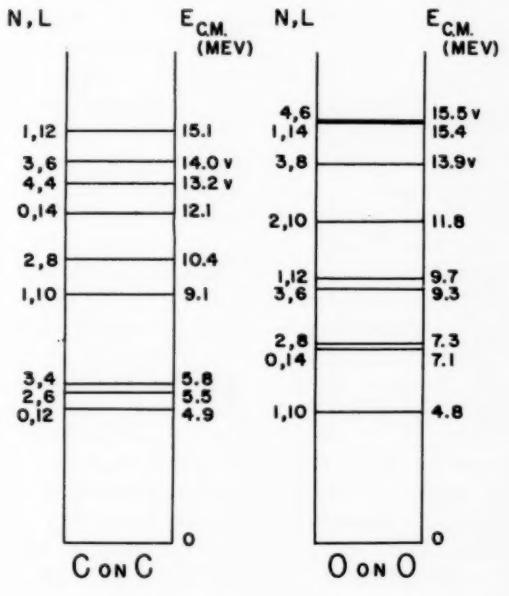

(b)

FIG. 1. (a) Interaction potential (center-of-mass) between two carbon nuclei is plotted against the separation R for various values of the orbital angular momentum quantum number L. The nuclear part of the interaction, V_{nuc}, is the real optical model potential (references 3 and 4), and R_0 is twice the assumed radius of a carbon nucleus. The levels correspond to vibrational oscillations of the carbon nuclei with respect to the center of mass and were calculated by approximating the potential wells with harmonic oscillator potentials. (b) Levels for carbon-carbon and oxygen-oxygen rotators are shown with rotation-vibration interaction included. The quantities N and $E_{c.m.}$ are the vibrational quantum number and the center-of-mass excitation energy, respectively. States lying above the potential barrier are labelled v.

suming the value of the diffuseness parameter given by Igo,[3] $r_0 = 1.2$ f, and a depth of 40 Mev, the nuclear potential has the form

$$V = -40\{1 + \exp[(R - R_0)/0.574]\}^{-1} \text{ Mev}, \qquad (2)$$

where $R_0 = r_0(A_1^{1/3} + A_2^{1/3})$ and R is the separation in fermis; A_1 and A_2 are the mass numbers of the projected and target nuclei.

The Coulomb and centrifugal potentials have their usual forms,

$$V_c = Z_1 Z_2 e^2/R,$$

$$V_m = (\hbar^2/2\mathcal{I})L(L+1),$$

where Z_1 and Z_2 are the atomic numbers of the incident and target nuclei, and L is the orbital angular momentum quantum number. The moment of inertia, $\mathcal{I}$, is taken to be the reduced mass times the square of the particle separations.

The potentials for carbon on carbon elastic scattering are shown in Fig. 1(a) for various values of the orbital angular momentum. The superposition of the attractive and repulsive potentials results in the formation of a potential well, the width and depth of which depend on the orbital angular momentum quantum number for a given nuclear potential. Approximating the well by that of a harmonic oscillator, excitation energies for vibrational states have been calculated and the results are shown in Fig. 1(a) for carbon-carbon scattering.

When a correction for rotation-vibration interaction is made for the levels in Fig. 1(a), the level scheme is that given in Fig. 1(b). The results of a similar calculation for oxygen-oxygen scattering are also shown. The harmonic oscillator quantum number is given by N and the label v indicates a virtual level.

In Fig. 2, the resonance structure predicted by the model is compared with the carbon-carbon and oxygen-oxygen scattering data of Bromley et al.[1] Arrows indicate the location of states shown in Fig. 1(b). Predictions for low (0 or 1) values of N are most accurate in the harmonic oscillator approximation. While structure is observed at the predicted energies, the fit must be considered qualitative since the angular momentum of the states is not determined. It is of interest to note that except for a virtual and consequently very wide state at center-of-mass energy 13.9 Mev, no structure is predicted for oxygen-oxygen scattering between energies 11.8 and 15.4 Mev.

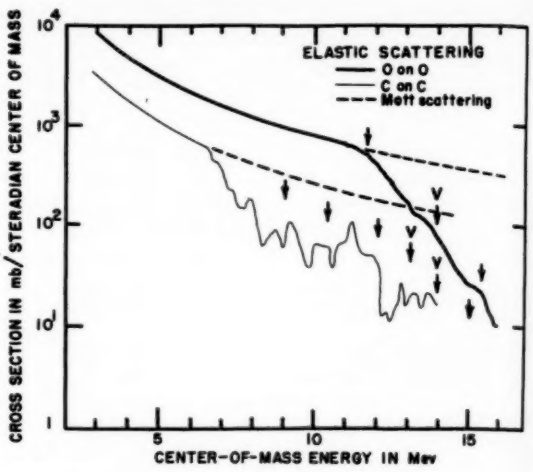

FIG. 2. Energies of predicted levels [Fig. 1(b)] are indicated by arrows above the experimentally observed excitation curves of reference 1. Only those states with excitation energies in the region of nuclear interaction are shown, and v denotes an excitation energy lying above the potential barrier. To make a detailed correlation, more information is needed about the absorption and resonant behavior of the partial waves. No sharp structure is expected in the oxygen-oxygen curve below the break at about 15.4 Mev since the level at 13.9 Mev is virtual.

An order-of-magnitude estimate of the cross section for the formation of a carbon-carbon rotator at 20 Mev (lab) is 5 mb for a level bound by 2 Mev. This appears somewhat lower than the experimental value even after interference enhancement. Structure due to the formation of such states should also be apparent in excitation curves for reactions other than elastic scattering.

---

*This work was supported in part by the Air Force Office of Scientific Research.

[1]D. A. Bromley, J. A. Kuehner, and E. Almquist, Phys. Rev. Letters 4, 365 (1960); also see three abstracts of papers by the same authors, Bull. Am. Phys. Soc. 5, 293 (1960).

[2]J. S. Blair, Phys. Rev. 95, 1218 (1954).

[3]G. Igo, Phys. Rev. Letters 1, 72 (1958).

[4]C. E. Porter, Phys. Rev. 112, 1722 (1958).

[5]R. H. Davis, Bull. Am. Phys. Soc. 5, 244 (1960).

TOTAL ABSORPTION RATE OF MUONS IN CARBON*

F. Russell Stannard
Lawrence Radiation Laboratory, University of California, Berkeley, California
(Received April 20, 1960)

The total absorption rate of muons in carbon has been determined from observations on 2519 muons stopped in a propane bubble chamber. The experimental method employed here leads to a considerable improvement over measurements made thus far with counters. Estimates based on the latter technique have, in fact, been limited to an accuracy of only about $\pm 25\%$.[1]

A negative muon stopped in propane (C_3H_8) is captured into orbits about a carbon nucleus.[2] The presence or absence of an electron at the end of the meson's track gives a direct indication whether the particle decayed or interacted. Assuming a value τ_d for the decay lifetime of the muon, one expresses the total absorption rate by

$$\Lambda_i = N_i/(N_d \tau_d), \qquad (1)$$

where N_i and N_d are the numbers of mesons interacting and decaying, respectively.

The photographs examined were taken with the 30-inch propane chamber. The muon beam had a background of approximately 1% pions. It was found that, out of a total of 2544 particles stopping in the chamber, 2338 decayed and 206 interacted. The prong distribution of the interactions is given in the first line of Table I.

The pion contamination was estimated from the difference in the prong distributions of pion and muon capture stars. Morinaga and Fry[3] have investigated the characteristics of muon interactions in the light elements of nuclear emulsion and found the maximum energy of the emitted protons to be about 15 Mev. Although many stars were seen to have two or more prongs, the energies of the secondaries were such that only rarely would more than a single prong have been resolvable had the events occurred in a bubble chamber. It follows that any star found in the chamber emitting a proton of energy greater than 15 Mev—or, alternatively, consisting of two or more prongs—is most unlikely to have arisen from muon capture, but rather from the interaction of a pion. In order to be able to estimate the total pion contamination, one needs to know the proportion of pion captures not giving these energetic disintegrations. The second line of Table I shows the prong distribution of a sample of 141 pion-capture stars. The final three columns give a total of 62 energetic stars, and these represent 44% of all pion captures. Hence, the total pion contamination, as estimated from 13 energetic stars, found in the sample of supposed muons becomes $13/0.44 = 30 \pm 5$. The remaining 176 events are attributed to muon interactions.

Table I. Characteristics of capture stars.

Primary particle	Number of prongs 0	1[a]	1[b]	2	3
Muons[c]	190	3	9	4	0
Pions	58	21	45	14	3

[a]The prong having an energy <15 Mev.
[b]The prong having an energy >15 Mev.
[c]Uncorrected as yet for pion contamination.

A study of the distribution of events throughout the chamber suggested that some five interactions had escaped detection near the windows and walls. This number then had to be added to the total.

It is expected that about 18% of muon captures[2] lead to the formation of B^{12}. B^{12} subsequently β decays to C^{12}, and some of the electrons from this source will have been photographed if the decay happened to occur between the arrival of the beam and the time of photography. An estimated four captures have been mistaken for decays in this way and consequently have had to be reclassified.

Other observational biases were found to be negligible. A sample of the propane was subjected to mass spectrographic analysis at the completion of chamber operation to test for the presence of impurities in the liquid, but none were found.

The corrected observations yield 185 interactions and 2334 decays from 2519 stopped muons. If one assumes a decay lifetime of 2.22×10^{-6} sec,[4] the estimate of the total capture rate becomes

$$\Lambda_i = (0.36 \pm 0.04) \times 10^5 \text{ sec}^{-1}. \qquad (2)$$

This compares with a previous measurement

of 0.45×10^5 sec^{-1}, based on 1000 muons stopped in a propane bubble chamber.[5] Combining these two results with estimates from counter work[1] gives a weighted mean of

$$\Lambda_t = (0.40\pm0.03)\times10^5 \text{ sec}^{-1}. \quad (3)$$

The theoretical value from Primakoff[6] is 0.44×10^5 sec^{-1}. This estimate has recently been modified by Flamand and Ford[7] to account for the effect of the finite nuclear size on the muon wave function. The experimental results are in good agreement with the modified prediction of 0.41×10^5 sec^{-1}.

Finally, it should be mentioned that several measurements recently have been made[8] of the partial rate for the muon-capture process leading to the ground state of B^{12}. These investigations provide a test of the Universal Fermi Interaction theory.[9] Although the value of the total rate, as found in this experiment, is somewhat lower than that previously accepted, the change does not significantly affect the measurements of the partial rate.

The author wishes to thank Dr. Wilson M. Powell, Dr. Robert W. Birge, and the other members of the propane chamber group without whose help this work would not have been possible. He is indebted to the Bevatron crew and staff, and also to Dr. Robert D. Sard for useful discussions.

*This work was performed under the auspices of the U. S. Atomic Energy Commission.

[1]J. C. Sens, Phys. Rev. 113, 679 (1959); W. E. Bell and E. P. Hincks, Phys. Rev. 88, 1424 (1952).

[2]W. K. H. Panofsky, L. Aamodt, and H. F. York, Phys. Rev. 78, 825 (1950).

[3]H. Morinaga and W. F. Fry, Nuovo cimento 10, 308 (1953).

[4]W. E. Bell and E. P. Hincks, Phys. Rev. 84, 1243 (1951); R. A. Swanson, R. A. Lundy, V. L. Telegdi, and D. D. Yovanovitch, Phys. Rev. Letters 2, 430 (1959); J. Fischer, B. Leontic, A. Lundby, R. Meunier, and J. P. Stroot, Phys. Rev. Letters 3, 349 (1959).

[5]T. H. Fields, R. L. McIlwain, and J. G. Fetkovich, Bull. Am. Phys. Soc. 4, 81 (1959).

[6]H. Primakoff, Proceedings of the Fifth Annual Rochester Conference on High-Energy Physics (Interscience Publishers, Inc., New York, 1955), p. 174.

[7]G. Flamand and K. W. Ford, Phys. Rev. 116, 1591 (1959).

[8]T. N. K. Godfrey, Phys. Rev. 92, 512 (1953); W. Love, S. Marder, I. Nadelhaft, R. Siegel, and A. E. Taylor, Bull. Am. Phys. Soc. 4, 81 (1959); J. G. Fetkovich, T. H. Fields, and R. L. McIlwain, Bull. Am. Phys. Soc. 4, 81 (1959); J. O. Burgman, J. Fischer, B. Leontic, A. Lundby, R. Meunier, J. P. Stroot, and J. D. Teja, Phys. Rev. Letters 1, 469 (1958); H. V. Argo, F. B. Harrison, H. W. Kruse, and A. D. McGuire, Phys. Rev. 114, 626 (1959).

[9]A. Fujii and H. Primakoff, Nuovo cimento 12, 327 (1959); L. Wolfenstein, Nuovo cimento 13, 319 (1959).

MODIFIED ANALYSIS OF NUCLEON-NUCLEON SCATTERING. p-p PHASE SHIFTS AT 210 Mev*

Malcolm H. MacGregor and Michael J. Moravcsik
Lawrence Radiation Laboratory, University of California, Livermore, California
(Received April 8, 1960)

The modified phase-shift analysis program[1,2] has been extended to measurements at 210 Mev. We find only two acceptable solutions, which correspond to the two Stapp solutions[2,3] at 310 Mev. This is one of the few instances in which the data[4-7] have been complete enough to yield a definitive result. Since the phase-shift sets thus obtained are of great value in dispersion relation calculations of the energy variation of phase shifts, and since the present analysis indicates what further experiments should be done to eliminate one of the two remaining phase-shift solution sets at 210 Mev (and therefore also at 310 Mev), we feel that the present results are of considerable interest, even though based on some preliminary data.

In the notation of Wolfenstein,[8] we have analyzed the recent Rochester 210-Mev measurements[4-6] of P, R, and A combined with an earlier Rochester 240-Mev measurement[7] of σ. Search problems were run from 30 random sets of phase shifts, using one-pion exchange contribution (OPEC) with a coupling constant $g^2=14.4$ for G and higher waves,[1] and searching on the 9 parameters S, P, D, F, ϵ_2. Since 35 pieces of data were used in the search program (the smallest angle cross-section point was excluded), a 9-parameter solution has an expected least-squares sum χ^2 of 26. The 30 random searches yielded 7 solution sets with χ^2 less than 200,

Table I. Nine-parameter phase shift[a] fits to 210-Mev data ($g^2 = 14.4$).

Soln.	χ^2	χ^2 corr.[b]	$^1S_0$	$^1D_2$	$^3P_0$	$^3P_1$	$^3P_2$	ϵ_2	$^3F_2$	$^3F_3$	$^3F_4$
a	43.08	28	12.8	0.5	-32.0	23.0	4.9	1.5	-6.0	-4.3	0.8
b	45.61	28	5.9	7.5	2.1	-20.9	17.0	-1.6	-0.4	-2.0	0.3
c	78.42	56	-15.7	2.8	-28.4	-2.1	17.9	-5.8	1.2	-2.3	1.0
d	94.59	81	-2.0	5.3	-41.6	-13.0	10.4	-4.6	-0.2	-3.6	1.1

[a]Phase shifts are nuclear bar phase shifts (see reference 3) in degrees.
[b]χ^2 corr. is the result when the three largest angle differential cross-section points are adjusted to give a contribution of 1 each to χ^2, as they should.

which we label *a* through *g* in order of increasing χ^2. Sets *a*-*d* are listed in Table I. Sets *e*-*g*, with χ^2 values of 115, 135, and 181, respectively, all feature $^1S_0$ phase shifts larger than +30°, and hence are ruled out by comparison with the negative $^1S_0$ phase shift required at 310 Mev.[2] An examination of the remaining sets *a*-*d* shows that the three largest angles in the differential cross-section data contribute unreasonable values to χ^2. When a correction is applied to allow for this, solutions *a* and *b* have about the expected χ^2 value of 26, as shown in Table I. Solution *c* has a χ^2 that, accepted at face value, has only one chance in a thousand of being correct. However, in view of the uncertainty with regard to the differential cross-section data, this cannot be considered sufficient evidence to rule out *c*. Solution *d* may possibly be ruled out by the χ^2 argument, but we will also present other reasons for discarding it.

The phase-shift analysis was extended for solution types *a*-*d* by treating the coupling constant g^2 as a parameter. A 9-parameter search gave the $\chi^2(g^2)$ values shown in Table II. The values of the coupling constant deduced from plots of these results are $g^2 = 14.3 \pm 2.5$, 15.8 ± 2.4, 21.0 ± 3.8, and ~28 for cases *a*, *b*, *c*, and *d*, respectively. Since the expected value of about 14 was obtained in a similar analysis at 310 Mev,[1] this casts some doubt on the validity of *c* and is another argument for ruling out *d*. Seven-parameter searches were also made in which first the $^3F_3$ and $^3F_4$ (high *J*) and then the $^3F_2$ and ϵ_2 (low *J*) phase shifts were calculated by OPEC, in addition to *G* and higher waves. The high-*J* case (Table II) gives parabolas for *a*, *b*, and *c* with minimum

Table II. Goodness-of-fit parameter χ^2 versus coupling constant g^2 for solutions *a*-*d*.

g^2	3	9.4	11.9	14.4	18	24	28.8
			9-parameter search S, P, D, F, ϵ_2				
a	121	49	44	43	45	52	55
b	65	50	47	46	46	53	64
c	105	87	82	78	75	75	84
d	150		104	95	85	78	84
			7-parameter search S, P, D, F_2, ϵ_2 (high J)				
a	227	105	73	54	48[a]	73	134
b	95	54	63	78	109[a]	102	178
c	106	103	113	129	90[a]	102	178
d	7723	105	73	54	90[a]	73	178
			7-parameter search S, P, D, F_3, F_4 (low J)				
a	390	253	235	326	263[a]	569	760
b	87	77[b]	278	419	151[a]	569	1561
c	524	278	169	97	151[a]	569	1561
d	306	449	386	458	263[a]	355	760

[a]$g^2 = 19.4$.
[b]$g^2 = 6$.

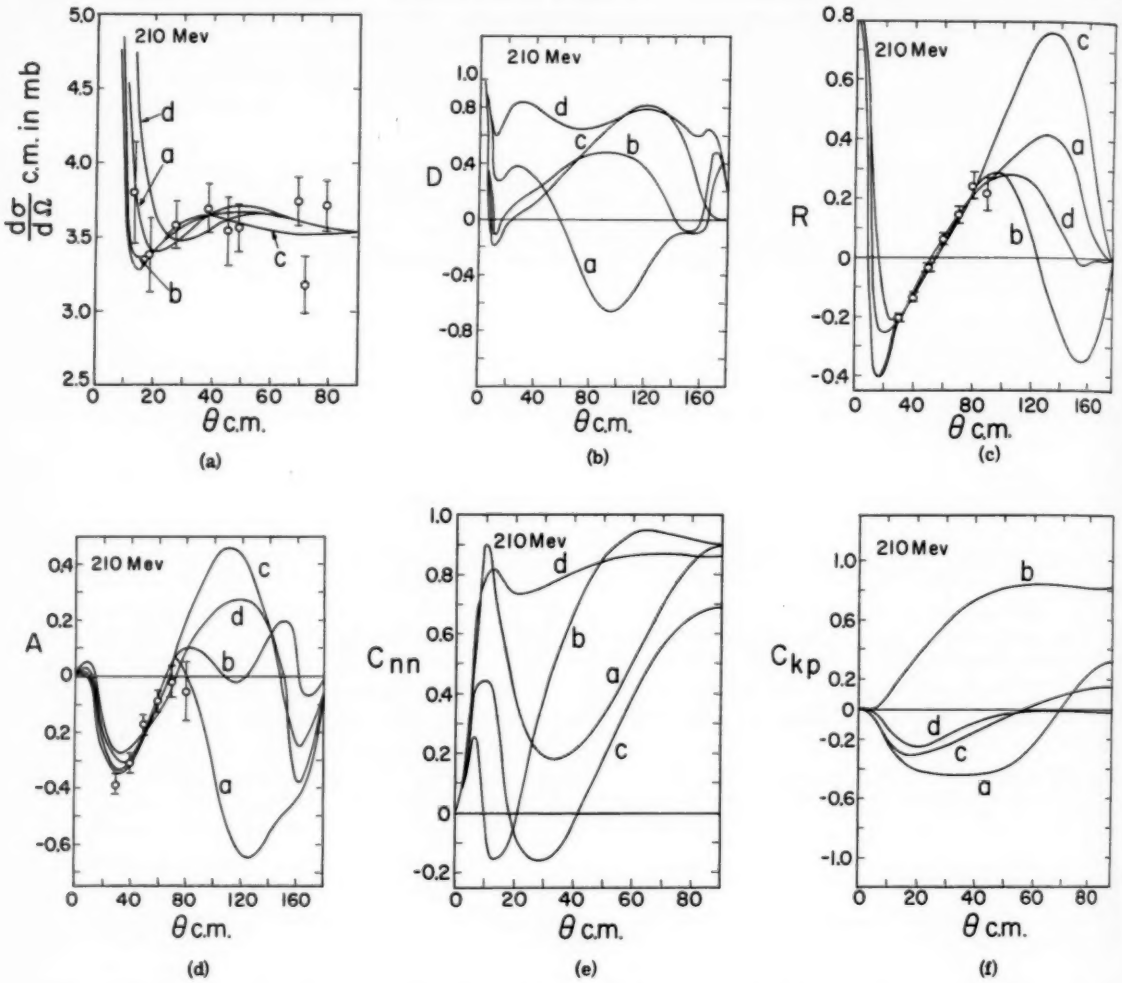

FIG. 1. Plots of the p-p scattering parameters σ, D, R, A, C_{nn}, C_{kp} predicted by solutions a-d, together with data used in the analysis.

χ^2 values of 48, 54, and 99 at $g^2 = 19$, 9, and 7, respectively. The shift to lower values for g^2 in the bases of b and c as the number of parameters is reduced from 9 to 7 is in agreement with a similar study at 310 Mev.[2] Solution d in the high-J case has lost its independent existence. The good χ^2 values for a and b show that they have ${}^3F_3$ and ${}^3F_4$ phase shifts similar to those predicted by OPEC. Solution c in the high-J approximation is not as good as a or b. When the low-J approximation was made, solutions a and d gave no χ^2 values less than 200 for any value of g^2. Solutions b and c had χ^2 minima of 77 and 97 at $g^2 = 5$ and 14, respectively. Hence the ${}^3F_2$ and ϵ_2 waves are not approximated by OPEC for a and d, and are only poorly approximated for b and c.

Comparison of the phase shift sets a-d with the Stapp solution sets[1-3] reveals that b is similar to Stapp solution 1, c is similar to 2, d is similar to 6, and a has no Stapp counterpart. Plots of the p-p scattering parameters σ, D, R, A, C_{nn}, and C_{kp} predicted by solutions a-d are given in Fig. 1. The polarization, not shown in the figure, is almost identical for the four solutions and is in good agreement with the experimental data. Solution d can be ruled out on the basis of χ^2 (Table I) and of erratic behavior

in the $\chi^2(g^2)$ plots, as mentioned above, and also because the corresponding Stapp solution 6 was shown to be spurious.[2] Solution a can probably be ruled out on three counts: (1) The $^1D_2$ value of 0.5° is not compatible with a required $^1D_2$ of either 4.8° or 11.9° at 310 Mev,[2] and the $^3P_1$ value of +23° is not compatible with a required $^3P_1$ value of -8.1° or -27.5° at 310 Mev.[2] (2) The predicted value for D [Fig. 1(b)] given by a disagrees radically with the actual shape of D as measured at 310 Mev.[3] (3) A large positive $^3P_1$ phase shift is in contradiction with analysis of the photodisintegration of the deuteron.[9] Solution a seems to be a spurious solution arising because of the lack of a D measurement at 210 Mev. On the basis of the present analysis, we rule out all phase-shift solution sets except b and c, and b is slightly favored over c. An examination of Fig. 1 shows that a single measurement of R', A', C_{nn}, or C_{kp} at an appropriate angle would choose among a, b, and c.

The question always arises in this kind of analysis as to whether 30 random searches are sufficient to span the space. Only four of the search problems did not end up with one or another of the sets a-g. In addition, search problems started from Gammel and Thaler[10] and from Bryan, Signell, and Marshak[11] phase shifts both ended up at solution b. Early phase-shift sets of Garren[12] and Klein,[13] using only S and P waves and only σ and P data, gave surprisingly good χ^2 values when applied to the complete set of data. Search problems started from four Garren and four Klein phase-shift sets ended up with our solution sets a, c, d, e, and b, d, e (twice), respectively, for the two cases. At 310 Mev, Stapp[3] used 400 random starts in the search for solution sets. The analogy between the results obtained at 210 Mev and at 310 Mev[1-3] makes us feel that additional 210-Mev random search problems would have a very small probability of producing additional solution sets.

It is a pleasure to acknowledge helpful discussions with Dr. H. P. Noyes throughout the course of this investigation.

---

*Work done under the auspices of the U. S. Atomic Energy Commission.

[1]P. Cziffra, M. H. MacGregor, M. J. Moravcsik, and H. P. Stapp, Phys. Rev. 114, 880 (1959).

[2]M. H. MacGregor, M. J. Moravcsik, and H. P. Stapp, Phys. Rev. 116, 1248 (1959).

[3]H. P. Stapp, T. J. Ypsilantis, and N. Metropolis, Phys. Rev. 105, 302 (1957).

[4]E. Baskir, E. M. Hafner, A. Roberts, and J. H. Tinlot, Phys. Rev. 106, 564 (1957).

[5]J. Tinlot, E. Heer, A. England, and W. Gibson, Bull. Am. Phys. Soc. 4, 242 (1959).

[6]A. England, W. Gibson, E. Heer, and J. Tinlot, Bull. Am. Phys. Soc. 5, 76 (1960). The authors advise us that the data in references 5 and 6 should be regarded as preliminary.

[7]C. L. Oxley and R. D. Shamberger, Phys. Rev. 85, 416 (1952); O. A. Towler, Phys. Rev. 85, 1024 (1952). The data were renormalized by W. Hess, Revs. Modern Phys. 30, 368 (1958).

[8]L. Wolfenstein, Phys. Rev. 96, 1654 (1954).

[9]G. Kramer, Nuclear Phys. 15, 60 (1960). We are grateful to Dr. Kramer for an interesting conversation on this subject.

[10]J. L. Gammel and R. Thaler, Phys. Rev. 107, 291 (1957).

[11]R. A. Bryan (private communication).

[12]A. Garren, Phys. Rev. 101, 419 (1956).

[13]C. A. Klein, Nuovo cimento 2, 1165 (1955).

POSSIBLE EVIDENCE FOR THE RADIATIVE DECAY OF THE Σ^+ HYPERON

E. M. Friedländer
Cosmic-Ray Laboratory, Institute of Atomic Physics, Bucharest, Rumania
(Received March 23, 1960)

An event most likely interpreted as a three-body decay of a Σ^+ hyperon, has been found during a systematic along-the-track scan of an Ilford G-5 emulsion stack exposed to the Bevatron K^- beam. Up till now this scan has yielded ~1500 σ_K stars.

A microprojection drawing of the event is shown in Fig. 1. The pertinent data are given in Table I. Track K is the incoming K^- which satisfied all the criteria for acceptance as a beam K^- meson. The three prongs OA, OB, and OC are all too short to allow identification. The thickness of OB suggests $Z \geq 2$ (recoil). Track π can be shown unambiguously to start at C,[1] and comes to rest in the same emulsion sheet, undergoing characteristic π-μ-e decay. A 13-Mev electron track is apparently copunctual with C. Upon closer examination, however, it proves to be a chance coincidence (a continuation beyond C was observed).

FIG. 1. A microprojection drawing of the event.

The only charged π^+-active product of K^- captures is the Σ^+ hyperon. If the Σ^+ decays at rest, the expected energy of the decay pion is 92.2 Mev, in striking disagreement with the value deduced from the observed range, viz., (24 ± 1) Mev. The length of track OC is too short to allow a distinction between decay at rest or in flight; a Σ^+ decay in flight could yield such a low-energy pion at the observed decay angle (26°) only if the kinetic energy of the Σ^+ is above 190 Mev. This exceeds considerably the maximum available energy in a K^- capture at rest, even if the Fermi momentum of the capturing nucleon is taken into account.

The event occurred near the center of the stopping zone of the K^- mesons in our stack. In order to exclude the possibility of any residual kinetic energy of the K^- at the point of capture, a comparative gap count was performed on the primary of this event and on that of a typical $K^- + p \rightarrow \Sigma^+ + \pi^-$ ($\Sigma^+ \rightarrow n + \pi^+$) event, occurring nearby in the same emulsion sheet. The results are plotted in Fig. 2 which shows that most probably the capture occurred at rest. This result was confirmed by a constant-sagitta scattering measurement which yielded (0.90 ± 0.22) of the expected sagitta.

The only possibility left for explaining the low energy of the pion is that—although it is emitted with high energy at C—it loses most of its energy in a nuclear collision without visible products

Table I. Pertinent data for the tracks associated with the event.

Track	Identity	Range (μ)	T (Mev)
OA	unidentified	1.8	0.3[a]
OB	unidentified	0.8	···
OC	unidentified	1.6	0.3[a]
π	pion	9522	24 ± 1
e	electron	···	13 ± 4[b]
μ	muon	622	4.2 ± 0.3

[a] If proton.
[b] From scattering.

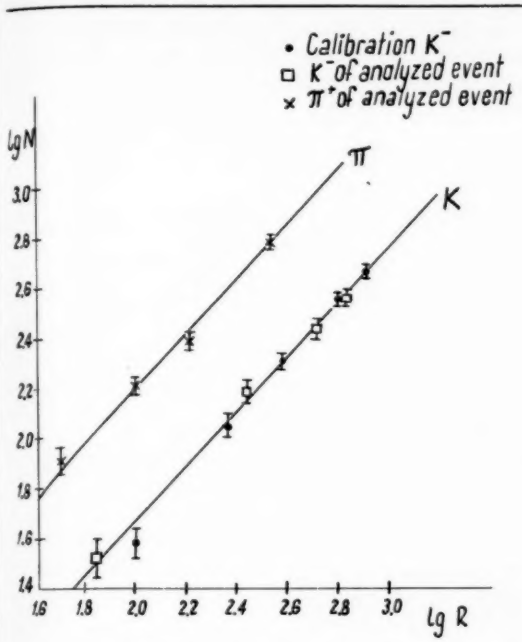

FIG. 2. Integral gap number distribution for tracks K and π and for the track of a calibration K^- meson.

before it stops and decays (the range of the decay muon proves that the $\pi - \mu$ decay occurred at rest). In order to check the assumption that the observed range is not equal to the ionization range, the following measurements were performed:

1. Constant sagitta scattering, yielding (1.18 ±0.32) of the expected value.

2. Total gap count (see curve π on Fig. 2), which compares favorably with the K^- results.

3. Constant-cell scattering near C, yielding a kinetic energy of 27 ± 4 Mev.

4. Gap count near C, compared to gap count on the calibration K meson, at a range corresponding to the same velocity as the pion's at C, viz., $R_K = R_\pi(M_K/M_\pi)$.

The ratio of gap densities was found to be 1.03 ±0.08, which proves that the pion was emitted from C with the energy corresponding to its observed range.

If we want to interpret this event in terms of known particles, we are forced to assume that besides the neutron, at least a second neutral particle is emitted in this Σ^+ decay. The simplest assumption[3] meeting the energy and angular momentum restrictions is that we are dealing with the radiative (inner bremsstrahlung) decay of the Σ^+:

$$\Sigma^+ \rightarrow n + \pi^+ + \gamma. \qquad (1)$$

The kinematics require $E_\gamma < 43$ Mev if the decay occurred at rest and correspondingly less if it occurred in flight.

The branching ratio for such a decay—which would have been expected to occur for very general reasons—has been computed recently by Barshay and Behrends.[4] The radiative decay with charged pion emission [Eq. (1)] is expected to occur most frequently (in ~3.5% of the decays). The (less frequent) $p + \pi^0 + \gamma$ decay mode might sometimes be mistaken for a one-prong Σ^--capture star, on account of its shorter proton track.

The only alternative explanation of this event requires an absurd piling up of chance coincidences, viz., scattering of incoming K^- at O, chance coincidence with two large blobs, followed by capture of the K^- at C with $\Sigma^- + \pi^+$ production, the Σ^- being captured within the same nucleus without visible recoil, while the pion energy is reduced by Fermi motion of the capturing nucleon. To illustrate the absurdity of such an interpretation the probability for chance coincidence of two blobs of the observed size with the assumed point of scattering was estimated from the emulsion background and was found to be $\sim 10^{-7}$.

The author is indebted to Professor J. Auslander, Professor C. M. G. Lattes, S. Bilenky, L. Lapidus, S. Alper, and E. M. Mayer for useful discussions. The event was found by Mrs. M. Radu.

Note added in proof: Recently, the Berne group, M. Nikolic, W. Koch, M. Schneeberger, and H. Winzeler, Nuclear Phys. 15, 519 (1960), have observed an event very similar to the one described here, but with a negative pion. An interesting feature of both observations is the close similarity between the pion kinetic energies (24 and 22 Mev, respectively).

---

[1]The extrapolation of track π passes at a distance of (0.67 ± 0.15) μ from point O.

[2]W. Barkas and A. Rosenfeld, University of California Radiation Laboratory Report UCRL-8030, 1958 (unpublished).

[3]It has been suggested that $OC \rightarrow \pi^+$ may represent the π^+-active decay of a hyperfragment ($\Lambda^0 p$). To the author's knowledge, no such case has been reported until now. A careful search among the ~150 hyperfragments recorded in the same stack has also failed to reveal any π^+-active hyperfragment. A somewhat less unlikely, but still very remote possibility could

be a $(\Sigma^+ n)$ compound. A possible $(\Sigma^+ p)$ compound was reported by M. Baldo-Ceolin et al., Nuovo cimento 6, 144 (1957). A similar event in which the identification of the Σ^+ hyperfragment was less certain, has been reported by S. Alper and E. M. Friedländer at the 1957 Dubna Conference on Cosmic Rays.

[4] S. Barshay and R. Behrends, Phys. Rev. 114, 931 (1959).

EVIDENCE FOR THE REACTION $\bar{p}+p \rightarrow \bar{\Sigma}^0+\Lambda^*$

Janice Button, Philippe Eberhard,† George R. Kalbfleisch, Joseph E. Lannutti,‡
Gerald R. Lynch, Bogdan C. Maglić, and M. Lynn Stevenson
Lawrence Radiation Laboratory, University of California, Berkeley, California
(Received April 22, 1960)

We have found an event which may be interpreted as the reaction $\bar{p}+p \rightarrow \bar{\Sigma}^0+\Lambda$.[1] The event was produced in the 72-in. liquid hydrogen bubble chamber. A highly purified beam of antiprotons of 1.99 ± 0.03 Bev/c was produced by using three velocity-selecting spectrometers. The approximate composition of this beam under normal operating conditions was $1.0\bar{p}$:$1.5\pi^-$:$1.9\mu^-$:$0.015K^-$. A description of the beam will be presented in a later publication.

Figure 1 is one of the three camera views of this event. Table I summarizes the measured momenta and directions of all the tracks. The table also summarizes the "best-fit" values obtained by assuming that (a) tracks 2, 3, and 4 correspond to a Λ and its decay fragments π^- and p, respectively, and (b) that tracks 5, 6, and 7 correspond to a $\bar{\Lambda}$ and its decay fragments $\bar{p}$ and π^+, respectively. The Λ is produced at an angle of 10.6 ± 0.4 deg and the $\bar{\Lambda}$ at an angle of 4.6 ± 0.3 deg with respect to the incident antiproton.

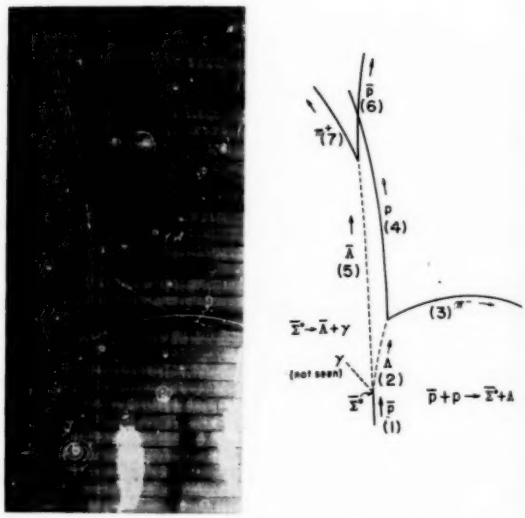

FIG. 1. One view of the event $\bar{p}+p \rightarrow \bar{\Sigma}^0+\Lambda$ or $\bar{\Lambda}+\Sigma^0$ found in the 72-in. hydrogen bubble chamber.

Table I. Track momenta and directions for event No. 265-608.

Track No.	Particle	Measured values: Momentum (Mev/c)	Azimuth (deg)	Dip (deg)	Fitted values from V decay: Momentum (Mev/c)	Azimuth (deg)	Dip (deg)
1	$\bar{p}$	2019 ± 20	89.6 ± 0.1	0.7 ± 0.1			
2	Λ		79.3 ± 0.1	-0.4 ± 0.8	506 ± 9	79.4 ± 0.1	-0.7 ± 0.3
3	π^-	107 ± 4	25.0 ± 1.6	39.7 ± 1.9	107 ± 2	25.3 ± 1.4	40.2 ± 1.4
4	p	463 ± 13	86.8 ± 0.4	-9.3 ± 0.5	470 ± 8	87.7 ± 0.2	-9.2 ± 0.3
5	$\bar{\Lambda}$		92.3 ± 0.1	4.6 ± 0.3	1384 ± 15	92.34 ± 0.03	4.7 ± 0.1
6	$\bar{p}$	1180 ± 15	88.5 ± 0.1	8.0 ± 0.1	1164 ± 13	88.6 ± 0.1	7.9 ± 0.1
7	π^+	271 ± 10	110.7 ± 0.4	-11.3 ± 0.6	245 ± 2	110.5 ± 0.2	-11.0 ± 0.3

Table II. Values of χ^2 for various hypotheses.

Tracks	Decay Interpretation	Decay χ^2	Decay Degrees of freedom	Production (and Σ decay) Interpretation	Production (and Σ decay) χ^2	Production (and Σ decay) Degrees of freedom
2, 3, 4	Λ	3.1	3	$\Lambda\bar{\Sigma}^0$	13	2
	$\bar{\Lambda}$	no fit	3	$\Sigma^0\bar{\Lambda}$	17	2
	K^0	450	3	$\Lambda\bar{\Lambda}$	560	4
5, 6, 7	$\bar{\Lambda}$	6.2	3	$\Lambda\bar{\Lambda}\pi^0$	90	1
	Λ	no fit	3			
	K^0	140	3			

Both V's were fitted by least-squares methods to the three different hypotheses of Λ, $\bar{\Lambda}$, or K_1^0 decay. The values of the resulting χ^2 functions are tabulated in Table II. The number of degrees of freedom (and therefore the expected value of χ^2) is three. The χ^2 values clearly indicate that tracks 2, 3, and 4 correspond to a Λ decay rather than a K_1^0 or $\bar{\Lambda}$ decay. Likewise, tracks 5, 6, and 7 are clearly the decay of a $\bar{\Lambda}$ rather than of a K_1^0 or Λ.

The next step was to decide to which of the following hyperon-antihyperon reactions this event corresponded:

(a) $\bar{p}+p\rightarrow\bar{\Lambda}+\Lambda$;

(b) $\bar{p}+p\rightarrow\bar{\Sigma}^0+\Lambda$, $\bar{\Sigma}^0\rightarrow\bar{\Lambda}+\gamma$;

(c) $\bar{p}+p\rightarrow\Sigma^0+\bar{\Lambda}$, $\Sigma^0\rightarrow\Lambda+\gamma$;

(d) $\bar{p}+p\rightarrow\bar{\Sigma}^0+\Sigma^0$, $\bar{\Sigma}^0\rightarrow\bar{\Lambda}+\gamma$, $\Sigma^0\rightarrow\Lambda+\gamma$;

(e) $\bar{p}+p\rightarrow\bar{\Lambda}+\Lambda+\pi^0$.

The most descriptive way found of displaying the dynamical differences between these reactions was to plot the possible values of the laboratory production angle versus the laboratory momentum of the Λ or $\bar{\Lambda}$ for each reaction. These were calculated by using the measured incident-beam momentum, 2.03 Bev/c, and are shown in Fig. 2. The solid line of Fig. 2(A) is a contour of allowed values of θ_Λ or p_Λ for the reaction $\bar{p}+p\rightarrow\bar{\Lambda}+\Lambda$. The shaded area is the region of allowed values for both the Λ and $\bar{\Lambda}$ if the reaction were $\bar{p}+p\rightarrow\bar{\Lambda}+\Lambda+\pi^0$. On all figures, 2(A) through 2(C), we have plotted the fitted values of p_Λ and θ_Λ as well as $p_{\bar{\Lambda}}$ and $\theta_{\bar{\Lambda}}$. The size of the black points indicates the size of the errors. Figure 2(B) displays the production and decay dynamics of $\bar{p}+p\rightarrow\bar{\Sigma}^0+\Lambda$. The shaded area is the region in which the $\bar{\Lambda}$ from $\bar{\Sigma}^0\rightarrow\bar{\Lambda}+\gamma$ decay may fall. The solid line is the contour of allowed values of θ_Λ and p_Λ for the directly produced Λ. We have also drawn a dotted line for Λ values corresponding to the best-fit beam momentum for reactions (b) and (c) obtained by fitting the production pro-

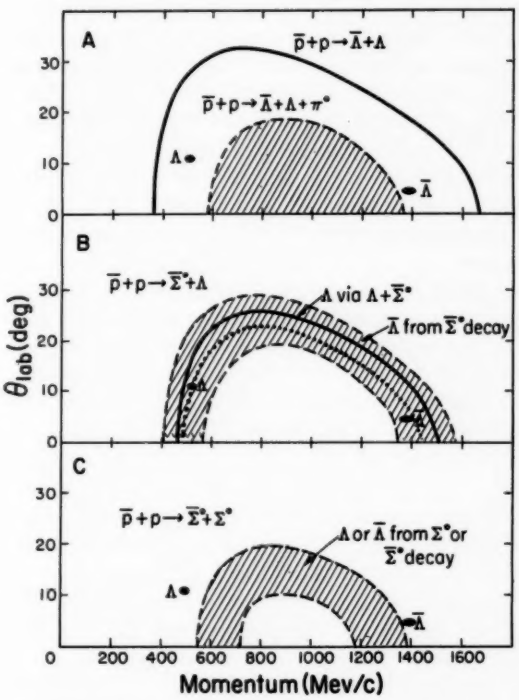

FIG. 2. Contours of θ_Λ vs p_Λ or $\theta_{\bar{\Lambda}}$ vs $p_{\bar{\Lambda}}$ for all possible antihyperon production reactions yielding Λ and $\bar{\Lambda}$. Momentum of the incident $\bar{p}$ is the measured value of 2.03 Bev/c. Fitted values of observed Λ and $\bar{\Lambda}$ of the $\Sigma-\Lambda$ event are indicated by black dots. In (B), the dotted curve represents Λ kinematics for the fitted 1.97-Bev/c incident momentum.

cess. A similar set of curves exists for $\bar{p}+p \rightarrow \Sigma^0+\bar{\Lambda}$, where we have $\bar{\Sigma}^0 \cong \Sigma^0$ and $\Lambda \cong \bar{\Lambda}$. The experimental points, of course, remain unchanged. Figure 2(C) shows the allowed region for the Λ or $\bar{\Lambda}$ coming from the decay of a Σ^0 or $\bar{\Sigma}^0$ produced in the reaction $\bar{p}+p \rightarrow \bar{\Sigma}^0+\Sigma^0$.

On the basis of these plots alone, we conclude that the most likely reaction is (b) $\bar{p}+p \rightarrow \bar{\Sigma}^0+\Lambda$. Reaction (c) appears next most likely. The other reactions are clearly ruled out.

There is additional information not shown on these graphs which may be gained by plotting this event on a stereographic projection or Wolff plot. Figure 3 is a reproduction of such a plot and shows that the two V's are not coplanar with the incident $\bar{p}$ track (track number 1). If we assume that the reaction is $\bar{\Sigma}^0+\Lambda$, then point "$\bar{\Sigma}^0$" would be the predicted direction of the $\bar{\Sigma}^0$. Its momentum would be 1485 ± 20 Mev/c. The angle $\theta_{\bar{\Lambda}\bar{\Sigma}}$ (3.0 ± 0.2 deg) and the observed $\bar{\Lambda}$ momentum (1380 ± 15 Mev/c) are consistent with the decay of a 1485-Mev/c $\bar{\Sigma}^0$. A similar analysis can be made assuming the event to be $\bar{p}+p \rightarrow \Sigma^0+\bar{\Lambda}$. Figure 4 is the resulting stereo projection. The predicted direction of the Σ^0 is given on this plot by the point "Σ^0," and its momentum is 580 ± 3 Mev/c. The angle $\theta_{\Lambda\Sigma}$ (7.5 ± 0.6 deg) and the observed Λ momentum (520 ± 9 Mev/c) are consistent with the decay of a 580-Mev/c Σ^0. Therefore, on the basis of decay, either reaction (b) or reaction (c) could fit the observed angles and momenta.

In order to summarize the relative likelihoods of reactions (b) and (c), we have constructed χ^2 functions for the production process plus the decay of the $\bar{\Sigma}$ or Σ. With the use of fitted values from the Λ and $\bar{\Lambda}$ decays, the number of degrees of freedom for this combination is two. For the

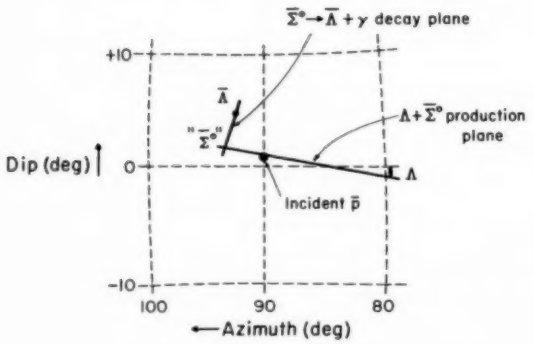

FIG. 3. Stereographic plot of the $\bar{\Sigma}^0+\Lambda$ interpretation.

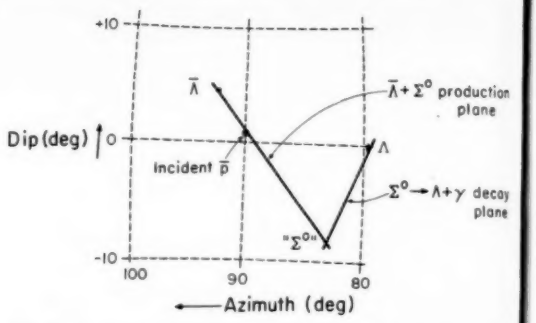

FIG. 4. Stereographic plot of the $\bar{\Lambda}+\Sigma^0$ interpretation.

reaction (b), the composite χ^2 is 13, and for the reaction (c), the composite χ^2 is 17. Admittedly obtaining a χ^2 of 13 or 17 when the expected value is 2 indicates that reactions (b) or (c) are not very likely. However, before we attach significance to the actual magnitude of χ^2, we must thoroughly understand the assigned measurement errors. At the present time, our information regarding systematic errors in the 72-in. chamber is fragmentary. We mention χ^2 only as an indication of the relative likelihood of the various hypotheses. In Table II we have summarized the composite χ^2 for the reactions that we could treat with our present techniques. It is clear that on the basis of χ^2 we cannot decide between reaction (b) and reaction (c). However, the two rates must be equal if CPT invariance is not violated by these strong interactions. On this basis, the observation of reaction (b) is evidence for reaction (c) and vice versa.

We have observed only one $\Lambda\bar{\Sigma}^0$ (or $\bar{\Lambda}\Sigma^0$) reaction in ≈ 6000 antiproton interactions. Since $\frac{2}{3} \times \frac{1}{3} = \frac{2}{9}$ of the reactions yielding $\bar{\Lambda}\Lambda$ will give an observable pair, we conclude that on the basis of one event, the frequency of production is about 1/3000. The known total cross section is about 90 mb.[2] This indicates that the $\Lambda+\bar{\Sigma}^0$ cross section is about 30 μb.

We have also considered the possibility that this event is the reaction $\pi^- + p \rightarrow K^0+\Lambda+\pi^0$, where the K^0 decays via the leptonic mode of decay in such a way as to look like a $\bar{\Lambda}$ decay. We have, therefore, calculated on the basis of dynamics alone the probability for a K_2^0 to decay giving the V that we have interpreted as Λ decay. It is impossible for $K_2^0 \rightarrow \pi^+ + \pi^- + \pi^0$ to fit. However, it is possible to obtain a fit for the decay modes $K_2^0 \rightarrow \mu^\pm + \pi^\mp + \nu$ and $K_2^0 \rightarrow e^\pm + \pi^\mp + \nu$. But when we estimate the number of events of this type that

we should expect to see on the basis of the known $\pi^- + p \rightarrow \Lambda + K^0 + n\pi^0$ background events and the conditions for ambiguity in K_2^0 vs $\bar{\Lambda}$ decay, we find less than 10^{-6} of an event.

It is also dynamically possible for the reaction $\bar{p} + p \rightarrow \bar{\Lambda} + \Lambda + \gamma$ to give rise to the observed event. This, however, is very unlikely because of the small probability of radiative production with a γ ray of 75 Mev/c.

This experiment would certainly not have been possible without the stimulation and foresight of Professor Luis W. Alvarez. An experiment of this difficulty owes its success to a great many people. Morris Pripstein and Ngyen H. Xuong have contributed long and tiring hours both in the development and in the operation of the antiproton beam. One can hardly overemphasize the indebtedness we owe to the people who built and operated the 72-in. bubble chamber, notably James D. Gow, Paul Hernandez, and Robert Watt. Members of Professor Burton J. Moyer's group contributed to the electronic aspect of the beam development and operation. Our thanks go to Dr. Margaret Alston and Dr. Hugh Bradner and the scanners for their contribution to the experiment. We are greatly indebted to Jon Peter Berge for assistance in the IBM analysis of our events. Finally we wish to thank the Bevatron crew who had the difficult task of producing the high-flux, short-spill beam that was necessary for this bubble chamber experiment.

*Work done under the auspices of the U. S. Atomic Energy Commission.

†Now at Laboratoire de Physique Atomique et Moleculaire, Collège de France, Paris.

‡On leave from Florida State University, Tallahassee, Florida.

[1]Janice Button, Bull. Am. Phys. Soc. 5, 54 (1960).

[2]R. Armenteros, C. Coombes, B. Cork, G. Lambertson, and W. Wenzel (to be published).

π^- CAPTURE IN COMPLEX NUCLEI AND NUCLEAR PAIR CORRELATIONS*

S. Ozaki,† R. Weinstein,‡ G. Glass, E. Loh, L. Neimala, and A. Wattenberg‖
Laboratory for Nuclear Science and Physics Department,
Massachusetts Institute of Technology, Cambridge, Massachusetts
(Received April 25, 1960)

A study was undertaken of the high-energy products of the capture of stopped π^- mesons in complex nuclei; scintillation counters in coincidence were used as detectors of neutrons and protons. By measuring the neutrons it was hoped to establish whether or not π^- capture in complex nuclei involves two nucleons, and if it does, to use the process to study the ratio of neutron-proton pairs to proton-proton pairs in complex nuclei.

Brueckner, Serber, and Watson[1] developed the hypothesis, which was also suggested by Perkins,[2] that low-energy π mesons would preferentially be absorbed by a pair of nucleons in complex nuclei. In the case of π^- absorption the reactions would be

$$\pi^- + p + n \rightarrow n + n, \qquad (1a)$$

$$\pi^- + p + p \rightarrow n + p. \qquad (1b)$$

Early measurements[3,4] on the interaction of π^+ mesons with carbon supported this hypothesis. Many studies of π^- capture have been made using radiochemical and emulsion techniques[5,6] and Ammiraju and Lederman[7] have made extensive measurements on π^- capture in light nuclei using a cloud chamber. The observations from most of these experiments were interpreted in terms of the two-body model with some modifications. All of these measurements lacked the possibility of observing the ejected neutrons and their angular correlations.

For the present set of measurements the π^- mesons were produced by bombarding beryllium with a bremsstrahlung beam from the MIT synchrotron. Coincidences were observed between two neutron counters in order to study reaction (1a), or between a neutron and a proton (telescope) counter in order to study reaction (1b); the latter experimental arrangement is shown in Fig. 1. For the results reported below, the neutron counters had an efficiency[8] of about 10% for 55-Mev neutrons, and the neutron counters were biased to observe only recoil protons with energies greater than 9 Mev. The proton counter system would accept protons of energy greater than 22 Mev and less than 112 Mev. We stopped π^- mesons in targets made of Li, C, Al, S, Cu, and Pb. Most effort was devoted to obtaining good statistics on the C and Al targets.

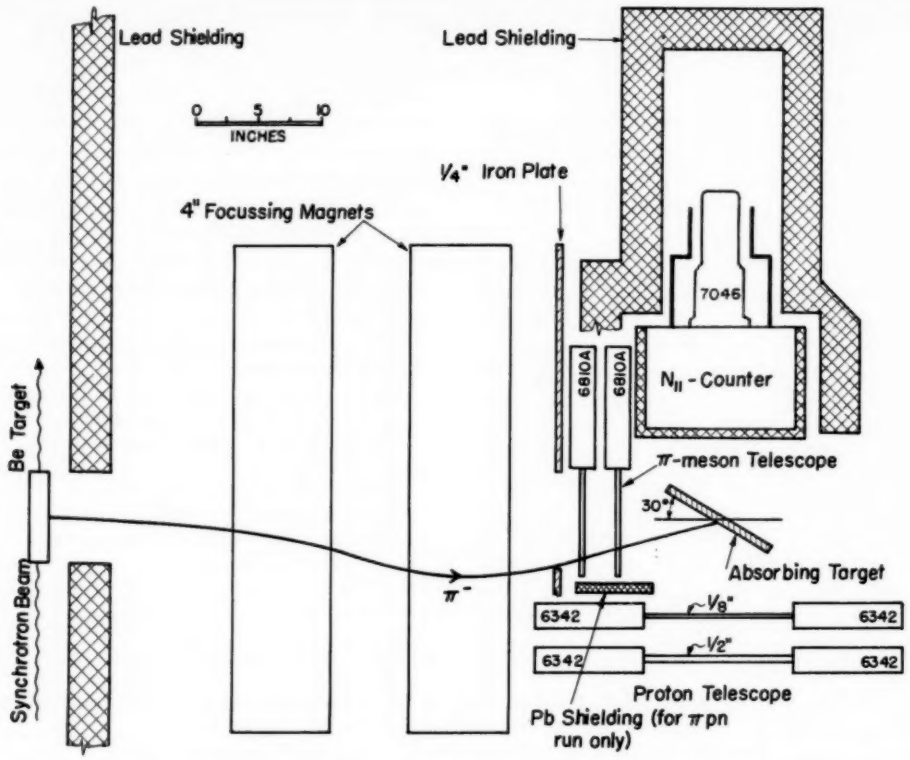

FIG. 1. The experimental arrangement of the apparatus which was used for the π^- + proton + neutron coincidence measurements at 180°. For the π^- + neutron + neutron coincidence measurements a neutron counter replaced the two proton counters so that the solid angle subtended would be approximately the same.

If the capture in a complex nucleus of a stopped π^- meson occurs according to reactions (1a) and (1b) (the two-nucleon model), kinematics requires that the nucleons come off essentially back to back if both nucleons escape from the nucleus without scattering inside the nucleus. The nucleons are not sharply correlated in angle because of the initial Fermi momentum of the pair of capturing nucleons.

In order to test the spatial correlation of the ejected nucleons, measurements were made with the counters at 180° to each other (Fig. 1) and with the counters at 90° to each other. The results for C are given in Table I. One sees in the data the 180° correlation required by the two-body model of Brueckner, Serber, and Watson.[1] The data of the other light elements agree but are not as statistically significant.

If one corrects for the relative probability of detecting the neutrons and protons, one obtains the following values of the ratio of n-n events [reaction (1a)] to n-p events [reaction (1b)]:

$$\text{ratio } (a/b) = 5.0 \pm 1.5 \text{ for carbon;}$$

$$\text{ratio } (a/b) = 3.9 \pm 1.2 \text{ for aluminum.}$$

Due to background subtractions and secondary events contributing more to the proton coincidence runs, we feel these observed ratios are to be taken as lower limits on the ratio of reaction (1a) to (1b). In other words, the capture of π^- mesons is likely to occur much more frequently

Table I. Coincidences as a function of angle.

Target	Neutron-proton coincidences per monitor unit		Neutron-neutron coincidences per monitor unit	
	90°	180°	90°	180°
C	0.8±1.1	4.8±0.7	2±7	25±3

with a neutron-proton pair than with a proton-proton pair. DeSabbata, Manaresi, and Puppi[9] and Tomasini[10] have previously found it necessary to assume this in order to explain data obtained on π^- capture in nuclear emulsions. Ammiraju and Lederman[7] drew the same conclusion from their data on capture in He.

If one assumes that only even angular momentum states are present between pairs of nucleons in complex nuclei (essentially the "Serber mixture of nuclear forces") and if one takes account of the Pauli principle only in the initial states, then the ratios one would expect from simple counting of the initial nucleon states are approximately 4.8 for both carbon and aluminum. If one includes odd angular momentum states, the expected ratios are approximately 2.4 which disagree with the observed ratios. On the above naive basis, one would say that the data are in agreement with the assumption of the "Serber mixture of nuclear forces" inside complex nuclei.

In the above estimates of the expected ratios, all final-state interactions have been neglected. However, it is of interest that the above conclusions are also valid if one takes account of the final states of the two nucleons.

In order to count the final states one has to take a particular model of the π^- capture process. We have assumed that the capture of π^- occurs when the π^- is in a p-state relative to one of the protons. The Pauli principle essentially inhibits some final states but only for reaction (1a), leading to a reduction in the expected ratio. Taking account of the Pauli principle and an angular momentum barrier, we get an expected ratio of about 3.4 for both elements.

In that we consider the observed ratios as lower limits, we have been led into reconsidering the assumptions used in obtaining an expected ratio that is somewhat less than the observed ratios.

In calculating the expected ratio we have neglected the fact that the momentum transfers involved correspond to short interaction distances, namely about 0.4×10^{-13} cm. For these small distances, the phenomenological nucleon-nucleon potentials[11,12] are much stronger for the triplet states than for the singlet state. The triplet states contribute to only the neutron-proton pairs [reaction (1a)] which would lead to the relative enhancement of the number of neutron-proton pairs at least in the above process. Thus the expected ratio would be in better agreement with the observed ratio if there are relatively fewer proton-proton pairs in the nucleus than the number given by a simple counting and the Pauli principle.

The authors appreciated very much discussions with Professor B. T. Feld, Professor H. Feshbach, and Professor V. F. Weisskopf. They also want to thank all the members of the Synchrotron Laboratory for their generous help. One of the authors (S. Ozaki) is greatly indebted to the U.S. Department of State and the Fulbright Committee for giving him the opportunity to do this work at MIT.

---

*This work has been supported in part by the Office of Naval Research and the U. S. Atomic Energy Commission.

†Fulbright Graduate Fellowship 1955-1959. Now at Brookhaven National Laboratory, Upton, New York.

‡Now at the Institute for Theoretical Physics, Copenhagen, Denmark.

‖Now at the University of Illinois, Urbana, Illinois.

[1]K. A. Brueckner, R. Serber, and K. M. Watson, Phys. Rev. 84, 258 (1951). Also see N. C. Francis and K. M. Watson, Am. J. Phys. 21, 659 (1953).

[2]D. H. Perkins, Phil. Mag. 40, 601 (1949).

[3]G. Bernardini and F. Levy, Phys. Rev. 84, 610 (1951).

[4]H. Byfield, J. Kessler, and L. M. Lederman, Phys. Rev. 86, 17 (1952).

[5]For references and a summary see p. 216 of N. Metropolis, R. Bivins, M. Storm, J. M. Miller, G. Friedlander, and A. Turkevich, Phys. Rev. 110, 204 (1958).

[6]S. A. Azimov, Y. G. Gulianov, E. A. Zanichalova, M. Nizametdinova, M. I. Podgoretskii, and A. Inidashev, J. Exptl. Theoret. Phys. (USSR) 31, 756 (1956)[translation: Soviet Phys.-JETP 4, 632 (1957)].

[7]P. Ammiraju and L. D. Lederman, Nuovo cimento 4, 281 (1956).

[8]The efficiency of the neutron counter was obtained in the same manner as employed by E. R. Christie, B. T. Feld, A. C. Odian, P. C. Stein, and A. Wattenberg, Rev. Sci. Instr. 27, 127 (1956).

[9]V. DeSabbata, E. Manaresi, and G. Puppi, Nuovo cimento 10, 1704 (1953).

[10]A. Tomasini, Nuovo cimento 3, 160 (1956).

[11]P. S. Signell and R. E. Marshak, Phys. Rev. 109, 1229 (1958).

[12]J. L. Gammel and R. M. Thaler, Phys. Rev. 107, 291 (1957); 107, 1337 (1957).

ROLE OF THE π-π INTERACTION IN HIGH-ENERGY π-NUCLEON INTERACTIONS

P. Carruthers* and H. A. Bethe
Laboratory of Nuclear Studies, Cornell University, Ithaca, New York
(Received April 18, 1960)

In this note we describe in a simple qualitative way the salient features of pion-nucleon interactions in the energy range 0.5 to 1.5 Bev from the point of view that every interaction is initiated by means of the scattering of the incident pion by a virtual pion of the nucleon.[1]

From the behavior[2] of the very high-energy (5 Bev) elastic and low-multiplicity inelastic events it is clear that there must be a large π-π cross section. One may therefore reasonably hope to explain the "intermediate" energy region ($0.5<E<1.5$ Bev) in terms of the two principal facts of pion physics: the 3-3 resonance and the large π-π cross section. Peierls[3] already used this general idea to explain the 600- and 900-Mev resonances in π^--p scattering. He, as well as Wong and Ross,[4] consider these and other higher resonances as occurring primarily in the system N-π-π; while the total angular momentum of the system may be high (up to $L=3$), each of the two individual pions in this model has a small angular momentum, $l=1$ or 0, relative to the nucleon.

The question then arises as to how the incident single pion, which has the full angular momentum L, gets "caught" by the nucleon and makes a "transition" to a small l corresponding to the N-π-π resonant state. We wish to suggest that this transition is effected by the π-π force acting between the incident π and a virtual π in the nucleon. No matter how the primary N-π-π resonance comes about, the transition will be strongly enhanced by resonances in the π-π system. From the point of simplicity alone this model deserves attention. Aside from this mechanism of initiating the reaction we wish to point out (a) that despite first appearances, the over-all behavior of the π^+-p data from 0.8 to 1.2 Bev is similar to that of the π^--p data from 0.6 to 1.0 Bev; (b) that present information on charge state ratios in single pion production events provides evidence for the dominance of the π-π isotopic spin state $t=1$ at 900-Mev pion lab energy, where the "third" resonance is located, in accord with the work of Frazer and Fulco[5] on the problem of nucleon form factors; (c) that the over-all behavior can be explained by assuming that the $t=0$ interaction in the pion system is dominant in the vicinity of the "second" resonance, from 400 up to about 700 Mev; above this energy the $t=1$ amplitude develops rapidly.

Evidence for point (a) comes from a comparison of the (π^--p) and (π^+-p) total cross sections.[6] Drawing $\lambda\!\!\!^{-2}$ ($\lambda\!\!\!^{-}$ = reduced c.m. wavelength) curves through the two π^--p peaks, one notes that, although the 1.3-Bev π^+-p peak is perhaps too broad to be considered as a single resonance, $\sigma(\pi^+$-$p)$ is qualitatively similar to $\sigma(\pi^-$-$p)$ but shifted upwards somewhat in energy. (Given the same angular momentum states, this increase in energy naturally suppresses the magnitude of the total cross section.) The similarity lies deeper than this, however. 1. It has been suggested[7] that the sudden rise of $\sigma(\pi^+$-$p)$ above 700 Mev is associated with the advent of a D_{33} resonance. (The notation is $L_{2T,2J}$ in extension of Fermi's notation for low-energy pion states.) For $\sigma(\pi^-$-$p)$ it has been reasonably well established that the second resonance (600 Mev) is D_{13}. 2. The π^+-p angular distribution for elastic scattering at 990 Mev displays a backwards bump similar to (but smaller than) that in π^--p scattering between 0.8 and 1 Bev.[8-12] 3. The work of Crittenden et al.[12] on π^--p interactions shows that the inelastic cross section rises abruptly to a maximum near the third resonance (900 Mev) although it is already large before. A similar behavior, but at higher energies, is shown by the inelastic π^+-p cross section although data are more scarce: $\sigma(\pi^+$-$p)$ increases slowly from about 3 mb at 500 Mev[13] to about 10.5 mb at 990 Mev[8] and then rises quickly to 16.5 mb at 1.1 Bev.[14] According to Peierls, the third resonance in π^--p is F_{15}. Hence it seems likely that an F state becomes important in $T=3/2$ (π^+-p) at about a Bev.

This evidence that the dynamical behavior of the π^+-p system is similar to that of the π^--p system, but develops at a higher energy, may be understood simply if we assume that the high-energy dynamics of the π-nucleon system, however complicated they may be, must be initiated by π-π interactions. The small π^+-p ($T=3/2$) cross section below 800 Mev is considered to be a consequence of the lack of any appreciable interaction in the $t=1$ and $t=2$ π-π states in this energy region. The rapid increase in $\sigma(\pi^+$-$p)$

above 800 Mev is interpreted as due to a strong $t=1$ interaction which reaches a maximum at about 900 Mev, according to the evidence considered in the next paragraph. On the other hand, the $T=1/2$ state of the π-nucleon system will, in our interpretation, be dominated by a $t=0$ resonance in the π-π system [point (c) above]. The simplest assumption for this $t=0$ state is that it is a two-pion S wave in the π-π center-of-mass system (P states are forbidden for two pions with $t=0$ by the Pauli principle). Another possibility would be the $t=0$, $J=1$ three-pion resonance, or bound state, suggested by Chew,[15] but this assumption would make it much more difficult to interpret the transition from a single incident pion to the resonant N-π-π state. Rodberg[16] has reported the results of a calculation of pion production using a π-π interaction, in which the s-wave $t=0$ amplitude dominates for energies less than 400 Mev. A reasonable fit to the data of Perkins et al.[17] is thereby obtained.

In order to get evidence for point (b) above, we consider the ratio r of the cross sections for the reactions $\pi^- + p \to \pi^- + \pi^+ + n$ and $\pi^- + p \to \pi^- + \pi^0 + p$.

$$r = \sigma(n+-)/\sigma(p-0). \qquad (1)$$

Note that the final pion state π^--π^0 cannot have $t=0$, while π^+-π^- is a mixture of $t=0$, 1, and 2. It is clear from the experiments that near the third resonance (900 Mev) the inelastic scattering is much greater in the $T=1/2$ state than in the $T=3/2$ state.[8,12,13] If now we combine first the isotopic spins of the pions in the final state and then couple these states of well-defined t to the nucleon to form a state with total isotopic spin $T=1/2$ (this eliminates $t=2$), then a simple use of Clebsch-Gordan coefficients gives the π-π amplitudes in terms of the charge state ratio:

$$|a_1|^2/|a_0|^2 = (r-\tfrac{1}{2})^{-1}. \qquad (2)$$

a_t is the amplitude for the state in which the π-π system has isotopic spin t. Figure 1 shows the value of the ratio (2) in the vicinity of the third resonance as measured by a number of authors.[10,11,18-20] Equation (2) says that $|a_0|$ decreases from about $1.4|a_1|$ at 800 Mev to only $\frac{1}{3}|a_1|$ at 900 Mev, rising again to about $1.2|a_1|$ at a Bev. The precise ratio of $|a_1|$ to $|a_0|$ depends on the experimental accuracy, and also on the $T=3/2$ admixture. However, if the data of Fig. 1 are reasonably correct, then it is easily seen that for any sensible amount of $T=3/2$ amplitude the same feature persists: $|a_1|^2/|a_0|^2$ goes through a pronounced maximum at 900 Mev.[21]

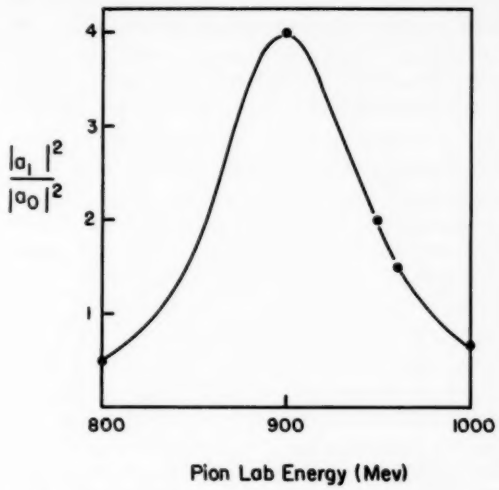

FIG. 1. The ratio of the $t=1$ $\pi-\pi$ amplitude to the $t=0$ $\pi-\pi$ amplitude, as deduced from Eq. (1), goes through a distinct maximum near 900 Mev. We consider this to be evidence for the $t=1$ $\pi-\pi$ resonance suggested by Frazer and Fulco.

Thus Fig. 1 seems to indicate a resonance in the $t=1$ state of the π-π system at 900-Mev lab pion kinetic energy. Since f waves in the π-π center-of-mass system are surely negligible at this energy, it seems that we have evidence for the $t=1$, p-wave π-π resonance suggested by Frazer and Fulco.[5] If the pion in the cloud is assumed to be essentially at rest, this lab energy corresponds to a total π-π center-of-mass energy $W \approx 4\mu$, also compatible with their work. Additional experimental information on charge state ratios would be very desirable. One might check to see if the isotopic spin zero amplitude shows a resonant behavior at 600 Mev, by methods similar to those of Fig. 1.

However, the narrow widths of $|a_1|^2$ makes it extremely unlikely that the third resonance is due only to a π-π resonance, owing to the momentum distribution of the virtual pions.[22] Therefore, it is of interest that the $J=5/2$, even-parity configuration of the 2-pion–nucleon system is just that in which both pions can interact with the nucleon in the 3-3 state, as pointed out by Peierls.[3] Further, Wong and Ross,[4] examining the two-meson propagator by means of the static theory, predict the energy of the $J=5/2$, $T=1/2$ even state to be near a Bev. Hence the third re-

sonance and also the sharpness of the π-π $t=1$ amplitude are very likely due to the effect of the resonant (3-3 state) interaction of both mesons with the nucleon. If this is true, then one cannot yet conclude that there is really a resonance in the π-π system, but only that the reaction goes through that channel in which the $t=1$ π-π interaction dominates.[23]

It is important to note that the "double isobar" picture of the F_{15} state by itself does not cause the behavior of $|a_1|^2/|a_0|^2$ shown in Fig. 1. This is seen by forming the $T=1/2$ state in three different ways: (a) first couple the nucleon and one meson together to form $T'=3/2$; (b) first couple the two mesons together to form a $t=1$ state; (c) first couple the two mesons in a $t=0$ state. Now the square of the projection of state (b) onto state (a), relative to the square of the projection of state (c) onto state (a), is just

$$3[W(\tfrac{1}{2}1\,\tfrac{1}{2}1;\,\tfrac{3}{2}1)]^2/[W(\tfrac{1}{2}1\,\tfrac{1}{2}1;\,\tfrac{3}{2}0)]^2=\tfrac{1}{2}, \quad (3)$$

where W is the Racah coefficient. Evidently $t=0$ is preferred, so far as the $T=1/2$ state is concerned.

Briefly, then, our picture of the high-energy resonances is as follows (see Fig. 2). The two-meson-plus-nucleon propagator is strongly enhanced by 3-3 resonance effects; for the channel with two p-wave mesons this amplitude probably displays a resonance (near 990 Mev). This two-meson channel is then considered to be coupled to the single (incident) meson channel only by the π-π interaction, which in turn may display resonances. With the over-all behavior controlled by the π-π channel, one may understand the difference between the interactions of positive and negative mesons with protons as outlined above. This picture emerges in a natural way (except for S-wave mesons) when a π-π interaction is added to the static theory. Limitations of space prevent our showing how this happens.

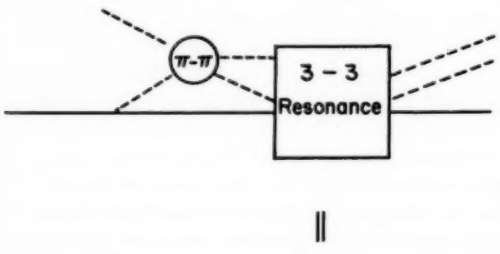

FIG. 2. A pion production event is pictured according to the model described in this Letter. The two-meson intermediate state, in which one or both mesons interact with the nucleon via the low-energy 3-3 resonance, is coupled to the incident meson through the π-π channel, which also may have resonances. (The mesons are represented by dashed lines, the physical nucleon by a solid line.)

The D_{13} and D_{33} resonances can presumably not be explained by the 3-3 interaction alone because it would be difficult to get a sharp peak in the S-P amplitude. Crudely speaking, increasing the energy of the system would merely increase the energy of the nonresonant S meson, leaving the p-wave at the resonant (3-3) energy. We therefore consider these resonances as due to cooperation between the 3-3 and a π-π resonance, of $t=0$ or $t=1$, respectively. The entrance into this state would also be through the π-π channel.

It was remarked earlier that the 1.3-Bev peak seems rather too broad to be made up from one state. Thus it is tempting to speculate that the $t=2$ π-π interaction becomes strong at this energy, since this would contribute to the $T=3/2$ (π^+-p) but not $T=1/2$ scattering. This interaction could possibly excite the P_{33} isobar found by Wong and Ross[4] in this energy range. It should be easy to check this experimentally; for example, one might expect the reaction $\pi^+ + p \to \pi^+ + \pi^+ + n$ to become important above a Bev, since two π^+ mesons have $t=2$.

Finally we wish to point out that the model here proposed explains why resonances exist in the $D_{3/2}$ (and $F_{5/2}$) state but not in $D_{5/2}$ (and $F_{7/2}$). We have assumed that the resonances arise from the two-meson configurations S-P (and P-P). Now from the vector model, the highest J obtainable from a state containing two mesons of orbital momenta l_1, l_2 and a nucleon of spin $s=1/2$ is

$$J_{\max}=l_1+l_2+1/2, \quad (4)$$

which gives $J_{\max}=3/2$ (5/2) for the S-P (P-P) configuration. This excludes $D_{5/2}$ and $F_{7/2}$.

---

*National Science Foundation Predoctoral Fellow.

[1]References to most of the original work on π-π interactions may be found in a recent paper by C. J. Goebel, Phys. Rev. Letters 1, 337 (1958). See also G. F. Chew and S. Mandelstam, Lawrence Radiation Laboratory Report UCRL-8728, 1959 (unpublished).

[2]G. Maenchen et al., Phys. Rev. 108, 850 (1957); W. D. Walker, Phys. Rev. 108, 872 (1957).

[3]R. F. Peierls, Phys. Rev. 118, 325 (1960).

[4]W. N. Wong and M. Ross, Phys. Rev. Letters 3, 398 (1959).

[5]W. Frazer and J. Fulco, Phys. Rev. Letters 2,

365 (1959); Lawrence Radiation Laboratory Report UCRL-8880, 1959 (unpublished).
[6]Total $\pi^{\pm}-p$ cross sections in the energy range of interest in this paper are given by B. C. Barish, W. N. Hess, V. Perez-Mendez, and J. Solomon, Phys. Rev. Letters 4, 242 (1960).
[7]P. Carruthers, Phys. Rev. Letters 4, 303 (1960).
[8]A. Erwin, J. Kopp, and A. M. Shapiro (private communication from Dr. Erwin).
[9]A. Erwin and J. Kopp, Phys. Rev. 109, 1364 (1958).
[10]W. D. Walker, F. Hushfar, and W. D. Shephard, Phys. Rev. 104, 526 (1956).
[11]L. Bagget, Lawrence Radiation Laboratory Report UCRL-8302, 1958 (unpublished).
[12]R. R. Crittenden et al., Phys. Rev. Letters 2, 121 (1959).
[13]W. J. Willis, Phys. Rev. 116, 753 (1959).
[14]L. O. Roellig and D. A. Glaser, Phys. Rev. 116, 1001 (1959).
[15]G. F. Chew, Phys. Rev. Letters 4, 142 (1960).
[16]L. S. Rodberg, Phys. Rev. Letters 3, 58 (1959).
[17]W. Perkins et al., Phys. Rev. Letters 3, 56 (1959).
[18]V. Alles-Borelli et al., Nuovo cimento 14, 211 (1959).
[19]1958 Annual International Conference on High-Energy Physics at CERN, edited by B. Ferretti (CERN, Geneva, 1958), p. 68.
[20]I. Derado and N. Schmitz, Phys. Rev. 118, 309 (1960).
[21]It should be noted that according to the standard isobar model [R. M. Sternheimer and S. J. Lindenbaum, Phys. Rev. 109, 1723 (1958)] the value of r should increase, essentially because of the presence of the combination $\pi^{-}-n$ in the final state of the reaction $\pi^{-}+p\rightarrow\pi^{-}+\pi^{+}+n$.
[22]For a discussion of this point see R. Cool, O. Piccioni, and D. Clark, Phys. Rev. 103, 1082 (1956).
[23]Peierls has noted[3] that the angular distribution [K. Berkelman and J. Waggoner, Phys. Rev. (to be published)] of the π^0 in the reaction $\gamma+p\rightarrow p+\pi^0$ in the energy range 950-1050 Mev photon energy (corresponding to 800-900 Mev pion energy) can be interpreted as due to $D_{13}-F_{15}$ interference. The D state responsible for this behavior is probably not the 600-Mev resonance (D_{13}) but the 800-Mev resonance (D_{33}) because the latter is closer and has a larger Clebsch-Gordan coefficient. Since the angular distributions determine only the relative parity of the 800-900 Mev states, the F_{15} assignment for the 900-Mev resonance depends critically on the correctness of D_{33} for the 800-Mev state which in turn rests on the argument of reference 7 (i.e., if the 800-Mev state were P_{33}, then the 900-Mev state would be D_{15}). Earlier $\pi^{+}-p$ scattering experiments seemed to indicate that the D_{33} resonance could not appear below 850 Mev. However, the results of reference 7 suggest that 800 Mev is possible, which is more comfortable if the amplitude of this state is to be appreciable between 600-800 Mev.

ERRATA

REGENERATION AND MASS DIFFERENCE OF NEUTRAL K MESONS. Francis Muller, Robert W. Birge, William B. Fowler, Robert H. Good, Warner Hirsch, Robert P. Matsen, Larry Oswald, Wilson M. Powell, Howard S. White, and Oreste Piccioni [Phys. Rev. Letters 4, 418 (1960)].

We neglected to mention the results of Boldt et al.[1] which indicated that the mass difference (divided by $\hbar/\tau_1$) is more probably a number of the order of one than larger than ten. These authors emphasized that the principal outcome of their experiment was to demonstrate the feasibility of the method that they used.

There are two typographical errors: In the third line above Eq. (1), c_1 should read τ_1. In the paragraph below Eq. (3), $K3$ should read $K2$.

[1]E. Boldt, D. O. Caldwell, and V. Pal, Phys. Rev. Letters 1, 150 (1958).

RECOILLESS RAYLEIGH SCATTERING IN SOLIDS. C. Tzara and R. Barloutaud [Phys. Rev. Letters 4, 405 (1960)].

Instead of

$$\varphi_T=\exp\left\{-\frac{3}{2}\frac{E_R}{k\theta}\left[\frac{1}{4}+\frac{1}{x}\int_0^x\frac{udu}{e^u-1}\right]\right\},$$

where $x=T/\theta$, Eq. (1) should read:

$$\varphi_T=\exp\left\{-\frac{3}{2}\frac{E_R}{k\theta}\left[\frac{1}{4}+\frac{1}{x^2}\int_0^x\frac{udu}{e^u-1}\right]\right\},$$

where $x=\theta/T$.

ABSTRACTS

In this section are printed the abstracts of Articles that have been forwarded to The American Institute of Physics for publication in THE PHYSICAL REVIEW. In quoting information obtained from this section before the appearance of the corresponding Article, reference should be made to "Physical Review (to be published)" rather than to this Journal.

THERMODYNAMICS OF RADIATIVE EMISSION PROCESSES. M. A. Weinstein, Lamp Research Laboratory, General Electric Company, Nela Park, Cleveland, Ohio (Received March 3, 1960).

A basic assumption implicit in the application of thermodynamics to the electromagnetic field is that the laws of thermodynamics are locally valid for radiative emission and absorption processes. This means that a certain minimum amount of entropy must be created by the radiative process itself. It is shown, by considering the extreme case in which the spontaneous emission of a natural spectral line is the only process taking place, that this assumption is correct, and that its validity is essentially a consequence of the uncertainty principle as expressed by the reciprocal relationship between natural line breadth and lifetime.

CURRENT-CARRIER TRANSPORT AND PHOTOCONDUCTIVITY IN SEMICONDUCTORS WITH TRAPPING. W. van Roosbroeck, Bell Telephone Laboratories, Murray Hill, New Jersey (Received October 23, 1959; revised manuscript received March 28, 1960).

Fundamental differential equations are derived under the unrestricted approximation of electrical neutrality which admits trapping. Applied magnetic field is taken into account. The general transport equations derived hold without explicit reference to detailed trapping and recombination statistics. Modified ambipolar diffusivity, drift velocity, and lifetime function, which depend on two phenomenological differential "trapping ratios," apply in the steady state. The same diffusion length is shown to hold for both carriers, and a general "diffusion-length lifetime" is defined. Mass-action statistics are considered for cases of (one or) two energy levels. Certain "effective"—rather than physically proper—electron and hole capture and release frequencies or times that apply to concentration increments are defined, and a restriction from detailed balance to which they are subject is derived. Found widely useful is "capture concentration," the concentration of centers at equilibrium which are occupied times the fraction unoccupied. Criteria are given for minority-carrier trapping, recombination, and majority-carrier trapping, and for "shallow" and "deep" traps. Applications of the formulation include: the diffusion-length lifetime corresponding to the Shockley-Read electron and hole lifetimes, and that for recombination centers in the presence of (nonrecombinative) traps; linear and nonlinear steady-state and transient photoconductivity; the photomagnetoelectric effect; and drift of an injected pulse. The small- and large-signal nonlinearities that may occur with saturation of deep traps provide a single-level model for superlinearity. Photomagnetoelectric current is found to be decreased by minority-carrier trapping, through an increase in diffusion length. A simple general criterion is given for the local direction of drift of a concentration disturbance. With trapping, there may be "reverse drift," whose direction is normally that for the opposite conductivity type. With solutions of one type obtained for drift of an injected pulse, multiple trapping ultimately results in Gaussian mobile-carrier distributions which spread as if through diffusion and which drift at a fraction of the ambipolar velocity. With solutions of another type, related to reverse drift is the occurrence of local regions of mobile-carrier depletion which may in practice extend over appreciable distances.

ENTROPY AND CROSS RELAXATION IN SPIN SYSTEMS. A. E. Siegman, Stanford Electronics Laboratories, Stanford University, Stanford, California (Received February 25, 1960).

Several examples of cross relaxation and harmonic cross relaxation between magnetic resonance transitions, both nuclear and electronic, have recently been reported. In these experiments, the appropriate cross-relaxation rate equations have generally been invoked to predict the results observed. It is pointed out that if the phenomena can be described in thermodynamic terms using the spin temperatures, then the results can be predicted in a simple fashion by maximizing the spin entropy. A simple approximation for the entropy of a multilevel spin system in terms of the population differences

Δn_{ij} is derived and applied to a typical cross-relaxation problem.

EXCITONS AND THE ABSORPTION EDGE OF CADMIUM SULFIDE. D. G. Thomas, J. J. Hopfield, and M. Power, Bell Telephone Laboratories, Murray Hill, New Jersey (Received March 9, 1960).

Measurements of the absorption coefficient between 10 and 300 cm^{-1} have been made with crystals of CdS in polarized light between 20 and 300°K, at wavelengths near 5000 A. Analysis of the results at various temperatures near 70°K shows that the absorption is in agreement with that calculated for a process involving the simultaneous creation of an exciton and the absorption of a phonon, both particles having a small wave vector. This agreement is strong evidence that the conduction band minimum and the valence band maximum in CdS both occur at the center of the Brillouin zone.

PHOTOEMISSION FROM Si INDUCED BY AN INTERNAL ELECTRIC FIELD. R. E. Simon and W. E. Spicer, Radio Corporation of America Laboratories, Princeton, New Jersey (Received February 18, 1960).

External photoelectric emission from silicon with a threshold of response corresponding to the band gap (1.05 ev) has been observed from a back-biased p-n junction which had received a cesium surface treatment. This emission current is proportional to the intensity of the incident light. The spectral distribution of this field-induced photoemission has been simply related to the spectral distribution of the fundamental absorption of silicon.

ELECTRICAL AND OPTICAL INVESTIGATION OF ABSORPTION CENTERS IN RUTILE SINGLE CRYSTALS. K. G. Srivastava,* Laboratory for Insulation Research, Massachusetts Institute of Technology, Cambridge, Massachusetts (Received August 28, 1959; revised manuscript received March 21, 1960).

Absorption centers in single crystals of rutile, causing relaxation spectra in the low-frequency range, can be produced by thermal quenching or optical irradiation at the edge of the characteristic absorption region (4200 A). They are observed only when the ac field is applied parallel to the optic axis. The temperature dependence of the main dispersion peak indicates an activation energy of 0.18 ev. Introduction of silver or copper by thermal diffusion did not produce low-frequency absorption maxima.

*Present address: Allahabad University, Allahabad, India.

TRANSFER OF ELECTRIC CHARGES THROUGH RUTILE SINGLE CRYSTALS. K. G. Srivastava,* Laboratory for Insulation Research, Massachusetts Institute of Technology, Cambridge, Massachusetts (Received August 28, 1959; revised manuscript received March 21, 1960).

Electron transfer and onset of field emission has been investigated in TiO_2 single crystals with dc current-time characteristics parallel and perpendicular to the optic axis as functions of voltage, temperature, electrode material, and light absorption. The currents are much larger and field emission sets in at lower voltage when the field is parallel to the optic axis. Higher temperature favors the current transfer by increasing the carrier mobility. The effect of different electrode materials proved minor, except in the case of Ti, which as cathode raised the current by about one order of magnitude. Photoelectric measurements showed that, in the critical voltage region of incipient field emission, light absorption can apparently force the current reversibly into the field-emitting stage.

*Present address: Allahabad University, Allahabad, India.

MEASUREMENT OF THE EQUILIBRIUM CONCENTRATION OF LATTICE VACANCIES IN SILVER NEAR THE MELTING POINT. R. O. Simmons and R. W. Balluffi, University of Illinois, Urbana, Illinois (Received March 11, 1960).

Relative changes in macroscopic length, $\Delta L/L$, and x-ray lattice parameter, $\Delta a/a$, of a 99.999% silver bar have been measured from 14 to 956°C, using a rigid parallel pair of filar micrometer microscopes and a rotating-single-crystal x-ray method. The expansions agree within experimental precision (about $1:10^5$) at the lower temperatures. At the higher temperatures ($\Delta L/L - \Delta a/a$) progressively increases, showing that

atomic sites are added, corresponding to the thermal generation of vacancy-type defects. The concentration of added sites, $\Delta N/N = 3(\Delta L/L - \Delta a/a)$, at the melting point (obtained by a 4° extrapolation) is $(1.7 \pm 0.5) \times 10^{-4}$. This value is only 1/5.5 of the corresponding value found for aluminum by the same technique. For reasonable values of the binding energies of vacancy aggregates, it is concluded that more than 90% of these extra sites are present as single vacancies. For an entropy of formation of $(1.5 \pm 0.5)k$ an energy of formation for monovacancies of 1.09 ± 0.10 ev is obtained. This formation energy is slightly larger than half the activation energy for self-diffusion, as similar measurements have shown for aluminum and lead, and as quenching experiments have indicated for gold.

LINEAR ANTIFERROMAGNETIC CHAIN. T. W. Ruijgrok,* Department of Physics, University of Washington, Seattle, Washington, and S. Rodriguez, Department of Physics, University of Illinois, Urbana, Illinois (Received February 16, 1960).

The properties of the low-lying states of the antiferromagnetic chain are studied by means of a variational method. A trial wave function is exhibited which has an energy very close to that of the correct ground state and which displays a long-range order.

*On leave of absence from the Rijksuniversiteit, Utrecht, The Netherlands.

FAR-INFRARED ENERGY GAP MEASUREMENTS IN BULK SUPERCONDUCTING In, Sn, Hg, Ta, V, Pb, AND Nb. P. L. Richards* and M. Tinkham, Department of Physics, University of California, Berkeley, California (Received February 17, 1960).

Measurements of the onset of absorption due to excitation of electrons across the energy gap were made on a variety of superconductors. Using the onset of the main absorption edge as a measure of the energy gap, the values of $E_g(0)$, the energy gap at absolute zero, were found to be $(4.1 \pm 0.2)kT_c$ for indium, $(3.6 \pm 0.2)kT_c$ for tin, $(4.6 \pm 0.2)kT_c$ for mercury, $\leq 3.0kT_c$ for tantalum, $(3.4 \pm 0.2)kT_c$ for vanadium, $(4.1 \pm 0.2)kT_c$ for lead, and $(2.8 \pm 0.3)kT_c$ for niobium. The deviations of these values of the energy gap from the Bardeen-Cooper-Schrieffer value of $3.5kT_c$ are a fairly smooth function of the Debye temperature alone, but a less smooth one of the ratio of the Debye temperature to the critical temperature. Structure was found on the absorption curves of lead and mercury. Its interpretation is discussed in terms of possible states in the gap, anisotropy of the gap, and of a possible dielectric anomaly. The position of the main absorption edge seemed to scale with temperature according to the temperature dependence of the energy gap predicted by the Bardeen-Cooper-Schrieffer theory, and the structure appeared to have a roughly similar temperature dependence. The absorption curves for pure superconductors are compared with predictions based on the theory of the skin effect in the normal and superconducting states. Two alloy superconductors were measured. They appeared to have less well-defined gaps than the pure superconductors.

*Now at the Royal Society Mond Laboratory, Cambridge, England.

INTERPRETATION OF RELATIVE THERMOELECTRIC PHENOMENA AT LOW TEMPERATURES WITH SPECIAL CONSIDERATION OF THE EFFECTS OF COLD WORK ON COPPER. W. B. Pearson, Division of Pure Physics, National Research Council, Ottawa, Canada (Received February 23, 1960).

Formulas first derived by Kohler and more recently discussed by MacDonald are used to account for relative thermoelectric effects at low temperatures in pure metals, dilute alloys, and cold-worked copper. Since calculations based on these formulas give diffusion thermoelectricity, phonon drag contributions to thermoelectricity should appear as differences between the calculated and measured curves of thermoelectric power as a function of temperature.

LCAO TREATMENT OF EXCITON STRUCTURE IN ALKALI HALIDE CRYSTALS. R. A. Pappert,* Cornell University, Ithaca, New York (Received July 16, 1959; revised manuscript received March 7, 1960).

A Heitler-London treatment is applied to the transfer mechanism which has been traditionally associated with the fundamental absorption of alkali halide crystals. In particular, detailed

calculations are made for NaCl using the free-atom Na 3s Hartree-Fock solution for the one-electron transfer function and the free-ion Hartree-Fock solutions for the remaining one-electron functions. The energy and oscillator strength so determined are irreconcilable with experiment, showing that the free-atom Na 3s function cannot be used in conjunction with the transfer model if the model is to yield sensible results. In a very semiquantitative way it is shown that an electron-hole overlap integral of about 0.1 coupled with Overhauser's exciton model leads to a doublet structure which is in agreement with experimental results for many of the chlorides, bromides, and iodides. These findings do not distinguish the transfer model from the "excitation model."

*Present address: Convair, San Diego, California.

GAUGE-INVARIANT FORMULATION OF THE BARDEEN-COOPER-SCHRIEFFER THEORY OF SUPERCONDUCTIVITY. T. A. Oliphant and W. Tobocman, The Rice Institute, Houston, Texas (Received February 29, 1960; revised manuscript received March 30, 1960).

The Bardeen-Cooper-Schrieffer theory of superconductivity is reformulated in a way which is manifestly gauge invariant. The method used is to pair electrons having equal and opposite angular momentum rather than equal and opposite linear momentum.

ANTIFERROMAGNETIC SUPEREXCHANGE EFFECT. R. K. Nesbet, Department of Physics, Boston University, Boston, Massachusetts (Received December 21, 1959).

The delocalization effect recently proposed by Anderson as the principal contribution to the antiferromagnetic coupling of magnetic ions is analyzed by methods used in an earlier paper to derive the Heisenberg exchange operator formalism for both ferromagnetic and antiferromagnetic coupling. It is shown that Anderson's effect can be included, together with the superexchange correlation effect treated previously, as contributions to the Heisenberg exchange integral for ions of arbitrary spin. In the case of the antiferromagnetic oxides MnO, FeO, CoO, and NiO, these two effects are found to be of comparable size, although the correlation effect is larger and determines the qualitative behavior of the Néel temperatures, which increase with decreasing spin through this sequence of transition metal ions. Agreement with the experimental Néel temperatures is significantly improved by including both effects.

THEORY OF DIAMAGNETISM OF GRAPHITE. J. W. McClure, Parma Research Laboratory, Union Carbide Corporation, Cleveland, Ohio (Received March 14, 1960).

The conduction-electron diamagnetism has been calculated for the three-dimensional band structure of graphite. The magnetic energy levels are found and the susceptibility calculated by analytically carrying out the free-energy sum. Agreement with experiment is found for values of the band parameters nearly equal to those which give agreement with the de Haas–van Alphen effect and other phenomena. The value of γ_0 is found to be 2.8 ± 0.1 ev. The results indicate the γ_1 is about 0.27 ev and Δ is about 0.025. The other band parameters do not have an important influence upon the value of the susceptibility. The relation to the general treatments of conduction-electron diamagnetism is also discussed.

BREADTH OF THE *F* BAND IN NaCl. A. M. Karo, Lawrence Radiation Laboratory, Livermore, California, C. W. McCombie, Department of Natural Philosophy, University of Aberdeen, Aberdeen, Scotland, and A. M. Murray, Department of Physics, The University, Sheffield, England (Received March 1, 1960).

The breadth of the *F* band in NaCl is calculated for various temperatures, primarily in order to investigate the status of the semiempirical configuration coordinate treatment of such problems. The main new feature of the calculation, which involves no adjustable parameters, is the use of the realistic normal modes employed in the Born-Blackman theory of specific heats. The eigenvectors as well as the eigenfrequencies of these modes are used. Modifications of the modes due to the missing ion at the *F* center are ignored. The coupling to the *F* center is determined from electrostatic forces on individual ions. Simpson's *F*-center wave functions are used and the calculated breadths are all about

85% of the experimental values. It is found that the main contributions to the breadth come from modes in a fairly small range of frequencies (much lower than the frequencies of the longitudinal optical modes considered in previous calculations) which includes the empirical configuration coordinate frequency. This last result helps to clarify the relation of the hypothetical configuration coordinate mode to the actual modes of lattice vibration.

THERMAL RESISTANCE DUE TO POINT DEFECTS AT HIGH TEMPERATURES. P. G. Klemens, Westinghouse Research Laboratories, Beulah Road, Churchill Borough, Pittsburgh, Pennsylvania (Received March 7, 1960).

An expression is obtained for the lattice thermal conductivity at high temperatures in the limit when the scattering of phonons by point defects is stronger than by umklapp processes. The latter limit the phonon mean free path at low frequencies and most of the heat is transported at frequencies such that the point defect and umklapp mean free paths are equal. The conductivity varies as $(AT)^{-1/2}$, where A is proportional to the strength of the point defect scattering and T is the temperature. The theory is in rough agreement with the thermal conductivity of Ge-Si alloys, measured by Steele and Rosi.

RADIATION EFFECTS OF BOMBARDMENT OF QUARTZ AND VITREOUS SILICA BY 7.5-kev TO 59-kev POSITIVE IONS. R. L. Hines and R. Arndt, Northwestern University, Evanston, Illinois (Received December 14, 1959; revised manuscript received April 8, 1960).

Bombardment of quartz or vitreous silica by positive ions produces a surface layer of altered refractive index whose depth and refractive index is found from reflection coefficient measurements at 650 mμ, 600 mμ, 550 mμ, 500 mμ, and 450 mμ. The layer depths and the changes in refractive index versus integrated flux are given for H_2^+, D_2^+, He^+, Ne^+, A^+, Kr^+, and Xe^+ ions with energies from 7.5 kev to 59 kev. All bombardments give approximately equal changes in refractive index for a given energy input per unit volume of material as long as the ion energy is low enough so that energy loss by ionization is negligible. The changes produced by ion bombardment are attributed to direct lattice displacements and are shown to be consistent with the known changes produced in quartz and vitreous silica by fast neutron bombardment. Thermal spikes produced by knock-on atoms in quartz and vitreous silica are experimentally shown to be unimportant for knock-on energies near 45 kev.

FUNDAMENTAL LATTICE DISPERSION FREQUENCIES OF NaCl AND KCl at 82°K. Marvin Hass, U. S. Naval Research Laboratory, Washington, D. C. (Received February 17, 1960).

The infrared dispersion frequencies of NaCl and KCl at 82°K were measured by infrared absorption of thin films and were found to be 170 ± 2 cm^{-1} and 149 ± 2 cm^{-1}, respectively. These values can be compared with those predicted by formulas of Szigeti, Odelevski, Lundqvist, and others relating the dispersion frequency to the elastic and dielectric constants. Good agreement seems to be obtained using the Szigeti formula or a combination of the Lundqvist and Odelevski formulas at low temperatures where anharmonic effects are small.

SURFACE ELASTIC WAVES IN CUBIC CRYSTALS. Denos C. Gazis and Robert Herman, Research Laboratories, General Motors Corporation, Warren, Michigan, and Richard F. Wallis, U. S. Naval Research Laboratory, Washington, D. C. (Received March 7, 1960).

A theoretical investigation of surface elastic waves in cubic crystals has been carried out using a theory developed by Stoneley. The range of elastic constants for which Rayleigh-type surface waves exist on a (100) free surface has been determined. For other allowed values of the elastic constants, generalized Rayleigh waves exist which are characterized by complex attenuation constants. In either case waves may not be propagated in certain directions parallel to the surface depending on the values of the elastic constants. A lattice dynamical theory of surface waves has been developed for a monatomic simple cubic lattice with nearest and next nearest neighbor central forces and angle-bending forces involving successive nearest neighbors. The surface waves exhibit dispersion when the wavelength is comparable to the lattice spacing. In the case of Rayleigh waves a critical wavelength exists, in general, such that for

shorter wavelengths the atomic displacements show a reversal in phase between successive layers parallel to the surface.

COMPARISON OF STRUCTURES OF SURFACES PREPARED IN HIGH VACUUM BY CLEAVING AND BY ION BOMBARDMENT AND ANNEALING. D. Haneman, Barus Physics Laboratory, Brown University, Providence, Rhode Island (Received December 18, 1959).

A comparison has been made for a bismuth telluride crystal of the structure of (0001) surfaces produced by cleaving in high vacuum, with similar surfaces prepared by the ion-bombardment and annealing technique. The low-energy electron-diffraction patterns of the two surfaces were found to be similar and of approximately the same intensities. Only integral order beams were present. It is concluded that both methods produce essentially clean surfaces with the same atomic arrangements, in the case of this crystal.

ADSORPTION AND BONDING PROPERTIES OF CLEAVAGE SURFACES OF BISMUTH TELLURIDE. D. Haneman, Barus Physics Laboratory, Brown University, Providence, Rhode Island (Received February 16, 1960).

No measurable adsorption of oxygen, nitrogen, or carbon monoxide was found for any of the clean surfaces produced. Water vapor has a very low sticking coefficient of the order of 10^{-5}. The results are discussed in terms of the chemical bonding of bismuth telluride. It is concluded that the atoms on cleavage faces are in a saturated-bond condition.

DECREASE OF F-CENTER PHOTOCONDUCTIVITY UPON BLEACHING. Fred C. Hardtke, Allen B. Scott, and Robert E. Woodley, Department of Chemistry, Oregon State College, Corvallis, Oregon (Received February 17, 1960).

A quantitative study of the rapid decrease in photoconductivity accompanying the relatively less rapid bleaching of F centers in additively colored KCl is reported. The experimental observations agree, except during very early stages of bleaching, with an equation for the variation of sensitivity with total light absorbed derived upon the assumption that negative-ion vacancies are created and traps of smaller cross section are filled during bleaching. Except during early stages, where several kinds of traps may be present in low concentration, only one kind of trap other than the negative-ion vacancy need be considered.

The effects of added divalent ions, both positive and negative, upon photoconductivity are reported.

SYMMETRY OF THE GREEN PHOSPHORESCENCE OF HEAT-PRETREATED COLORED KCl CRYSTALS. A. Halperin and N. Lewis, Department of Physics, The Hebrew University, Jerusalem, Israel (Received March 2, 1960).

On thermal pretreatment in the open air (at 700°C), the phosphorescence of KCl crystals after x-ray coloring at liquid-air temperature turned from violet to green. While the former phosphorescence showed no anisotropy, the green was found to become partially polarized after irradiation with [011] light. The irradiation also induced dichroic absorption at 3650 A. Both the polarization in the phosphorescence and the dichroic absorption persisted up to nearly 200°K.

The polarized light bleached the component of the 3650A absorption in parallel to it, but enhanced the green phosphorescence with the main effect on the perpendicular component.

It is suggested that oxygen which diffused into the crystal during the heat treatment is responsible for the asymmetric center.

TRAPPING AND DIFFUSION IN THE SURFACE REGION OF CADMIUM SULFIDE. James J. Brophy, Physics Division, Armour Research Foundation, Chicago, Illinois (Received February 19, 1960).

In lightly doped single-crystal CdS illuminated with 4400A radiation, hole-electron pairs generated at the surface diffuse into the crystal until the hole is trapped. The electrons experience multiple retrapping until they disappear through recombination. Current noise and photoconductivity measurements are used to study these processes. The noise data establish the ambipolar diffusion length as 30 microns, confirm that diffusion is important through the appearance of an $f^{-3/2}$ trend in the noise spectra, and show that discrete traps are located the same distance below the conduction band in the surface regions

as in the bulk. Discrete trap levels at 0.35, 0.40, and 0.43 ev below the conduction band are observed in the surface region. Trap densities of 10^6 traps/cm^3 volt, an order of magnitude greater than that in the bulk, are determined. The trap frequency factors are of the order 10^{10} sec^{-1}.

INFRARED ABSORPTION AND VALENCE BAND IN INDIUM ANTIMONIDE. G. W. Gobeli* and H. Y. Fan, Purdue University, Lafayette, Indiana (Received March 14, 1960).

Infrared absorption is studied at near liquid helium temperature for n- and p-type degenerate samples of various carrier concentrations. The absorption in p-type samples, at photon energies larger than the energy gap, depends on the hole concentration. The results show that the valence band is warped and that the energy at $k=0$ is very close to the maximum energy of the band. A step in the absorption of n-type samples is observed which gives an estimate of $\sim 0.012m$ for the effective mass of light holes. The long-wavelength absorption in p-type samples is characteristic of intervalence band transitions.

*Now at Bell Telephone Laboratories, Murray Hill, New Jersey.

MAGNETIC AFTER-EFFECT IN IRON DUE TO MOTION OF DISLOCATIONS. Giuseppe Biorci, Andrea Ferro,* and Giorgio Montalenti, Istituto Elettrotecnico Nazionale "Galileo Ferraris," Centro Studi per l'Elettrofisica del C. N. R., Torino, Italy (Received January 29, 1959; revised manuscript received February 25, 1960).

The magnetic after-effect in iron at high temperatures due to motion of dislocations is investigated. The specimens, consisting of a few large crystals, are examined, some after a careful annealing and some after a small plastic deformation. The intensity of the after-effect is measured as the horizontal displacement (viscosity field) between two magnetization curves: one taken immediately after demagnetization, and the other taken a long time later.

On annealed Armco iron the magnetic viscosity begins to appear above 320°C, reaching 0.3 amp-turn/m at about 450°C. On the other hand, in cold-worked specimens the viscosity field is appreciably larger and is already observable below 200°C. Similar results are obtained on high-purity electrolytic iron. Comparison with the relaxation of elastic modulus, occurring in the same temperature range, seems to confirm that the observed magnetic viscosity is due to dislocation motion.

An interpretation of the phenomenon, on the basis of the Vicena theory concerning the dependence of the coercive force on the dislocation density, is given.

*Istituto Nazionale di Fisica Nucleare, Sezione di Torino, Torino, Italia.

HALL COEFFICIENT IN TIN-BISMUTH ALLOYS. P. A. Bender and W. F. Love, Physics Department, University of Colorado, Boulder, Colorado (Received March 7, 1960; revised manuscript received April 8, 1960).

The Hall coefficient in a series of tin-bismuth alloys has been measured at 75°K as a function of composition. The results are compared with previous results on the band structure in these alloys. They indicate that hole conduction is present though not always dominant throughout the range of alloys studied.

WEAK-FIELD MAGNETORESISTANCE IN p-TYPE LEAD TELLURIDE AT ROOM TEMPERATURE AND 77°K. Robert S. Allgaier, U. S. Naval Ordnance Laboratory, White Oak, Silver Spring, Maryland (Received March 9, 1960).

The weak-field magnetoresistance of six single crystals of p-type PbTe was measured at room temperature and 77°K. The general predictions of weak-field theory were precisely obeyed in the range of magnetic-field intensities for which the theory should apply. In stronger fields at 77°K, deviations from weak-field behavior of three types were observed which agree with the Gold-Roth theory of magnetoresistance at arbitrary magnetic-field strengths. The weak-field data at both temperatures conformed very closely to the ⟨111⟩ ellipsoid-of-revolution multivalley model with values of the mass and scattering-time anisotropy parameter K of 4.7 (room temperature) and 4.2 (77°K), and with values of the statistical-scattering factor G of 1.17 (room temperature) and 1.016 (77°K). The dependence of the magnetoresistance at 77°K on the Fermi level

was used to make a rough calculation of the effective-mass components of the carriers in p-type PbTe which led to a total density-of-states effective mass of 0.16 times the free electron mass. Some preliminary room-temperature magnetoresistance data on n-type PbTe and on PbS and PbSe were also obtained which revealed that the longitudinal magneto resistance in both n- and p-type PbS and PbSe was an order of magnitude smaller than in p-type PbTe.

IONIZATION AND CHARGE TRANSFER IN PROTON-HYDROGEN ATOM COLLISIONS. Wade L. Fite, R. F. Stebbings, David G. Hummer,* and R. T. Brackmann, John Jay Hopkins Laboratory for Pure and Applied Science, General Atomic, San Diego, California (Received March 14, 1960).

The cross sections for charge transfer and for ionization in collisions between protons and hydrogen atoms have been determined over the energy range from 400 to 40 000 ev. The experiment used modulated crossed-beam techniques. Experimental results are compared with several theoretical predictions.

*Present address: Department of Physics, University College, London, England.

CHARGE TRANSFER AND ELECTRON PRODUCTION IN H^-+H COLLISIONS. David G. Hummer,* R. F. Stebbings, and Wade L. Fite, John Jay Hopkins Laboratory for Pure and Applied Science, General Atomic, San Diego, California, and Lewis M. Branscomb, National Bureau of Standards, Washington, D. C. (Received March 14, 1960).

The cross sections for charge transfer and electron production in collisions between hydrogen atoms and hydrogen negative ions (H^-) have been measured over the energy range 100 to 40 000 ev using modulated atomic-beam techniques in a crossed-beam experiment. Agreement of the experimental results with the perturbed-stationary-states calculation for charge transfer of Dalgarno and McDowell is quite satisfactory.

*Present address: Department of Physics, University College, London, England.

THEORY OF ADIABATIC SUSCEPTIBILITY. Tsunenobu Yamamoto,* Department of Chemistry, University of Oregon, Eugene, Oregon (Received February 26, 1960).

A general proof of the equivalence between χ_S and χ_{iso} is presented in the framework of statistical thermodynamics. It is based on the observation that transitions do occur during adiabatic processes due to the neglected small interactions which can hardly be included in the actual Hamiltonian. A new expression is found for χ_{iso} which is proved to coincide with χ_S and which is rederived straightforwardly from the ergodic theorem. As an example, a system of spins with a magnetic interaction under a strong magnetic field is considered by means of the perturbation method and shown to give consistent results.

*On leave from the Department of Chemistry, Faculty of Science, University of Kyoto, Kyoto, Japan.

CROSS SECTION FOR FORMATION OF DOUBLY-IONIZED HELIUM BY ELECTRON IMPACT. H. E. Stanton and J. E. Monahan, Argonne National Laboratory, Lemont, Illinois (Received March 7, 1960).

The cross section for the formation of He^{++} by electron impact has been measured relative to that of He^+ for electron energies between 100 ev and 2400 ev. A relative minimum in the measured ratio of the yields of He^+ to He^{++} at an energy of about 600 ev is believed to be real. For incident energies above 1400 ev the results are consistent with a constant value of 145 for this ratio.

COLLISION PROCESSES IN MIXTURES OF MERCURY VAPOR AND FOREIGN GASES. Donald E. Cunningham* and Leonard O. Olsen, Case Institute of Technology, Cleveland, Ohio (Received October 26, 1959; revised manuscript received April 4, 1960).

An extensive and quantitative study of collision processes occurring in mercury vapor–foreign gas mixtures has been performed. Measurement of the polarization of mercury resonance radiation allows a determination of the probability for quenching, adiabatic depolarizing, and nonadiabatic depolarizing collisions. The use of a photomultiplier circuit in securing the data, and of an

IBM 610 ccmputer in analysis of the data, made the breadth of this study possible. The most important result is that no adiabatic depolarization is needed to account for the results obtained for all foreign gases studied. All quenching and depolarizing probabilities obtained in this study, and in earlier studies at this laboratory, are summarized in tabular form.

*Now at American Institute of Physics, 335 East 45 Street, New York, New York.

OPTICAL PUMPING OF HELIUM IN THE $^3S_1$ METASTABLE STATE. F. D. Colegrove and P. A. Franken, Harrison M. Randall Laboratory of Physics, The University of Michigan, Ann Arbor, Michigan (Received March 14, 1960).

The alignment of He^4 atoms in the ($n=2$, metastable) $^3S_1$ state is described. Metastable atoms are produced by an rf discharge in a glass tube containing a few mm of pure helium, and the one-micron pumping light ($2\,^3P - 2\,^3S$) is provided by a helium lamp. A resonance signal is obtained from radio-frequency disorientation by monitoring the transmitted pumping light. The double maximum line shape of this signal for strong rf magnetic fields is discussed. Included also is a discussion of the angular dependence of the signal when unpolarized light is used and an explanation of the inversion of the resonance signal for certain densities of the metastable helium atoms.

The measured relaxation time of the oriented metastable atoms in the discharge is about 2.5×10^{-4} second and the pumping time is about a millisecond. A method is proposed and initial measurements are given for the cross section for destruction of metastable helium atoms by collision with foreign gas atoms. The application of optical pumping in helium to the measurement of weak magnetic fields is also discussed.

EFFECTS OF ADDED GASES ON THE SENSITIZED FLUORESCENCE SPECTRUM OF A Hg-Tl MIXTURE. Richard A. Anderson* and Robert H. McFarland, Department of Physics, Kansas State University, Manhattan, Kansas (Received October 29, 1959; revised manuscript received March 14, 1960).

An investigation of the sensitized fluorescence of a mercury-thallium mixture without and with the addition of argon and helium gases is discussed. Data taken without the addition of foreign gases are used to extend the theory of Frish and Karaulinya to a mercury-thallium mixture. Relative collision cross sections for the excitation of the thallium energy states, $9\,^2S_{1/2}$, $7\,^2D_{5/2,3/2}$, $8\,^2S_{1/2}$, $6\,^2D_{5/2}$, and $6\,^2D_{3/2}$ were calculated for mercury-thallium collisions. Data taken with the addition of argon and helium gases are given to indicate the variation of the intensity of the thallium lines as a function of argon and helium gas pressures at one constant thallium and three mercury temperatures. The explanation of the results depends on the role of mercury $6\,^3P_1$ excited atoms, metastable atoms, and mercury molecules in collision with thallium atoms for energy exchange, and also requires the use of Winans' partial selection rule and other generally accepted ideas concerning energy transfer, emission, and absorption.

*Present address: University of Missouri School of Mines and Metallurgy, Rolla, Missouri.

DISSIPATION IN QUANTUM MECHANICS. THE HARMONIC OSCILLATOR. I. R. Senitzky, U. S. Army Signal Research and Development Laboratory, Fort Monmouth, New Jersey (Received February 29, 1960).

The need for a quantum-mechanical formalism for systems with dissipation which is applicable to the radiation field of a cavity is discussed. Two methods that have been used in this connection are described. The first, which starts with the classical Newtonian equation of motion for a damped oscillator and applies the conventional formal quantization techniques, leads to an exact solution; but subsequent discussion shows that this method is invalid, the results being unacceptable from a quantum-mechanical viewpoint. The second method, which considers the interaction of two systems, the lossless oscillator and the loss mechanism, is adopted in the present article. No special model is used for the loss mechanism, but this mechanism is assumed to have a large number of densely-spaced energy states.

The approximations with respect to the loss mechanism that underlie the concept of dissipation are discussed. These approximations are then applied to the analysis, and a differential equation for a coordinate operator of the harmonic oscillator is obtained which has the for-

mal appearance of the Newtonian equation of motion for a driven damped harmonic oscillator, the driving term being an operator referring to the loss mechanism. The presence of the driving term is responsible for the difference between the present theory and that of the first method mentioned above. A solution of the differential equation for the coordinate operator is given explicitly. An examination of the physical significance of the solution shows that the driving term is responsible not only for the thermal fluctuations which are due to the loss mechanism, but also for the proper commutation relationship of the conjugate coordinates of the oscillator and for its zero-point fluctuations.

A generalization of the solution to provide for a classical driving force and coupled atomic systems is given. The results are then restated in a form that refers to the loss mechanism only through the two parameters by which it is usually described—the dissipation constant and the temperature.

ENERGY LEVELS OF THE SILICON ISOTOPES FROM INELASTIC PROTON SCATTERING. R. E. White,* Laboratory for Nuclear Science, Massachusetts Institute of Technology, Cambridge, Massachusetts (Received February 23, 1960; revised manuscript received March 24, 1960).

Energy levels of the stable isotopes of silicon, Si^{28}, Si^{29}, and Si^{30}, up to 6.5-Mev excitation have been investigated by studying the inelastic scattering of 7.5-Mev to 8.5-Mev protons from a thin silicon-dioxide target with a broad-range magnetic spectrograph. Several new levels are reported, and the significance of the Si^{28} results is discussed in regard to a previously proposed interpretation of the level spectrum.

*Now at Atomic Energy Research Establishment, Harwell, England.

POLARIZATION OF PROTONS SCATTERED FROM C^{12}. T. A. Tombrello, R. Barloutaud,* and G. C. Phillips, The Rice Institute, Houston, Texas (Received February 19, 1960).

The polarization of protons elastically scattered from carbon in the energy region between 4.65 and 5.0 Mev has been measured by double scattering from carbon targets. These results, together with the findings at Harwell by Evans and Grace, show that the polarizations predicted from the phase-shift analysis are somewhat in error. This disagreement may be explained by making small changes in the splitting of the P- and D-wave phase shifts without seriously affecting the fit to the angular distributions. It was found that in the energy range from 3.0 to 4.0 Mev the D-wave phases required from 1° to 4° additional splitting, while in the range from 4.0 to 5.0 Mev the splitting of the P-wave phases had to be reduced by 4°. These modified phase shifts give a revised contour map of spin polarization versus energy and angle.

*Now at Centre d'Etudes Nucléaires de Saclay, France.

EXCITED STATES OF P^{32}. D. Piraino, C. H. Paris,* and W. W. Buechner, Physics Department and Laboratory for Nuclear Science, Massachusetts Institute of Technology, Cambridge, Massachusetts (Received March 11, 1960).

The proton groups from the $P^{31}(d,p)P^{32}$ reaction have been studied at angles of 30, 50, 70, and 90 degrees. The incident deuteron energy was 6 Mev, and the protons were analyzed with a broad-range magnetic spectrograph. Fifty-two excited states were found in the region between the ground state and 6.2 Mev in P^{32}.

*Now with High Voltage Engineering Corporation, Amersfoort, Netherlands.

STATES OF EVEN-EVEN NUCLEI IN THE NEAR-HARMONIC REGION: SPECTRA OF Rn^{218}, Rn^{220}, AND Rn^{222}. F. S. Stephens, F. Asaro, and I. Perlman, Lawrence Radiation Laboratory and Department of Chemistry, University of California, Berkeley, California (Received March 2, 1960).

Gamma-ray singles and coincidence spectra have been measured in the alpha decay of Ra^{222}, Ra^{224}, and Ra^{226}. Excluding the prominent transitions from the first excited states, the energies (and abundances relative to total α emission) of the observed radiations were: Ra^{222}: 325 kev (8.4×10^{-5}), 475 kev (7×10^{-5}), 525 kev (2×10^{-5}), and 798 kev (2.5×10^{-4}); Ra^{224}: 290 kev (9×10^{-5}), 410 kev (4×10^{-5}), 650 kev (6×10^{-5}); Ra^{226}: 260 kev (0.9×10^{-4}), 420 kev (7×10^{-6}), 450 kev (3×10^{-6}), 610 kev (1.0×10^{-5}). The observed gamma-gamma coincidences were Ra^{222}: 325-325 kev, 325-475 kev, and 325-525 kev; Ra^{224}:

241-290 kev and 241-410 kev; Ra^{226}: 188-260 kev and 188-420 kev. It was not strictly determined that the Ra^{222} radiations were not due to other members of the Th^{226} family. These data have been used to deduce the following levels, spins, and parities in the daughter Rn nuclides: Rn^{218}: 650 kev, 2+; 800 kev, 1-; and, possibly, 850 kev, 4+. Rn^{220}: 530 kev, 2+; and 650 kev, 1-. Rn^{222}: 448 kev, 2+; and 610 kev, 1-. The 2+ states in Rn^{220} and Rn^{222} have been previously assigned by Scharff-Goldhaber. These results are incorporated in a general energy level systematics of even-even nuclei in the heavy element region.

DECAY OF 6.3-min Br^{78}. William R. Pierson and Charles D. Coryell, Department of Chemistry and Laboratory for Nuclear Science, Massachusetts Institute of Technology, Cambridge, Massachusetts (Received February 26, 1960).

The nuclide 6.3-min Br^{78} has been made by the reactions (γ, n), $(n, 2n)$, (p, n), $(d, 2n)$, and (α, n), and its decay properties have been investigated by positron decay-curve analysis, by application of a standard chemical isomer separation procedure, by searching for conversion electrons, and by studying the gamma-ray and positron-gamma-coincidence spectra. The early portion of the positron decay curve exhibited a single 6.25 ± 0.2 min component, and no active daughter of this species was chemically separable from active CBr_4. Conversion electrons were not found, and soft gamma rays were shown to be absent. There are 12-kev x rays, of intensity about 0.05 relative to the positrons and therefore presumed to be K x rays of Se resulting from electron capture. These results show that 6.3-min Br^{78} has no daughter isomer and probably no >10-sec parent isomer. There is a 615-kev gamma ray, in coincidence with positrons, and of intensity 0.139 that of all positrons, representing decay of Br^{78} to Se^{78} in the 615-kev 2+ state. However, no evidence for decay to Se^{78} in the 1.32-Mev state could be found. From these data it was deduced that 6.3-min Br^{78} decays 81% by positron emission and 6% by electron capture to ground-state Se^{78}, 11% by positron emission and 2% by electron capture to Se^{78} in the 615-kev state, and <1% to Se^{78} in the 1.32-Mev state. The disintegrations or Br^{78} to Se^{78} in the ground state and 615-kev state have logft values of 4.8 and 5.2, respectively, indicating that the spin of ground-state Br^{78} is 1, with even parity. The absence of isomerism is discussed in terms of the locations of expected energy levels, with reference to the known locations of these levels in Br^{80}.

TENSOR FORCE EFFECTS IN ODD-ODD NUCLEI. Neal D. Newby, Jr., Lawrence Radiation Laboratory, University of California, Berkeley, California (Received March 3, 1960).

A study of the ground-state coupling rules in odd-odd nuclei reveals that in almost all cases where Nordheim's weak rule is applicable both particles have spin and orbital angular momentum parallel rather than antiparallel. A semiclassical model is employed to indicate that an attractive n-p tensor force will tend to break down Nordheim's weak rule. Examination of the quantum mechanical formula substantiates this finding.

DECAY OF $_{66}Dy^{166}$. R. G. Helmer and S. B. Burson, Argonne National Laboratory, Lemont, Illinois (Received March 10, 1960).

Samples of Dy^{166} were produced by successive neutron capture in stable Dy^{164}. This isotope decays by beta-ray emission with an 80.2-hr half-life to states in Ho^{166}. This isotopic assignment of previous authors is confirmed. Separations of the parent and daughter activities were carried out by use of an ion-exchange column. Scintillation studies were made with a 256-channel scintillation coincidence spectrometer. Internal-conversion electrons were measured in magnetic spectrographs with permanent magnets and the continuous beta spectra were observed with a 180° magnetic spectrometer with a variable field. The seven gamma-ray transitions observed had energies of 28.1, 54.2, 82.5, 288, 344, 375, and 428 kev. Beta-ray branches of 481 and 402 kev were observed with the magnetic spectrometer; two others of 114 and 56 kev are postulated for the decay scheme. The decay scheme presented indicates the existence of five levels in $_{67}Ho^{166}$ at 0 (0^-), 54 (2^-), 82 (1^-), 370, and 428 (1^+) kev. The ground state and first two excited states are interpreted as members of a rotational band with $K = 0$. This interpretation implies that in odd-odd nuclei the level sequence can be inverted for the first two excited states of such a band.

EVIDENCE FOR SMALL DEVIATIONS IN THE ALLOWED POSITRON SPECTRUM OF Zr^{89}. J. H. Hamilton, Physics Department, Indiana University, Bloomington, Indiana and Vanderbilt University, Nashville, Tennessee, L. M. Langer, Physics Department, Indiana University, Bloomington, Indiana, and W. G. Smith, Physics Department, Indiana University, Bloomington, Indiana and Purdue University, Lafayette, Indiana (Received February 23, 1960).

The decay of Zr^{89} has been carefully studied with magnetic and scintillation spectrometers with special emphasis on the detailed shape of the positron spectrum. The decay scheme has been verified. The positron decay is by a single, allowed group followed by a single 915-kev gamma ray. The Zr^{89} spectrum has a nonstatistical shape corresponding to an excess of low-energy beta particles. Theoretical refinements for screening and finite deBroglie wavelength were applied but were found to be much too small to explain the observed deviation from a statistical spectrum. The same shape factor that was found to fit the In^{114}, Y^{90}, P^{32}, and Na^{22} data (in addition to the once forbidden, unique shape factor for Y^{90}) also fits the Zr^{89} data, i.e., $(1+b/W)$ with $0.2 \leq b \leq 0.4$. It is significant that the deviation has the same direction and approximate magnitude as was found for the electron spectra.

SOME (d,p) AND (d,t) REACTIONS ON MAGNESIUM ISOTOPES. E. W. Hamburger* and A. G. Blair, University of Pittsburgh, Pittsburgh, Pennsylvania (Received February 16, 1960).

Natural and enriched magnesium targets were bombarded with 14.8-Mev deuterons from the University of Pittsburgh cyclotron. The reaction products were magnetically analyzed and detected in a scintillation counter. Angular distributions from 10° to 60° (in some cases to 90°) were obtained for most of the following reactions: $Mg^{24}(d,p)$ to the 0-, 1.61-, and 1.96-Mev levels of Mg^{25}, $Mg^{25}(d,t)$ to the 0-, 1.37-, 4.12-, 4.24-, 5.24-, 6.01-, 7.33-, and 7.60-Mev levels of Mg^{24}, and $Mg^{26}(d,t)$ to the 0-, 0.58-, 0.98-, 1.61-, 1.96-, 2.56-, 2.74-, 2.80-, 3.40-, and 3.90-Mev levels of Mg^{25}. The level at 7.60 Mev in Mg^{24} has not been reported before. The observed angular distributions are compared to stripping theory, and l values and absolute reduced widths are extracted. An anomaly in the angular distribution was found for the transitions between the Mg^{24} and Mg^{25} ground states and was studied as a function of incident deuteron energy. The reduced widths obtained are compared to the predictions of the rotational model, and, in general, good agreement is found; however, an admixture (of $\approx 15\%$) of higher rotational bands was found in the Mg^{26} ground-state wave function.

*Now at Departamento de Fisica, Faculdade de Filosofia, Universidade de São Paulo, São Paulo, Brazil.

RESULTS OF STRIPPING ANALYSIS OF THE $Co^{59}(d,p)Co^{60}$ REACTION. H. A. Enge, D. L. Jarrell, and C. C. Angleman, Physics Department and Laboratory for Nuclear Science, Massachusetts Institute of Technology, Cambridge, Massachusetts (Received February 29, 1960).

The MIT-ONR electrostatic generator and broad-range magnetic spectrograph have been used to investigate proton groups produced by bombarding thin cobalt targets with 6.0-Mev deuterons. The angular distributions of the twenty-eight most intense proton groups corresponding to as many levels in Co^{60} were analyzed in terms of stripping theory to determine the orbital angular momentum of the captured neutron. The Q values of the (d,p) reaction were measured for sixty levels of Co^{60}. The ground-state Q value was found to be 5.262 ± 0.011 Mev.

PHOTONEUTRON REACTIONS: C^{12}, N^{14}, O^{16}, AND F^{19} NEAR THRESHOLD. K. N. Geller, J. Halpern, and E. G. Muirhead,* Physics Department, University of Pennsylvania, Philadelphia, Pennsylvania (Received February 25, 1960).

Photoneutron reactions in carbon, nitrogen, oxygen, and fluorine have been studied in the region of threshold using improved efficiency for the detection of the residual activity. The betatron energy calibration used is based on thresholds of deuterium, bismuth, copper, and for scattering from the 15.12-Mev level in carbon. Results show that the thresholds for nitrogen and fluorine correspond well with the expected values for the respective neutron separation energies. For oxygen, the position of threshold is also in good agreement. Assuming a

linear extrapolation of the betatron calibration above 15 Mev, it is found that the carbon threshold is 52 kev above the accepted value of the separation energy. The successful correlation between the assignment of known resonance energies with the positions of many of the breaks in the yield curves corroborates the assumed linearity of the betatron energy scale above 15 Mev. It follows that previous betatron calibrations using the carbon threshold must be in error by approximately 100 kev at 18.7 Mev.

*Permanent address: University of Melbourne, Melbourne, Australia.

PHOTOPROTON AND PHOTONEUTRON PRODUCTION IN ALUMINUM AND COPPER. R. E. Chrien* and A. H. Benade, Case Institute of Technology, Cleveland, Ohio (Received March 2, 1960).

The ratio of proton to neutron yields from aluminum and copper irradiated with betatron x rays up to 20.8 Mev in energy has been measured. Simultaneous detection of protons and neutrons is accomplished by placing two samples of the same element in series in the x-ray beam. Direct detection methods are used in each case, a shallow proportional counter for protons and a boron-lined detector for neutrons. A photon difference method has been used to reduce yield data to cross-section form. The proton and neutron yields for aluminum are found to be approximately equal at 20 Mev with cross sections of 19 and 21 millibarns, respectively. At 20.8 Mev a yield ratio of one proton to about 6 neutrons is found for copper, with a peak photoproton cross section of 23 millibarns. The results are compared to a calculation based on the assumption that these reactions proceed through the formation of a compound nucleus.

*Now at Brookhaven National Laboratory, Upton, New York.

SCATTERING OF SLOW NEUTRONS BY WATER. Mark Nelkin, John Jay Hopkins Laboratory for Pure and Applied Science, General Atomic, San Diego, California (Received February 18, 1960).

The motions of hydrogen atoms in water are considered in terms of the H_2O molecule as the basic dynamical unit. Vibrations, hindered rotations, and translations of the molecule are included. For the numerical calculations, the hindrance of the translations is neglected, and the hindered rotations are replaced by a torsional oscillation with a single energy, $h\nu = 0.06$ ev. When certain approximations are made in the average over molecular orientation, this model allows for the computation of differential and total slow-neutron cross sections. The computed cross sections are in good agreement with most of the available slow-neutron scattering data. The features of the high-resolution experiments directly associated with the hindrance of the molecular translation in the liquid are not reproduced.

ODD-EVEN DEPENDENCE OF NUCLEAR LEVEL DENSITY PARAMETERS. R. E. Bullock and R. G. Moore, Jr., Convair, Fort Worth, Texas (Received February 23, 1960).

Previously reported experimental (n, p) and (n, α) cross-section data have been analyzed to determine nuclear level density parameters for the Fermi gas model which best fit the experimental data for target nuclei ranging in mass number from 9 to 64. Level density parameters for odd-odd and even-even nuclei are obtained in terms of those for the better-known odd A values. The results of this analysis are $\frac{1}{2}C_{\text{odd-odd}} = C_{\text{odd } A} = 5C_{\text{even-even}}$. Brief mention is made of the direct-interaction contribution in (n, p) reactions. Experimental measurements which would be most beneficial for further theoretical analysis are suggested.

MULTIPLE MESON PRODUCTION BY PHOTONS IN HYDROGEN. B. M. Chasan, G. Cocconi,* V. T. Cocconi,* R. M. Schectman, and D. H. White, Laboratory of Nuclear Studies, Cornell University, Ithaca, New York (Received February 19, 1960).

The analysis of 235 events of double meson production by photons up to 1.1 Bev (reaction $\gamma + p \rightarrow p + \pi^+ + \pi^-$) observed in a H_2 diffusion cloud chamber has produced the following results. The cross section rises rapidly at about 500 Mev to a value of approximately 70 μb. The angular, momentum, and Q distributions of the reaction products cannot be satisfactorily accounted for either by a pure statistical model, or by a pure isobaric state model, or by a model assuming interaction of the incoming photon with the meson

cloud of the proton, leading to $\pi-\pi$ interaction. The observation of 14 cases of the reactions $\gamma+p\rightarrow p+\pi^{+}+\pi^{-}+\pi^{0}$ and $\gamma+p\rightarrow n+\pi^{+}+\pi^{+}+\pi^{-}$ suggests that the combined cross sections for these reactions is about 10 μb between 700 and 1000 Mev.

*Now on leave at CERN, Geneva, Switzerland.

ELECTRON PAIR PRODUCTION IN $\pi^{-}+d$ CAPTURE. David W. Joseph,* The Enrico Fermi Institute for Nuclear Studies and the Department of Physics, The University of Chicago, Chicago, Illinois (Received February 25, 1960).

The internal conversion coefficient $\rho(p)=(dW_{2e}/dp)/(dW_{\gamma}/dp)$, relating the $\pi^{-}+d$ capture processes yielding $2n+e^{+}+e^{-}$ and $2n+\gamma$, is calculated as a function of the $n-n$ relative momentum p. It is found to be a slowly varying function of p, insensitive to the strength of the $n-n$ force. The spectrum of the electron pair energies (or of the momentum p) therefore depends sensitively on the $n-n$ scattering length, just as Watson and Stuart found to be the case for the photon spectrum. Thus, observation of the pair production process is an alternative method of measuring the $n-n$ scattering length.

*Now at Purdue University, Lafayette, Indiana.

DEPOLARIZATION OF A MUON BY HYPERFINE INTERACTION. Elihu Lubkin, Lawrence Radiation Laboratory, University of California, Berkeley, California (Received February 29, 1960).

The further depolarization of a muon captured in the 1s Bohr orbit by hyperfine interaction with a nucleus of spin j is calculated. The main result is that the asymmetry parameters of the decay electrons from the $J=j\pm\frac{1}{2}$ states are multiplied by respective asymmetry reduction factors $\frac{1}{3}[1\pm 2/(2j+1)]$.

COMMUTATION RELATIONS OF QUANTUM MECHANICS. Joseph V. Lepore, Lawrence Radiation Laboratory, University of California, Berkeley, California (Received February 29, 1960).

The mathematical and physical meaning of the commutation relations of nonrelativistic quantum mechanics is discussed in terms of the representation of translations, Galilean transformations, and rotations of the coordinate system by unitary transformations acting on the unitary vector space of quantum states.

PROPOSAL FOR DETERMINATION OF $\Sigma\Lambda$ RELATIVE PARITY FROM CHEW AND LOW ANALYSIS OF REACTIONS OF THE FORM $A+B\rightarrow C+D+E+\cdots$. Murray Muraskin, Department of Physics, University of Illinois, Urbana, Illinois (Received March 14, 1960).

We use the Chew and Low analysis of reactions of the form $A+B\rightarrow C+D+E+\cdots$, which makes use of the existence of a pole in the S matrix, to propose an experiment to determine the $\Sigma\Lambda$ relative parity and the coupling constant for the $\Sigma\Lambda\pi$ interaction. It is found that the sign of the extrapolated cross section for the reaction $\Sigma^{+}+d\rightarrow\Lambda^{0}+p+p$ is different for the two parity cases. Other applications of the Chew and Low method to strange particle reactions are briefly studied.